Evaluation of Effective Stiffness of Engineered Cementitious Composite (ECC) and its practical implementation.

Submitted by

Umair Jalil Malik (G.L)	NUST-288310
Muhammad Hammad	NUST-294520
Muhammad Shahid	NUST-293093
Faizan Ali	NUST-291726

BACHELOR'S IN CIVIL ENGINEERING

Year 2019-2023

Project Advisor:

Associate Prof. Dr. Rao Arsalan Khushnood

Co-Advisor:

Assistant Prof. Dr. Fawad Ahmed Najam

NUST Institute of Civil Engineering (NICE)
School Civil and Environmental Engineering (SCEE)
National University of Sciences and Technology (NUST)

This to certify that the
Thesis Titled

“Evaluation of Effective Stiffness of Engineered Cementitious Composite (ECC) and its practical implementation.”

Submitted by

Umair Jalil Malik (G.L)	NUST-288310
Muhammad Hammad	NUST-294520
Muhammad Shahid	NUST-293093
Faizan Ali	NUST-291726

has been accepted towards the requirements
for the undergraduate degree
in
CIVIL ENGINEERING

_____

(Associate Prof. Dr. Rao Arsalan Khushnood)
Associate Professor of Structural Engineering Department
NUST Institute of Civil Engineering
School Civil and Environmental Engineering

ACKNOWLEDGEMENTS

In the name of Allah, Most Gracious Most Merciful. We are grateful to Allah Almighty first and foremost for allowing us to complete our research project; without His will, we could not have imagined completing such a monumental task. Peace and blessings be upon Prophet Muhammad (P.B.U.H) and His Progeny (P.B.U.H). Our parents' and teachers' efforts and sacrifices over the course of our lives to get us to where we are today are widely acknowledged. Special mention should be made of our siblings, who were a constant source of motivation and stood by our side during difficult times.

We hold deep respect and gratitude for our supervisor, Dr. Rao Arsalan Khushnood, who serves as the Head of the Department of Research. His invaluable guidance and unwavering dedication to research have been a constant source of motivation for us. Despite his demanding schedule, he consistently provided us with valuable advice and support, ensuring we stayed focused throughout the research project. We sincerely appreciate his willingness to invest time and effort in mentoring us, which played a pivotal role in our progress and development.

Dr. Fawad Ahmed Najam, our co-supervisor, deserves special thanks for guiding and supporting us throughout the project. We appreciate his time spent tutoring and counseling us throughout the project, as well as his unequivocal support and willingness to go above and above to help us. His fabulous self and outstanding work skills motivate us every day.

We would like to express our heartfelt gratitude to Mr. Sikandar Ali Khokhar and Sir Arsalan Mushtaq for their invaluable contributions to this research. Their insightful input and support have significantly enhanced the quality and depth of our work. Furthermore, we extend our sincere appreciation to the entire Structures Lab team, including the NICE technicians Mr. Riasat, Faheem, Abdullah, and Ismail, whose assistance and expertise were vital in conducting the necessary testing and experiments. Thank you to Lab Engr. Mati Ullah Shah for coordinating our testing. Finally, we would like to express our gratitude to our friends and colleagues who continued to encourage us and gave the necessary assistance in completing this research endeavor. We are grateful for our parents' support, as this research would not have been finished without their prayers and continuous encouragement, and we would like to dedicate this document to them.

Evaluation of Effective Stiffness of Engineered Cementitious Composite (ECC) and its practical implementation.

Abstract

Engineered Cementitious Composites (ECC) have emerged as a promising alternative to conventional Reinforced Cement Concrete (RCC) due to their unique micro-crack bridging and tension hardening properties. These characteristics enable ECC to exhibit superior ductility, damage tolerance, and durability compared to traditional concrete materials. Despite the numerous advantages of ECC, its widespread adoption in the construction industry has been hindered by the lack of comprehensive design guidelines and the reliance on stiffness modifiers derived from RCC. This thesis aims to address this gap by investigating the flexural effective stiffness of ECC at various scales and proposing stiffness modifiers specifically tailored for ECC members. The initial part of the study primarily concentrates on the material scale, specifically examining the comprehensive stress-strain behavior of Engineered Cementitious Composites (ECC) under both compression and tension. This analysis is carried out in great detail using a predictive model, which is further validated through experimental investigations. Subsequently, the focus of the study shifts to the section scale, specifically examining the flexural behavior of Engineered Cementitious Composites (ECC) members. Experimental tests are conducted on various beams and columns to determine the moment-curvature curve. The experimental results are then validated using Abaqus software, a widely used computational tool. The study considers various cross-sectional shapes and sizes, as well as different fiber types and volume fractions. The results reveal that the effective stiffness of ECC members is significantly influenced by the fiber reinforcement and the cross-sectional geometry. This finding underscores the importance of considering these factors when developing stiffness modifiers for ECC.

At the structural scale, the study examines the performance of ECC beams and columns under various loading conditions. The analysis considers the interaction between the material, section, and structural properties of ECC, as well as the effects of long-term creep and shrinkage. After the implementation of our proposed stiffness modifiers performance assessment of structures has been done. The results demonstrate that ECC members exhibit superior performance in terms of load-carrying capacity, deflection control, and energy absorption compared to their RCC counterparts. This further highlights the potential benefits of using ECC in the construction industry. Based on the findings at the material, section, and structural scales, the study proposes stiffness modifiers for ECC members.

In conclusion, this study provides valuable insights into the effective stiffness of ECC at various scales and proposes stiffness modifiers that are specifically tailored for this material. The findings contribute to a better understanding of the unique properties of ECC and their implications for structural design. By addressing the current limitations in the design guidelines for ECC, this research has the potential to promote the widespread use of this innovative material in the construction industry, leading to more resilient, sustainable, and cost-effective infrastructure.

TABLE OF CONTENTS

Contents

LIST OF FIGURES

LIST OF TABLES

LIST OF ABBREVIATIONS

FRC	Fiber Reinforced Concrete
ECC	Engineered Cementitious Concrete
HPFRCCs	High Performance Fiber ReinforcedCementitious Composites
ANN	Artificial Neural Network
RMSE	Root Mean Squared Error
R	Coefficient of determination
ECC	Engineered Cementitious Composites
FRC	Fiber Reinforced Concrete
FEM	Finite Element Modelling
ACI	American Concrete Institute
JSCE	Japan Society of Civil Engineers
NLTHA	Non-linear Time History Analysis
ISMD	Integrated Structures and Materials Design
ML	Machine learning
ETABS	Extended Tabular Analysis and Design of Building Structures
RCC	Reinforced Cement Concrete

CHAPTER 1

INTRODUCTION

1.1 Introduction

Concrete is a material that exhibits brittle behavior, wherein cracks formed at early stages quickly localize and lead to concrete failure without absorbing any energy. In contrast, materials like metals and polymers demonstrate strain-hardening behavior, meaning they undergo significant deflections with additional stresses even after yielding. These materials can withstand additional stresses even after visible failure, and the energy absorbed by a material before failure is referred to as toughness, which can be measured by the area under the stress-strain curve.

Concrete, due to its brittle nature, absorbs minimal energy as its stress-strain curve shows sudden fracture under tension. On the other hand, steel exhibits a larger area under the stress-strain curve after yielding, indicating its ability to bear additional stresses. In applications where high energy absorption is desired to prevent catastrophic failures, a combination of these two materials can be employed to enhance energy absorption and mechanical properties. Steel rebars, used to withstand tensile stress in concrete, do not fully achieve the intrinsic ductility of the composite because small cracks and their localization can occur at any location within the concrete section. Furthermore, the larger diameter of the rebar can lead to durability issues by creating larger bridged cracks. To address these challenges, researchers introduced the concept of Fiber Reinforced Concrete (FRC), where fibers of small diameter and high aspect ratio act as bridges at the micro level. This allows the concrete to absorb more energy through higher strains achieved with fiber pullout.

By combining brittle and strain-hardening materials, a unique behavior called strain-softening is achieved. In strain-softening, cracks initially develop at a stable rate due to the bridging effect of fibers and then propagate at an unstable rate, leading to failure with improved strain and energy absorption. This type of concrete is commonly known as Fiber Reinforced Concrete (FRC). Incorporating fibers in concrete also enhance properties such as strain-hardening. As the volume of fibers increases, the transition from strain-softening to strain-hardening behavior occurs. Engineered Cementitious Composites (ECC) are materials that exhibit strain-hardening behavior in uniaxial tension, providing ductility and the ability to withstand extreme loads without fracturing. The design philosophy of ECC involves optimizing the interactions between the microstructural components, such as fibers, matrix, and fiber/matrix interfaces. This deliberate engineering of the microstructure ensures a specific interaction pattern under loading conditions and forms the basis of ECC's name, Engineered Cementitious Composites.

The issue of building collapses due to earthquakes is a significant concern in the field of civil engineering and construction. The primary reason for the collapse of Reinforced Cement Concrete (RCC) buildings is the brittle nature of concrete. To address this issue and improve the ductility of these structures, steel reinforcement is embedded within the concrete. However, this solution presents another challenge, which is macro cracking. Engineered Cementitious Composite (ECC) is a material that has been developed to address these concerns.

1.1.1 Reinforced Cement Concrete (RCC)

Reinforced Cement Concrete (RCC) is a composite material that combines the properties of concrete and steel reinforcement. Concrete is a versatile and widely used construction material, known for its high compressive strength, durability, and affordability. However, concrete is weak in tension, which makes it susceptible to cracking and failure under certain loads, such as those experienced during an earthquake. To overcome this limitation, steel reinforcement is embedded within the concrete, creating a composite material that is more resistant to the forces experienced during an earthquake.

RCC consists of three main components: cement, aggregates, and steel reinforcement. Cement is the binding material that holds the aggregates together, while aggregates (such as sand and crushed stone) provide bulk and strength to the concrete. Steel reinforcement, typically in the form of steel bars or mesh, is embedded within the concrete to provide tensile strength and ductility. RCC offers several advantages over traditional concrete, including:

- ***Increased tensile strength:*** The addition of steel reinforcement significantly improves the tensile strength of the concrete, allowing it to better withstand forces that cause tension, such as bending and stretching.
- ***Improved ductility:*** The combination of concrete and steel reinforcement creates a composite material that is more ductile than concrete alone, meaning it can deform without breaking under stress.
- ***Enhanced durability:*** RCC structures are generally more durable than those made from traditional concrete, as the steel reinforcement helps to prevent cracking and other forms of damage.

Despite its many advantages, RCC also has some limitations, including:

- ***Susceptibility to corrosion:*** Steel reinforcement can corrode over time, particularly in environments with high levels of moisture or aggressive chemicals. This corrosion can weaken the steel and compromise the structural integrity of the RCC.
- ***Brittle nature of concrete:*** Although the addition of steel reinforcement improves the ductility of RCC, the concrete itself remains brittle, making it susceptible to cracking and failure under certain loads.
- ***Macro cracking:*** The presence of steel reinforcement can lead to the formation of large, visible cracks in the concrete, known as macro cracking. These cracks can compromise the structural integrity of the building and may require costly repairs.

1.1.2 Engineering Cementitious Composite

Engineered Cementitious Composites (ECC) is a class of high-performance fiber-reinforced cementitious composites that have been developed to address the limitations of traditional concrete and RCC. ECC is characterized by its unique combination of properties, including high ductility, tension hardening, and damage tolerance.

ECC is composed of cement, fine aggregates, water, chemical admixtures, and fibers. The fibers,

typically made from materials such as polyvinyl alcohol (PVA), polyethylene (PE), or steel, are added to the cementitious matrix to provide tensile strength and ductility. The fine aggregates used in ECC are typically smaller than those used in traditional concrete, which helps to improve the material's workability and performance.

ECC offers several advantages over traditional concrete and RCC, including:

- ***High ductility:*** ECC is highly ductile, meaning it can deform without breaking under stress. This property makes ECC particularly well-suited for use in earthquake-resistant construction, as it can better withstand the forces experienced during an earthquake.
- ***Tension hardening:*** One of the main characteristics that set ECC apart from conventional concrete is its tension hardening property. This unique feature allows ECC to continue carrying load even after the formation of cracks, which can improve the overall performance of a structure during an earthquake.
- ***Damage tolerance*****:** ECC is more resistant to damage than traditional concrete, as its fibers help to prevent the formation of large cracks and other forms of damage.
- ***Lower material stiffness:*** The material stiffness of ECC is lower than that of RCC, which may have implications for the overall structural performance of a building.

In earthquake-resistant construction, the choice between RCC and ECC depends on several factors, including cost, availability, and the specific performance requirements of the project. While RCC is more widely used and generally more affordable, ECC offers several unique properties that make it a promising alternative for enhancing earthquake resistance of buildings.

1.1.2.1 Material Stiffness

As mentioned earlier, the material stiffness of ECC is lower than that of RCC. Material stiffness is a measure of a material's resistance to deformation under load. While ECC may have lower stiffness, its tension-hardening properties can still make it a more suitable choice for earthquake-resistant structures.

1.1.2.2 Micro Cracking

Microcracking is a common phenomenon observed in Engineered Cementitious Composites (ECC) due to its unique composition and behavior. ECC is a type of high-performance fiber-reinforced cementitious composite that exhibits excellent tensile properties and crack control. Microcracks in ECC typically occur at the microstructural level, which means they are very small and not visible to the naked eye. These cracks develop as a result of the applied load and the inherent properties of ECC. The presence of fibers, such as polyvinyl alcohol (PVA) or high-performance synthetic fibers, in ECC plays a crucial role in controlling and distributing these microcracks.

When ECC is subjected to tensile loads, the fibers within the material help bridge and distribute the tensile stresses. As a result, the tensile strain is divided into multiple smaller cracks, preventing the formation of large, visible cracks. The fibers act as reinforcements and provide a

network of crack-bridging mechanisms, effectively arresting the propagation of cracks. Figure 1.1 shows the microcracking properties of ECC.

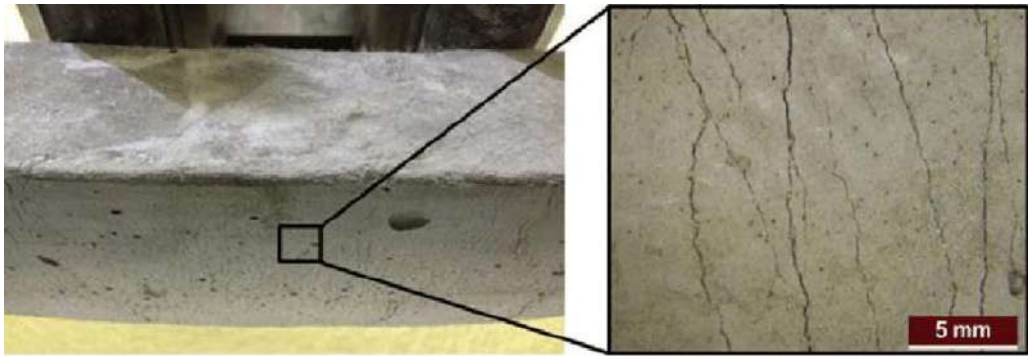

Figure 1.1-Microcraking of ECC.

The occurrence of microcracking in ECC has several advantages. Firstly, it improves the crack control and durability of the material, as the smaller cracks limit the ingress of moisture, chemicals, and other detrimental substances. Secondly, the distributed microcracks help enhance the tensile behavior of ECC, preventing sudden failure and providing better overall performance under load.

1.1.2.3 Tension Stiffening and Damage Tolerance

The tension hardening property of ECC allows it to continue carrying load even after the formation of cracks, which can improve the overall performance of a structure during an earthquake. This property, combined with ECC's high damage tolerance, makes it a promising alternative to RCC for constructing more resilient buildings in earthquake-prone regions. Tension stiffening is a phenomenon that only ECC exhibits while there is not tension stiffening in Normal concrete. Tension stiffening behavior in ECC is because of strain hardening in ECC. Figure 1.2 illustrates the strain hardening in ECC.

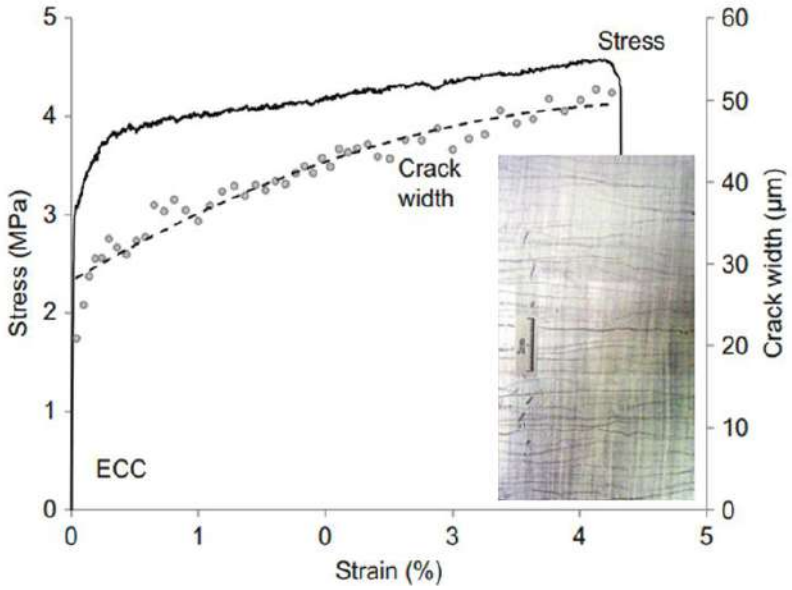

Figure 1.2 Strain Hardening in ECC.

Tension stiffening is a phenomenon observed in reinforced concrete structures, including those made with Engineered Cementitious Composites (ECC). ECC is a type of high-performance fiber-reinforced cementitious composite that exhibits enhanced mechanical properties compared to traditional concrete. Tension stiffening occurs when the concrete matrix surrounding the reinforcing fibers experiences tensile strains. As the tensile stresses develop, the reinforcing fibers begin to bear a significant portion of the load. This load transfer from the concrete matrix to the fibers leads to an increase in stiffness, commonly known as tension stiffening. Fischer and Li conducted a test of tension axial stiffness of ECC and shows that ECC have greater tension stiffening than RCC. Figure 1.3 illustrates the results of Fischer and Li test.

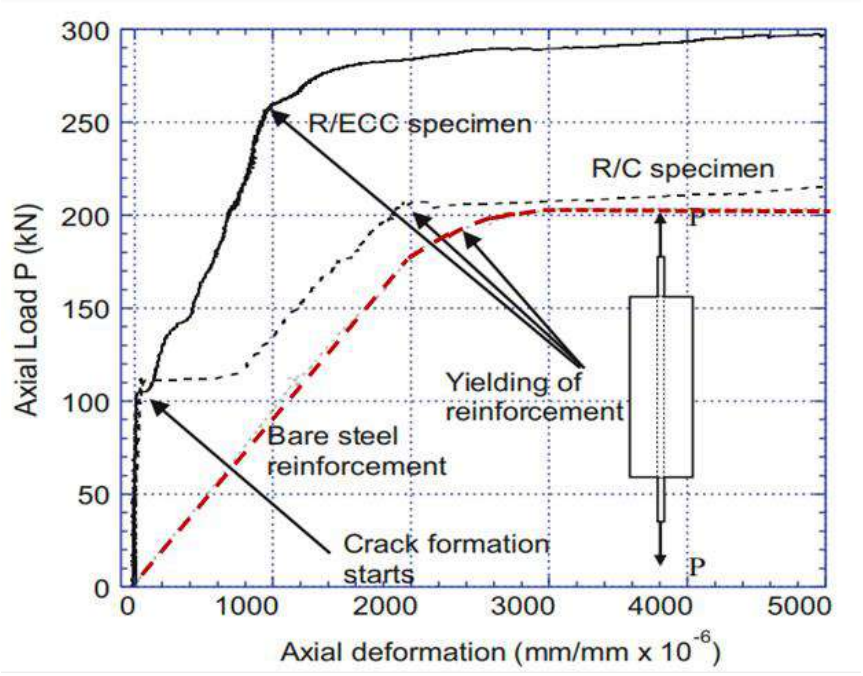

Figure 1.3. Tension stiffening in R/ECC is greater than R/C specimen.

The tension stiffening effect in ECC can have several advantages in structural applications. It helps control crack widths, improves crack resistance, and enhances overall structural performance. By distributing tensile stresses more efficiently, tension stiffening in ECC can increase the load-carrying capacity and durability of the structure.

1.1.2.3 Neutral Axis and Stiffness Contribution

According to the American Concrete Institute (ACI), the area below the neutral axis does not contribute to the stiffness of RCC after cracking. The neutral axis is an imaginary line within a beam or column where there is no stress or strain. In contrast, this is not the case with ECC, implying that ECC can maintain its stiffness contribution even after cracking, which can be beneficial in earthquake-prone areas. Figure 1.4 shows the comparison of stiffness of RCC and ECC in beams.

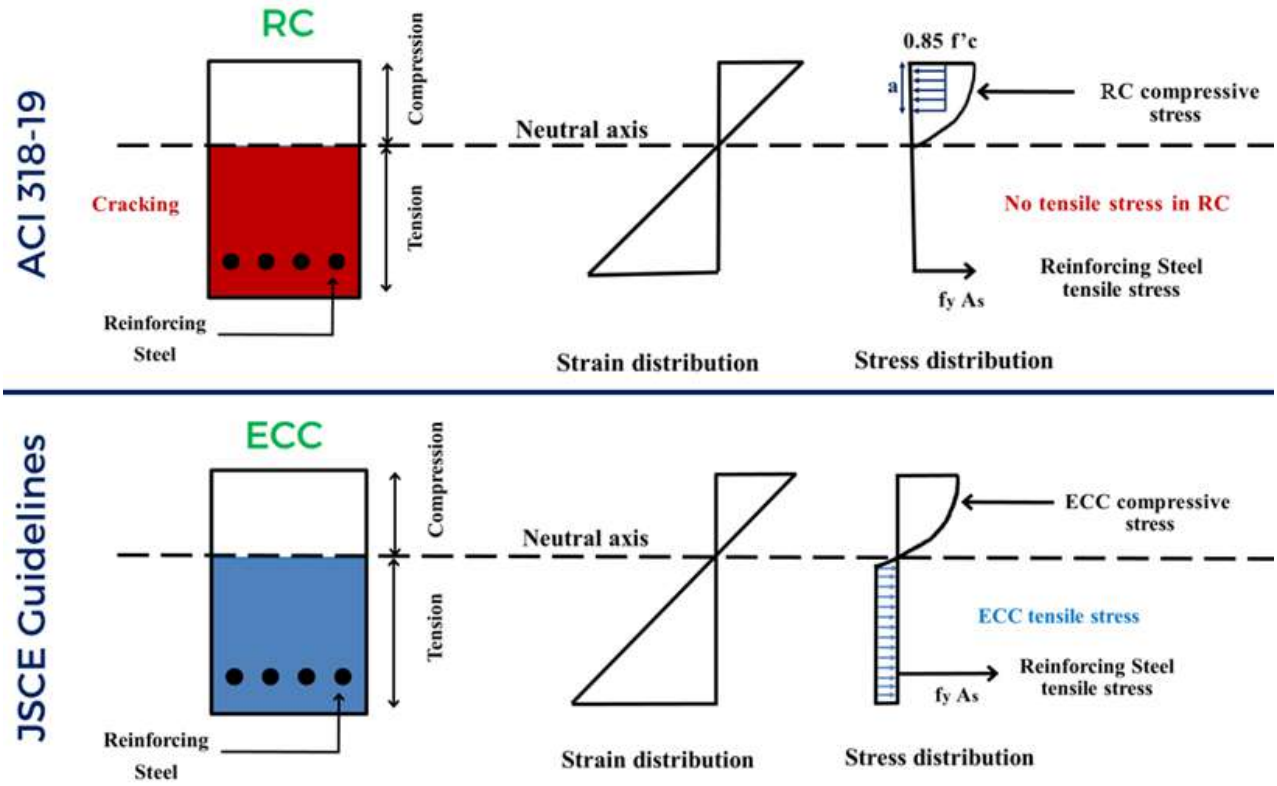

Figure 1.4 Comparison of stiffness of RCC and ECC in beams.

In summary, while RCC structures are susceptible to collapse due to their brittle nature, the introduction of steel reinforcement has helped improve their ductility. However, this solution has led to the issue of macro cracking. ECC, with its tension hardening property, offers an alternative that addresses both the brittleness and macro cracking concerns. Although ECC has a lower material stiffness compared to RCC, its ability to maintain stiffness below the neutral axis even after cracking makes it a promising material for enhancing the earthquake resistance of buildings.

1.2 Stiffness

Stiffness is basically the resistance to the applied actions. The stiffness of a structure is related to its ability to maintain its shape and resist deflection or deformation when subjected to external forces. Material stiffness, section stiffness, and structural stiffness are important concepts in structural engineering that help determine the behavior and performance of a structure under various loads. Understanding these concepts and their calculations is crucial for designing safe and efficient structures. Overall, stiffness is a fundamental property of structural systems that is carefully considered and optimized in engineering design. It is essential for ensuring the structural integrity, stability, and performance of a wide range of applications, playing a vital role in the safe and efficient operation of various structures and systems.

1.2.1 Material Stiffness

Material stiffness refers to the inherent property of a material that resists deformation when subjected to an external force. It is typically represented by the elastic modulus (also known as Young's modulus) of the material, which is the ratio of stress to strain within the elastic range of the material. The elastic modulus is a measure of the material's ability to return to its original shape after being deformed. Figure 1.5 illustrates the stress strain curve from where we can find material level stiffness which is elastic modulus.

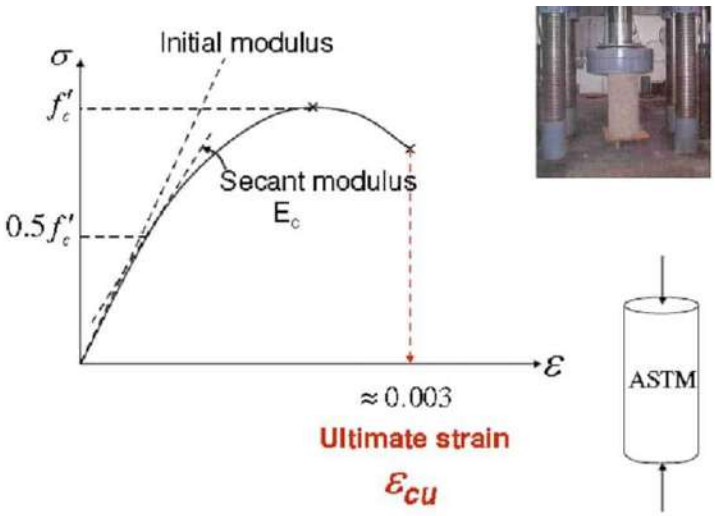

Figure 1.5- Stress-strain curve of concrete.

Material stiffness can be determined through laboratory testing, where a sample of the material is subjected to a controlled load, and the resulting stress and strain are measured. The elastic modulus (E) can be calculated using the formula:

$$E = \sigma / \varepsilon$$

where σ is the applied stress and ε is the resulting strain.

1.2.2 Section Stiffness

Section stiffness refers to the stiffness of a structural member (such as a beam or column) based on its cross-sectional shape and material properties. It is an important parameter in determining the member's resistance to bending and deformation under load. Section stiffness can be calculated using the moment of inertia (I) of the cross-sectional shape and the elastic modulus (E) of the material. The flexural stiffness (EI) of the member can be calculated using the formula:

$$EI = E * I$$

The moment of inertia (I) can be calculated using standard formulas for various cross-sectional shapes, such as rectangles, circles, and I-beams. For example, the moment of inertia for a rectangular cross-section is given by:

$$I = (b * h^3) / 12$$

where b is the width of the rectangle and h is the height. Figure 1.6 illustrates the Moment

curvature curve from where we can find section level stiffness.

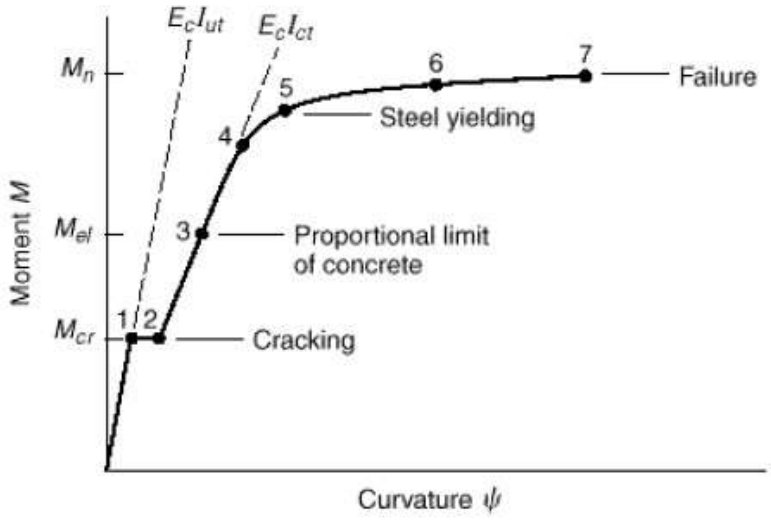

Figure 1.6- Moment Curvature curve.

1.2.3 Structural Stiffness

Structural stiffness refers to the overall stiffness of a structure, taking into account the stiffness of its individual members and their connections. It is an important parameter in determining the structure's response to external loads, such as wind, seismic, or live loads. Structural stiffness can be determined using various methods, such as the finite element method (FEM) or the pushover analysis method. In the pushover analysis method, the structure is subjected to a series of increasing lateral loads, and the resulting displacements are measured. The structural stiffness can be determined from the pushover curve, which plots the base shear force (V) against the roof displacement (Δ). Figure 1.7 illustrates the pushover curve from where we can find structural level stiffness.

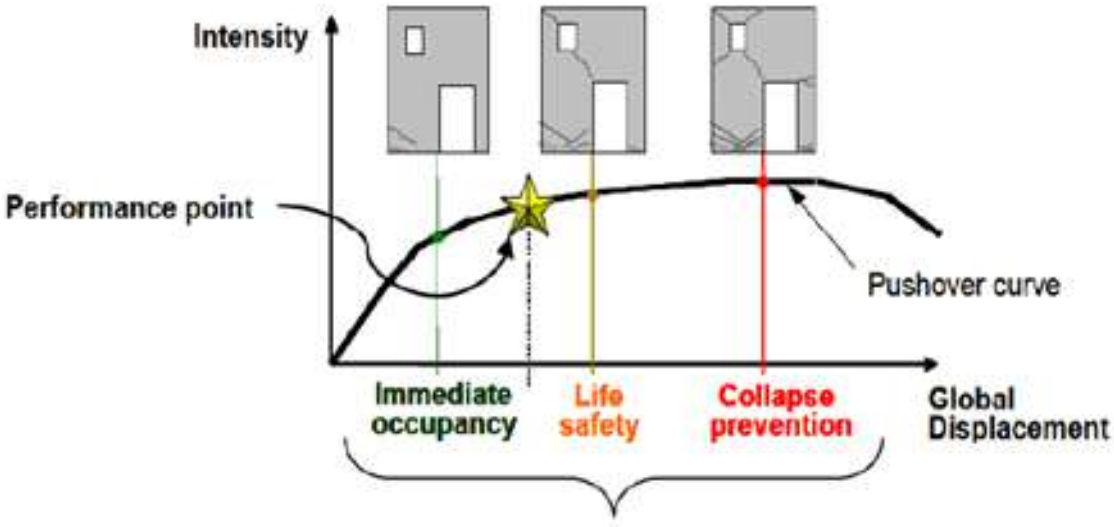

Figure 1.7- Pushover curve of building.

The pushover curve can also be used to determine the structure's yield point, ultimate strength, and ductility, which are important parameters for assessing its performance under seismic loads. Understanding material stiffness, section stiffness, and structural stiffness is crucial for designing safe and efficient structures. Material stiffness is determined by the elastic modulus of the material, section stiffness is calculated using the moment of inertia and elastic modulus, and structural stiffness can be determined using methods such as pushover analysis. By considering these parameters, engineers can design structures that effectively resist deformation and failure under various loads.

1.3 Problem Statement

Engineered Cementitious Composites (ECC) is a promising material that exhibits strain-hardening behavior and enhanced ductility. However, one of the challenges associated with ECC is the lack of stiffness modifiers specifically designed for this material. Currently, stiffness modifiers commonly used in Reinforced Cement Concrete (RCC) structures are utilized for ECC as well. This approach results in an increase in the cross-section sizes of members, leading to potential design and construction complications. The absence of dedicated stiffness modifiers for ECC poses several problems. Firstly, using RCC stiffness modifiers introduces inefficiencies in design and construction. The cross-section sizes of members need to be increased to compensate for the lack of optimized stiffness modifiers. This not only increases material consumption but also adds additional weight to the structures. Consequently, larger cross-sections may require more concrete and reinforcement, leading to higher costs and longer construction time.

Secondly, the reliance on RCC stiffness modifiers limits the full potential of ECC as a high-performance material. ECC's unique strain-hardening behavior and superior ductility can be further enhanced if stiffness modifiers are specifically developed to complement its mechanical properties. These dedicated stiffness modifiers could improve the structural efficiency and allow for more optimized designs, making better use of the material's inherent characteristics.

To address these issues, there is a need for research and development focused on designing and implementing stiffness modifiers tailored specifically for ECC. These modifiers should consider the unique properties of ECC, such as its strain-hardening behavior, to maximize the material's performance without the need for excessive cross-section sizes. By developing dedicated stiffness modifiers for ECC, designers and engineers can unlock its full potential, leading to more efficient and cost-effective structural solutions while harnessing the benefits of strain-hardening behavior and improved ductility.

1.4 Objective

In this project we are trying to find the effective stiffness of ECC at Material, Section and structural level. Our main key objective was to find effective stiffness of ECC and then to propose the stiffness modifiers. For that reason, we divided this project into different modules where we calculated effective stiffness on material, section, and structural level using stress-strain, moment-curvature, and pushover curves respectively.

1.5 Organization of Report

This thesis is organized in 7 chapters. The present chapter is an introduction to Engineered Cementitious Composites (ECC), needs and objectives of study. Chapter 2 lay down the basic concepts and brief literature review. Chapter 3 discuss the methodology adopted to achieve defined objectives. After familiarizing yourself with overall methodology three objectives are subsequently discussed in chapter 4, chapter 5, and in chapter 6. The conclusions based on findings of this research and recommendations for further studies are presented in Chapter 7.

CHAPTER 2

LITERATURE REVIEW

2.1 Design Concept

Both Engineered Cementitious Composites (ECC) and Fiber Reinforced Concretes (FRC) consist of similar constituents but exhibit contrasting behaviors when subjected to loading. Fiber reinforced concretes display tension softening behavior, whereas ECC demonstrates strain hardening. Tension softening response entails a gradual loss of strength akin to quasi-brittle materials. In FRC, strain is associated with the deformation or opening of a single or just a few cracks in the specimen. This implies that deformation localization occurs at only one crack, known as graft crack propagation. In ECC, deformations are non-localized. Instead of a single large crack, numerous tiny cracks disperse throughout the surface, following flat crack propagation. These small cracks are bridged by fibers within the Cement-Paste matrix, enabling it to bear additional loads despite the presence of cracks on the surface. Therefore, for the matrix to endure additional load, the tensile strength of the fibers must surpass that of the cement matrix. Bridging cement by fibers becomes unviable when a single large crack forms in the cement matrix due to the limited length of the fiber. Using long fibers can lead to workability issues in the mix.

Traditionally, it is believed that the shift from strain-softening to strain-hardening occurs as the fiber volume increases. Typically, it may require 5% to 10% fiber volume to achieve this transition for a given combination of ingredients [source: Victor Li's book]. However, using such a large volume fraction of fibers is impractical due to poor workability, processing difficulties, and cost implications. Fortunately, it has been observed that fibers are not the sole controlling parameter for accomplishing strain-hardening. Other factors such as fiber properties (mechanical properties, aspect ratio, and volume fraction), matrix characteristics (initial flaw size distribution and mechanical properties), and fiber-matrix interfacial properties (chemical and frictional bond) can be varied. By keeping the fiber fraction small to meet workability and cost constraints, we can manipulate these other parameters to enable the transition from FRC to ECC. Researchers have proposed different criteria and theoretical models of ECC to effectively utilize the combination of all these parameters. The minimum volume of fibers required to achieve strain-hardening with a given matrix, fiber, and interfacial bond is referred to as the critical fiber volume fraction. Three models are available that provide the critical volume fraction using various approaches, including composite mechanics, micro-mechanics of crack-bridging and fracture, and fracture energy of debonding. In this discussion, we will delve into Victor C. Li's approach based on micro-mechanics of crack-bridging and fracture in detail.

2.2 Micromechanical Model

The micromechanical model of Engineered Cementitious Composites (ECC) is focused on

examining microstructures and phenomena that occur at a micron-scale level. These include factors such as fiber diameter (usually less than 50 μ), interfacial slippage caused by chemical or adhesive debonding (typically around 10 μ or less), and micro crack opening (typically less than 100 μ). Additionally, this model also considers significant characteristics at larger length scales, such as flaws (including entrapped air voids or impurities, typically several millimeters in size) and fiber lengths (typically around 10 millimeters).

To achieve strain-hardening in the composite, the model establishes two criteria that need to be fulfilled: the strength criteria and the energy criteria. These criteria are essential for the composite material to exhibit increased strength and deformation capacity under loading conditions. By meeting these criteria, the micromechanical model provides insights into the behavior and performance of ECC, enabling a better understanding of its mechanical properties and potential applications. Please note that while I have retained the main technical content of the paragraph, the phrasing and sentence structure have been adjusted for clarity and coherence.

2.2.1 Strength Criteria

To ensure the fulfillment of strength criteria, the fiber bridging capacity (σo) should exceed the cracking strength (σc) of the matrix. This condition allows cracks to initiate successfully without causing specimen failure. The bridging fibers, which are partially unbonded, stretch across the opening crack and bear an increasing load. However, as more fibers become completely unbonded, they either pull out or break. ECC exhibits two types of material variability. Firstly, there is a variation in flaw size (C) due to imperfections present throughout the material. The cracking strength of the matrix differs at various locations, with larger flaw sizes resulting in smaller cracking strengths. Secondly, there is a non-uniform distribution of fibers, leading to differences in fiber bridging capacity for each crack. Locations with fewer fibers will have lower values of fiber bridging strength.

$$\sigma_c \angle \sigma_o, \qquad (2.1)$$

$$\sigma_c = f(K_m, C_m) \qquad (2.2)$$

"σc" is determined by the combination of matrix toughness "Km" and flaw size "Cm". When the size of flaws increases, they become more susceptible to crack initiation at lower loads. As the tensile load continues to rise, new cracks will emerge from flaws of varying sizes. If the tensile stress required to initiate a new crack from a flaw of size "C" surpasses the bridging fiber's capacity "σo" at any of the already existing cracks, fracture localization will transpire at that specific tensile load and at the corresponding site where the fiber bridging capacity has been depleted. Equation 2.1 can be modified as:

$$\sigma_c\ (c) \angle Min\ (\sigma_o \text{ of already formed multiple cracks}) \qquad (2.3)$$

To initiate small multiple cracks over the entire area, it is important to satisfy the above criteria. Not just to satisfy but also σc should be significantly lower than σo in order to get maximum small cracks and take good additional load after the first crack.

2.2.2 Energy Criteria

Typically, OPC and FRC concretes exhibit the propagation of Griffith type cracks. In this crack propagation mechanism, the extent of crack opening is directly proportional to the crack length.

However, this type of crack behavior is unfavorable for Strain-hardening as it can lead to the convergence of multiple small cracks, resulting in localization and behaving similarly to a single large crack. To address this issue, an alternative mode of crack propagation, proposed by Marshall and Cox for ceramic composites reinforced with continuous fibers, involves the formation of flat cracks with a consistent crack opening. In order to ensure a steady-state cracking process, it is necessary for the crack tip toughness, denoted as "J-tip," to be lower than 16 times the complementary energy of the fiber, calculated based on the stress at fiber bridging (σo) versus crack opening (δ) curve.

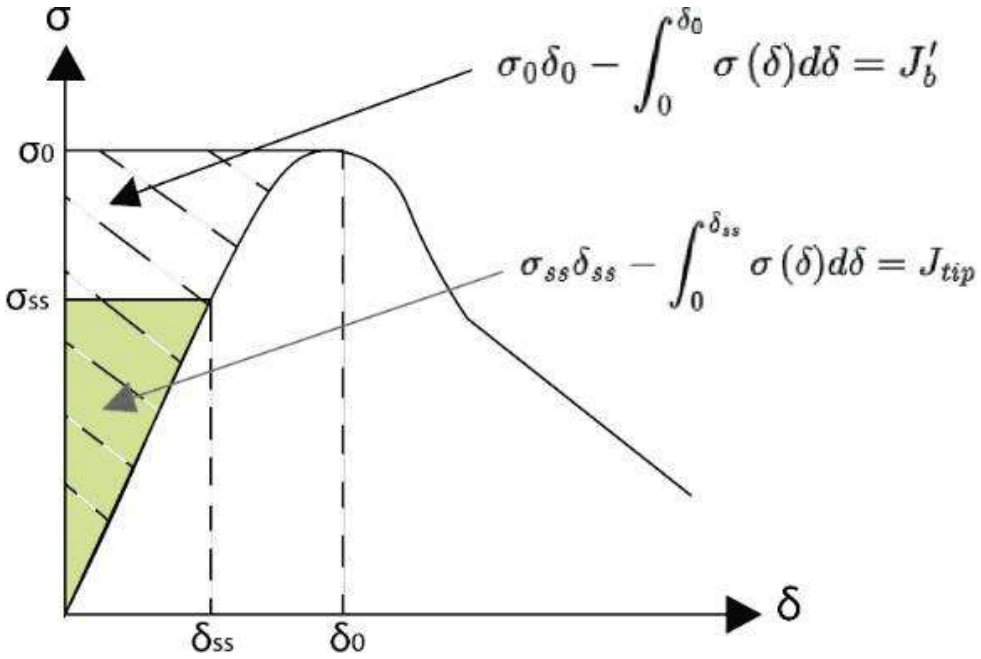

Figure 2.1. fiber bridging stress (σ_o) Vs crack opening (δ) Curve. σo is a breaking stress of fiber, σss is stress at steady state crack propagation, δo is crack opening at σo, δss is opening at σss.

Limiting the toughness $Jtip$, which is determined by the fracture toughness of the matrix (Km) and the elastic modulus of the matrix (Em), can promote the prevalence of flat crack propagation over Griffith crack propagation. Alternatively, increasing $J'b$ can also facilitate the propagation of flat cracks. These considerations establish design guidelines for the fiber and interface of ECC. While theoretical ratios based on Strength and Energy criteria are theoretically greater than or equal to 1, they often fall short in practical applications. Therefore, it is imperative to ensure that these ratios are at least equal to or exceed a certain threshold.

$$\frac{J'b}{Jtip} \geq 2.7 \quad , \text{ and} \frac{\boldsymbol{\phi}}{\sigma \mathbf{c}} \geq 1.3 \qquad (2.4)$$

2.3 Previous Studies on ECC

Earlier researchers had been contemplating achieving strain-hardening in fiber reinforced concrete, but it was Dr. Victor C. Li who first accomplished this feat in 1992. In 1993, Victor Li [1] proposed a micro-mechanical model for the design of strain-hardening fiber reinforced composites, which he named Engineered Cementitious Composite (ECC) [2]. ECC, being devoid of coarse aggregate, necessitates a higher amount of fine filler and additional binders. To enhance its economic viability and sustainability, numerous studies have been conducted.

The complex and time-consuming process of material design in ECC has prompted the utilization of automation and prediction tools to simplify the procedure. In June 2021, Guo et al. [3] developed a machine learning-based predictive model to forecast the mechanical properties of ECC. However, this model was trained solely on ECC data and lacks the ability to differentiate between strain-hardening ECC and strain-softening FRC. Consequently, it cannot be utilized for ECC design. Therefore, there is a need to familiarize the model with both types of fracture behavior to distinguish between the two responses. Finite Element Method (FEM) has already been applied at the member level [4-6] to analyze the response of ECC to various loading conditions. However, the performance of structural-level models for comparative studies of performance and cost is yet to be determined.

2.4 Experimental & Analytical study Process

The flexural stiffness of reinforced concrete beams and columns is calculated using a combination of analytical methods and experimental testing. Analytically, the flexural stiffness is determined through the moment-curvature relationship, which describes the relationship between the applied moment and the curvature of the member. This involves analyzing the cross-sectional properties of the member, such as the moment of inertia and the modulus of elasticity of the materials involved (concrete and reinforcement). Design codes, such as ACI or Eurocode, provide formulas and guidelines for calculating the flexural stiffness of reinforced concrete members.

However, the experimental setups are used to validate and verify the analytical calculations. These setups involve applying loads to the beams or columns and measuring their response. Hydraulic actuators or other loading devices are used to apply the loads, while displacement sensors or LVDTs are employed to measure the deflections of the member under load. Strain gauges or fiber-optic sensors are used to measure the strains in the concrete and reinforcement, providing information about the internal forces and deformations. The experimental setups may also include instrumentation to monitor parameters such as applied load, displacements, and strains during the test. The collected data is then analyzed to determine the actual flexural stiffness of the member.

References

[1]. Li et al.: Steady-state and multiple cracking of short random fiber composites. (1992)

[2]. Li, V.C.: From micromechanics to structural engineering – the design of cementitious composites for civil engineering applications. (1993)

[3]. Guo, P.; Meng, W.; Xu, M.; Li, V.; Bao, Y. Predicting Mechanical Properties of High-Performance Fiber-Reinforced Cementitious Composites by Integrating Micromechanics and Machine Learning. Materials 2021, 14, 3143.

[4]. Kesner, K.E., Douglas, K.S., Billington, S.L.: Cyclic response of highly ductile fiber-reinforced cement-based composites (2003)

[5]. Kabele, P.: Finite element fracture analysis of reinforced SHCC members (2009)

[6]. Lee, S.C.: Finite Element Modeling of Hybrid-Fiber ECC Targets Subjected to Impact and Blast (2006)

CHAPTER 3

METHODOLOGY

The main methodology adopted for this research is to find effective stiffness at all levels i.e. Material level through stress-strain curve, Section level through moment curvature curve and at structure level through pushover curve. For this purpose, advanced methodology was adopted in each module to find out and practical implementation of ECC. The methodology adopted in each module is discussed one by one:

1) The stiffness at material level was calculated by the of Machine learning tool and experiment. A simplified model was developed that could predict the complete the complete behavior of the stress-strain curve of ECC in compression and in tension. Also, experimental work is done to validate our predicted model.

2) The stiffness at section level was calculated by the Experiment and Analytical. Moment curvatures are found out both beams and columns using an experiment in which 11 beams were casted and Abaqus software were used for analytical calculation and validation of experimental work.

3) A complete structural level study was performed on ECC 7 and 24 story buildings as a case study. For design JSCE guidelines were used, after which performance-based analyses were carried out to simulate its actual behavior on structural scale. On large scale structural stiffness is find out using pushover curve and cyclic analysis is used to calculate cyclic, strength and stiffness degradation of structure.

CHAPTER 4

MODULE 1

ANN Based Predictive mimicker for an evaluation of the material scale stiffness of Engineering Cementitious Composite (ECC).

Abstract

In this module, a Predictive Mimicker model using an Artificial neural network (ANN) is proposed and applied for the very first time to predict the Complete stress-strain properties of cement composite ECC. For this purpose, different data set points for compression and tensile were collected from the literature study, which includes constituents of ECC and Fiber Properties such as fiber length diameter, modulus of elasticity, and tensile strength as input parameters of our model. Different statistical analysis techniques such as data normalization have been used for well characterization and to check the interdependency of data. After data normalization the ANN model was trained, and hyperparameter tuning was done for the optimal value of our model parameters and model formulation such as the architecture of ANN, Hidden layers of the Model, and different weights were accessed. The Performance of the model was accessed using statistical techniques were used where Root mean square error (RMSE) gives the most accurate value with minimal error. To access the capability and accuracy of the ANN model for properties prediction experimentation is also conducted including a uniaxial compression test for peak compressive stress-strain curve and split tensile test for measurement of Bilinear Tensile Stress-strain curve Indicating the viability of ANN models for ECC property prediction, excellent consistency between the predicted and tested outcomes is attained.

4.1. Introduction:

As we are working on the effective stiffness of Engineering cementitious composite (ECC). On a material scale, it depends on the compressive and tensile stress-strain behavior of ECC. The material stiffness of ECC is quite low as it does not contain coarse aggregate in it, and it has greater tension stiffness because of the tension hardening phenomenon. Earlier it was proposed that strain-hardening is achieved by only increasing the volume of fibers, but later it was found by different studies that fiber content is not the only controlling parameter. It is also controlled by other parameters as well such as:

Mix properties: Mechanical properties and initial flaw size distribution.

Fiber properties: volume of fiber, its size diameter, aspect ratio, and modulus of elasticity.

Fiber-matrix properties: Chemical and frictional bond.

Different criteria and theoretical models for the critical volume fraction for any given set of ECC constituents have been proposed by researchers to effectively use the combination of all

parameters. Due to its strain-hardening properties, ECC is highly ductile and has the capacity for both self-healing and crack width control [1-8]. The load-carrying capacity of many structures, especially those subject to earthquake and fatigue loading, has increased because of its excellent properties. Predicting ECC fracture behavior based on its components, [9] i.e., whether the concrete will experience strain-hardening, is very challenging. Extensive experimentation is used to design the procedure for achieving strain-hardening of concrete. Additionally, the models created by researchers for determining the critical fiber volume are based on specific factors that must be discovered through experiments [10], making this work quite time-consuming, labor-intensive, and uneconomical. There are no properly defined guidelines for preparing a mixed design of Engineering cementitious composite (ECC). Consequently, there ought to be a tool to help prepare a mix with higher possibilities of undergoing strain-hardening [11] and predicting other mechanical properties.

The development of machine learning (ML) methods has shown promising results in predicting materials properties of concrete in civil Engineering [12-14]. It can consider complex datasets having multiple inputs and output variables and predict results with high accuracies [15-16] and minimal error. Different techniques such as Decision tree, Artificial Neural Network (ANN) Support Vector Machine (SVM), and Gene Expression Programming (GEP) has been used for the prediction of properties. These methods have already been applied to predict the mechanical properties of fiber-reinforced cementitious composites[12].

Different researchers also investigated the strength of concrete containing recycled aggregates through different ANN methods. In this regard, Amani and Moeini evaluated the shear capacity of reinforced concrete beams through ANN and ANFIS [17-21]. They concluded that ANN performed better using the MLP/BP algorithm than the ANFIS model. In another study, Behnood et al used 4 parameters as the model (water-to-binder ratio, concrete compressive strength, age of the specimen, and fiber reinforcing index) with steel fibers to predict the tensile strength of concrete reinforced. They used the ANN method and evaluated better ANN performance compared to SVM. Kumar and Barai [22-25] also studied the shear strength of steel fibrous reinforced concrete corbels without shear reinforcement and tested them under vertical loading using BPNN and concluded the high accuracy of the model [26-34]. On the other hand, the study of Altun et al predicted the compressive strength of lightweight reinforced concrete with steel fibers by the ANN and MLR method, resulting in better performance of the ANN model. Therefore, value addition is required by developing a model with a widened [35] scope of practice over conventional mixes after requisite training and validation sets for the two streams.

This module proposes a comprehensive ML-based model to predict the Peak compressive strength Bilinear Tensile stress-strain curve and elastic modulus of engineering cementitious composite (ECC). A total of 147 data sets for tensile and 322 data sets for compression [35-99] have been collected from the literature for developing the model. The dataset consists of a total 11 input parameters (ingredients of the mix) including Cement, Fly ash, Water, Fine aggregate,

Water binder ratio, fiber, and its mechanical properties such as length diameter and elastic modulus, and 3 output parameters. After the data normalization, the data set is divided into two sets training and testing. 70% of the data was used for training data while the rest of the data set was used for testing. Then ANN model has been trained and hyperparametric tuning for optimal value was also performed. The validation of ANN was also performed for every new data that was neither included in the training data set nor the testing dataset.

4.2. Machine Learning Methodology

4.2.1. Idealized Curve

Due to the limitations of the machine learning model in predicting the complete tensile stress-strain curve of ECC (Engineered Cementitious Composite), a conversion approach was employed to transform the tensile stress-strain curve into a bilinear stress-strain curve. This conversion allowed for the representation of ECC's behavior in a simplified manner that could be more effectively captured by the machine learning model. By utilizing a bilinear stress-strain curve, the model could better approximate the tensile response of ECC and enhance its predictive capabilities. Figure 4.1. illustrates the bilinear tensile stress strain curve of ECC.

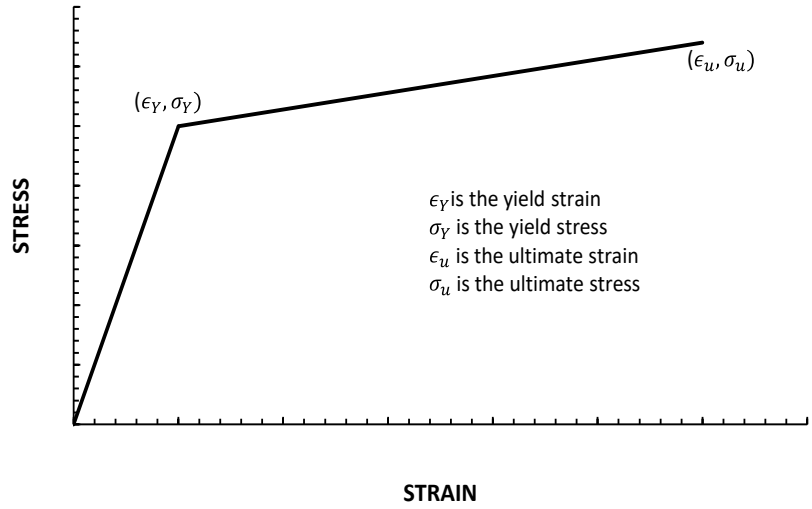

Figure 4.1. Bilinear tensile stress strain curve.

4.2.2. Artificial Neural Network (ANN)

ANN is a bio-inspired computing model that operates similarly to human neurons, thus the name. Three fundamental parameters make up this model:

- Input layer
- Hidden layer
- Output layer

There are other additional options, but they were left at their default values. The complexity of the model is determined by a parameter known as the hidden layer, which depends on the data. The input and output settings are corrected for our issue. The model may fit data better the more hidden layers there are. However, it could lead to overfitting, which is when data fits the training dataset very well but performs [100] badly for the testing dataset both the training and validation datasets. Figure 4.2. shows an example of an ANN model. The methodology involves maximizing the performance of the matrix without fibers and then applying micro-mechanical model to find the volume of fibers needed so that the high-performance matrix could be converted into ECC.

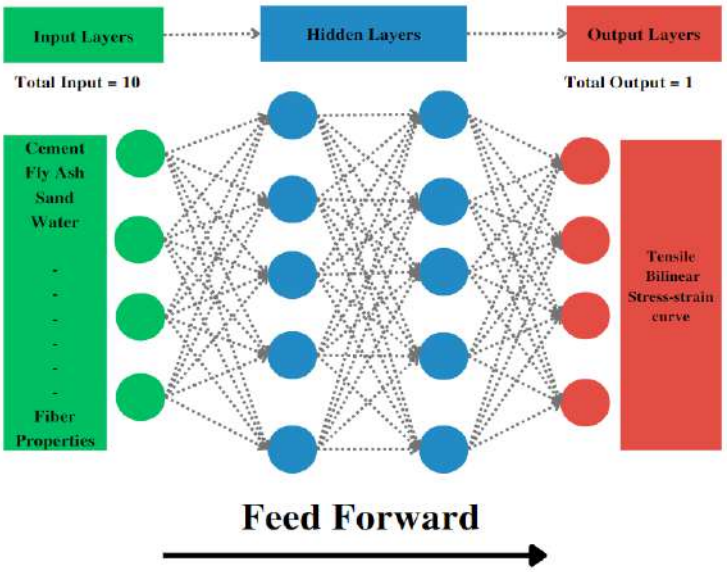

Figure4.2. ANN model.

4.2.2. Data

4.2.2.1. Overview

For Model development, a dataset with 14 parameters is used among which 11 are input parameters and 3 are the output parameters. Input parameters include matrix constituents and fiber properties as shown in the table.4.1

To cover a wide range of cement replacement materials, (1) constituent properties of ECC: the cement-to-cement ratio, the sand-to-cement ratio, the fly ash-to-cement ratio, the water-to-binder ratio, the fiber content, and the superplasticizer content was used. Major parameters that define (2) fiber properties are: the length, diameter, fiber, the fiber elastic modulus, and tensile strength, and the elastic modulus of fiber used.

Table 4.1. The statistical details of input parameters.

	Unit	***Range***	***Mean***	***Median***	***Mode***	***Standard Deviation***	***Sample Variance***	***Kurtosis***	***Skewness***
Cement	kg/m^3	190-1218	613.23	578.00	820.00	219.25	48070.70	-0.52	0.25

Fly ash	kg/m^3	109-1644.86	780.34	822.00	205.00	319.01	101765.17	0.49	-0.11
Water	kg/m^3	185-726.73	368.89	331.00	379.25	106.22	11282.53	3.10	1.80
Sand	kg/m^3	129-1237.67	518.75	474.40	656.00	154.81	23964.63	3.40	0.93
Super Plasticizer (HRWRA)	kg/m^3	0-156.18	14.87	5.52	0.00	29.86	891.62	12.34	3.58
Fibers Content	kg/m^3	6.41-48	22.88	26.00	26.00	7.51	56.47	0.71	-0.45
Length of Fibers	mm	8-13.0	10.76	12.00	12.00	1.86	3.44	-1.34	-0.79
Diameter of Fiber	µm	8-200	39.74	39.00	39.00	19.52	381.04	61.89	7.60
Nominal strength of Fiber	MPa	626-3000	1688.75	1620.00	1620.00	312.17	97447.03	8.39	2.33
Elastic modulus of Fiber	GPa	6-210	47.23	42.80	42.80	23.17	536.71	33.44	5.38

4.2.2.2. Data Normalization

The data set collected from the literature study is in raw form and the range of data is quite large. For example, cement content is in the range of 1 but another parameter like elastic modulus and diameter is in the hundred. So, the sensitivity of each parameter data normalization is important which ultimately affects the result. We keep data in the range of 0 to 1 following the data normalization technique used.

$$x* = \frac{x - x(\min)}{x(\min) - x(\max)}$$

where x(min) is the lowest value of the parameter, x(max) shows the highest value of the parameter x shows the original value of the input parameter and x* shows the normal value of the parameter.

4.2.2.3. Data Normalization

Hyperparametric tuning is the most important parameter while training the machine learning model. it is used to evaluate the optimal value of the parameters. In Artificial Neural Network (ANN) technique it corresponds to the number of hidden layers and neurons present and the learning rate. A repetitive process is used for optimal value by changing the weights of parameters. The parameters are selected to counter the overfitting and underfitting data.

4.2.2.4.Data Normalization

Performances evaluation is basically to test the accuracy of the model which relates the predicted

results (Ypre) and Actual results (Yactual). 4 basic parameters
(1) Mean absolute error (MAE),
(2) Root mean square error (RMSE),
(3) Coefficient of determination (R2) and
(4) Pearson correlation coefficient (R) are used for the performance evaluation of our model.

$$RMSE=\sqrt{\frac{1}{n}.\sum_{i=1}^{n}(Ypre-Yactual)^2}, \quad (2)$$

$$R=\frac{\sum_{i}^{n}=1(Ypre-\overline{Ypre}).(Yactual-\overline{Yactual})}{\sqrt{\sum_{i}^{n}=1(Ypre-\overline{Ypre})^2}.\sqrt{\sum_{i}^{n}=1(Yactual-\overline{Yactual})^2}} \quad (3)$$

$$R^2=\frac{\sum_{i}^{n}=1(Ypre-\overline{Ypre})}{\sum_{i}^{n}=1(Yactual-\overline{Yactual})} \quad (4)$$

4.2.3. Training Process

The machine learning model was trained using the optimal hyperparameters. Careful consideration was given to avoid both under-fitting and over-fitting of the model. The training process was carried out, and the performance of each model was evaluated separately using the training and testing datasets, following the parameters defined in next Section. The training approach is illustrated in Figure 4.3.

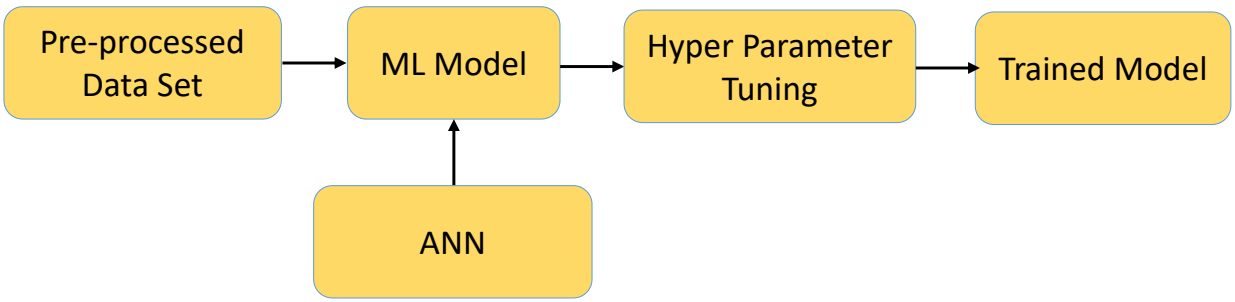

Figure 4.3. Training Process of predictive model.

4.3. Experimentation Methodology

4.3.1. ECC Designing

ECC is a composite that exhibits strain hardening under uniaxial tension. Initially, it was believed that strain hardening could only be achieved by increasing the fiber content. However, this option was not practical due to excessive cost and issues related to the workability of the mix. Later, it was found that fiber content is not the only parameter to achieve this behavior [59]; other essential parameters which could govern the behavior of FRC in tension could be matrix toughness, matrix tensile strength, fiber properties (elastic modulus, yield strength, aspect ratio,

etc.), and matrix- fiber interfacial properties (frictional bond, snubbing coefficient etc.) [4,60]. Many researchers have come up with their idea for finding out critical volume fraction (minimum volume of fibers needed for strain hardening) by comparing the above-mentioned properties. Some of the models that give critical volume fraction using different approaches are [61-66]

- An approach based on Composite mechanics
- Based on micro-mechanics of crack-bridging and fracture
- An approach based on fracture energy of debonding

4.3.2. Materials, mixture proportions and specimens preparations

The ingredients used in the production of ECC mixture included ordinary Portland cement (OPC), silica sand, fly ash (FA), water, polyvinyl alcohol (PVA), steel fibers and polycarboxylate based superplasticizer. The cement silica sand and fly ash used in this study were locally available and chemical composition of cement and fly ash is shown in table 4.3.The particle size of ingredients are shown in the table: The PVA fibers used in this study and their specifications are shown in Table 4.2.

The summary of mix proportion use in this study are listed in table 4.4. A mortar mixer with a rotating blade was used to mix the PVA-ECC. First, the solid ingredients (cement, fly ash, and sand) were thoroughly mixed for two minutes. In the meantime, the HRWR was mixed with the measured water to make a liquid solution. The HRWR solution was then gradually introduced into the mix. The fibres were slowly and manually added to achieve an even dispersion after the mixture became uniform and consistent. Finally, all the ingredients were thoroughly mixed for 5-10 minutes. When the mixing was finished, the fresh mixture was poured into greased moulds and vibrated for a few minutes. After casting, the specimens were covered with lids and demoulded 24 hours later. The specimens were then cured at a constant temperature of 25 degrees Celsius. At the age of 28 days, all the tests described in this paper were performed.

For the uniaxial compression test, three 150 mm x 150 mm x 150 mm cube specimens of each mix were cast. The uniaxial tension test was performed on six dog-bone specimens of each mix, each with a gauge length of 80 mm and a reduced section measuring 80 mm, 36 mm, and 20 mm in the middle.

Table 4.2 Fibers used in this study.

Properties of Fibres						
Type	length of fiber (mm)	Diameter of fiber (µm)	Density (kg/m^3)	Nominal Strength (Mpa)	Young's Modulus (Gpa)	Elongation (%)
PVA Fiber	12	39	1300	1620	43	6
Steel Fiber	13	200	7850	2500	210	8

Table 4.3. Chemical Composition of cement and fly ash.

Material	SiO2 (%)	Al2O3 (%)	Fe2O3 (%)	CaO (%)	MgO (%)	SO3 (%)	Na2O (%)	K2O (%)
Cement	18.11	3.07	3.03	65.88	1.87	3.37	0.47	0.19
Fly ash	49.98	25.32	5.31	5.92	1.51	0.62	0.83	0.89

Table 4.4. Mix proportion use in this study

Mix ID	Cement (kg/m^3)	Sand (kg/m^3)	Fly ash (kg/m^3)	Water (kg/m^3)	Superplasticizer (kg/m^3)	PVA fibers (kg/m^3)	Steel fibers (kg/m^3)
Mix1	572	456	686	332	7	26	0
Mix 2	447	456	763	332	7	26	0
Mix 3	412	456	824	326	6	26	0
Mix 4	572	440	686	332	4	0	157

4.3.3. Experimentation Setup

The experimental study, including the uniaxial tensile test and the compression test, are conducted in this present research. 6 Dog bone-shaped specimens and 3 cubes of each mix design were prepared as per the Japan Society of Civil Engineers (JSCE) and ASTM C-1273. The samples were cured for 28 days. The tension test was conducted using universal testing machine (UTM) with a loading rate of 0.3mm/min. In order to measure the elongation in the Dog bone samples the lateral faces were fixed with two double cantilever clips on gauges with gauge length 80mm. Casting of specimens is shown in Fig. 4.4 (a). The testing of dog bone and cubes are shown in Fig. 4.4 (b).

Figure 4.4. (a) Casting of Dog bone sample dimensions as per JSCE and cubes (b) Uniaxial tension testing setup and compressive testing .

4.4. Result and Discussions

4.4.1. Predicted Results (Compressive and Tensile stress strain curve)

Based on the above-mentioned input parameters and model specifications, the Elastic modulus, Peak compressive strength, and Bilinear Stress-strain curve can be predicted. Table no 4.5. shows the comparison between actual results and predicted results of defined output parameters. The prediction accuracy was measured in terms of the R-value. Its larger value indicates high prediction accuracy of the model, while in the case of RMSE value, a low value indicates high accuracy which is quite low in our model. Figure 4.5 illustrates comparison between predicted and actual tensile stress strain curve result using ANN model.

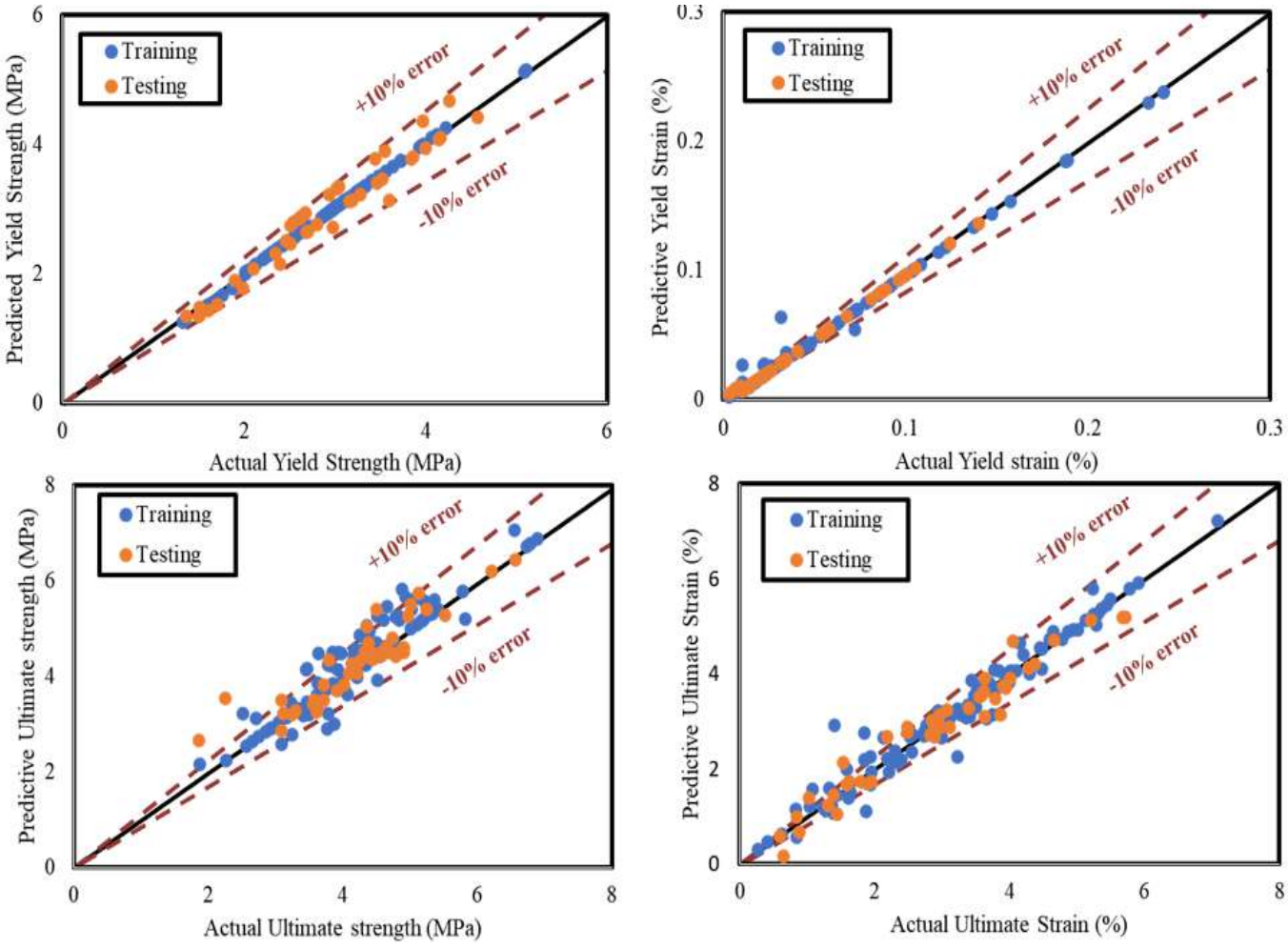

Figure 4.5 illustrates comparison between predicted and actual Elastic modulus and peak compressive stress strain result using ANN model.

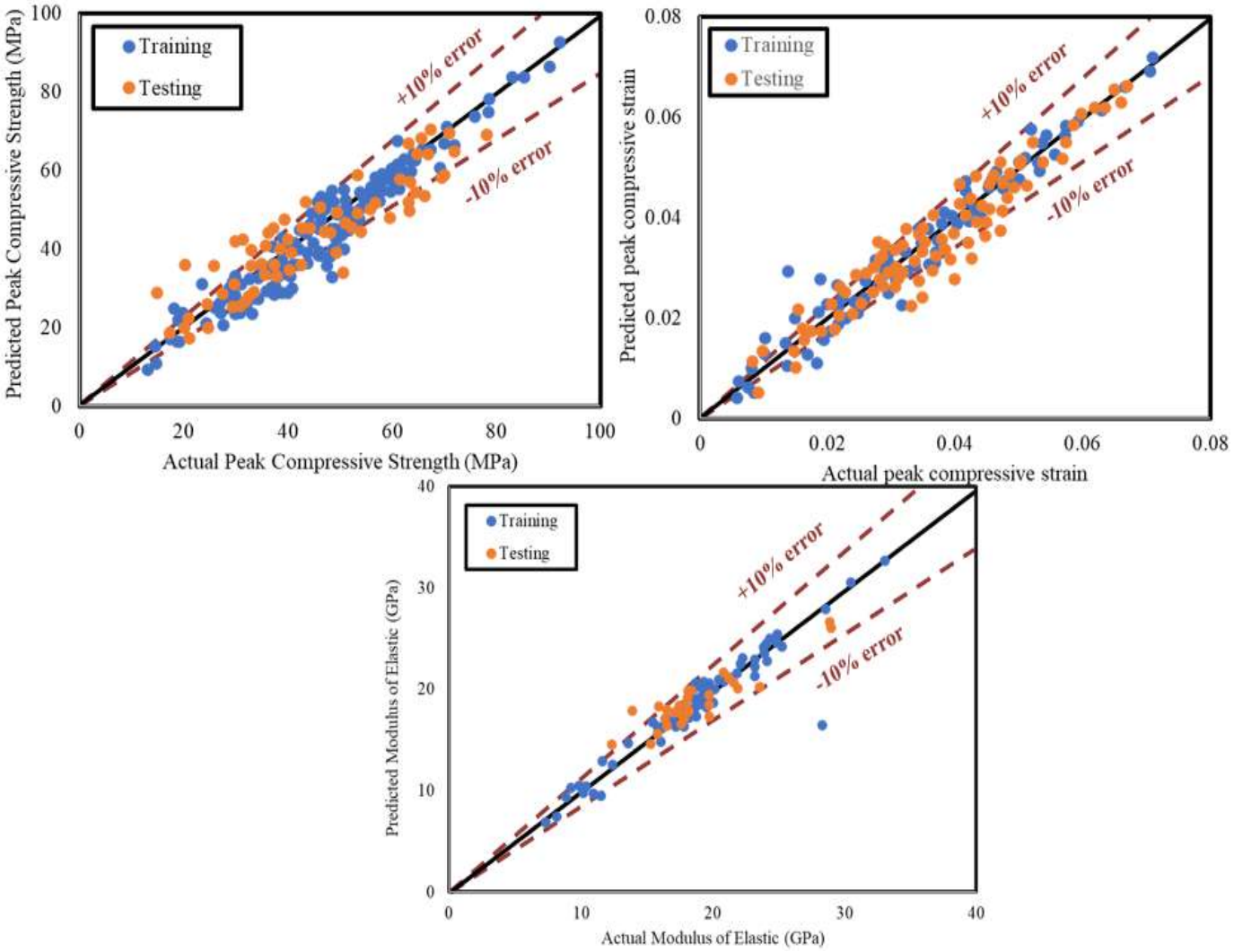

Figure 4.6. The actual vs predicted plots (a) peak compressive stress (b) peak compressive strain (c) Elastic Modulus.

The performance of the model using different statistical techniques is summarized in Table 4.5. The predicted and experimental results are compared to avoid underfitting and overfitting. Among all techniques Root mean square error technique give the more accurate result with the minimal error value of 0.004. The complete working process is discussed in figure 4.7.

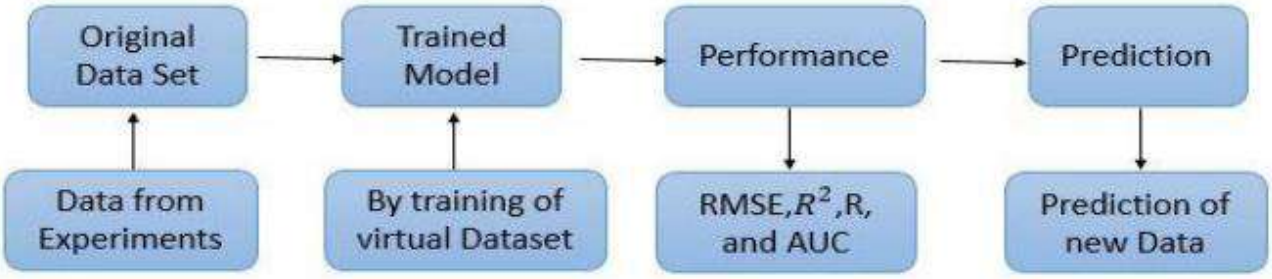

Figure 4.7. Working of predictive model

Table 4.5. Performance matrix of the predictive models

Set	Evaluation	Yield Strain	Yield Strength	Ultimate Strain	Ultimate Strength
Training	RMSE	0.002891213	0.041949141	0.299858336	0.366442867
	R2	0.997262609	0.999418716	0.95409944	0.962854906
	R	0.998625611	0.999709316	0.976780139	0.981251704
	MAE	0.002136898	0.036973608	0.195095418	0.239105176
Testing	RMSE	0.004844452	0.204988848	0.313352972	0.374143339
	R2	0.993670434	0.948956659	0.95089776	0.832592686
	R	0.996834538	0.974144065	0.975139867	0.91246517
	MAE	0.003818182	0.158527385	0.224998147	0.261403182

Set	Evaluation	Elastic Modulus	Peak Compressive Strength	Peak Compressive Strain
Training	RMSE	0.96	3.5	0.21
	R2	0.956	0.96	0.97
	R	0.99	0.98	0.99
	MAE	0.72	2.53	0.121
Testing	RMSE	2.08	5.77	0.95
	R2	0.899	0.899	0.887
	R	0.882	0.91	0.89
	MAE	1.5	4.32	0.65

4.4.2. Experimental Validation

It is clear from Table RMSE technique has the maximum accuracy with minimal error value compared to the other techniques. Thus, it was used to predict Peak compressive strength, Bilinear tensile strength, tensile strain, and elastic modulus (neither in original nor in virtual). The model was practiced for validation by published experiments' data. Samples are cast for 4 mixes of the model with varying input parameters of the model. Figure 4.8 and 4.9. shows the comparison of actual v/s predicted properties of Tensile and Compressive mixes respectively.

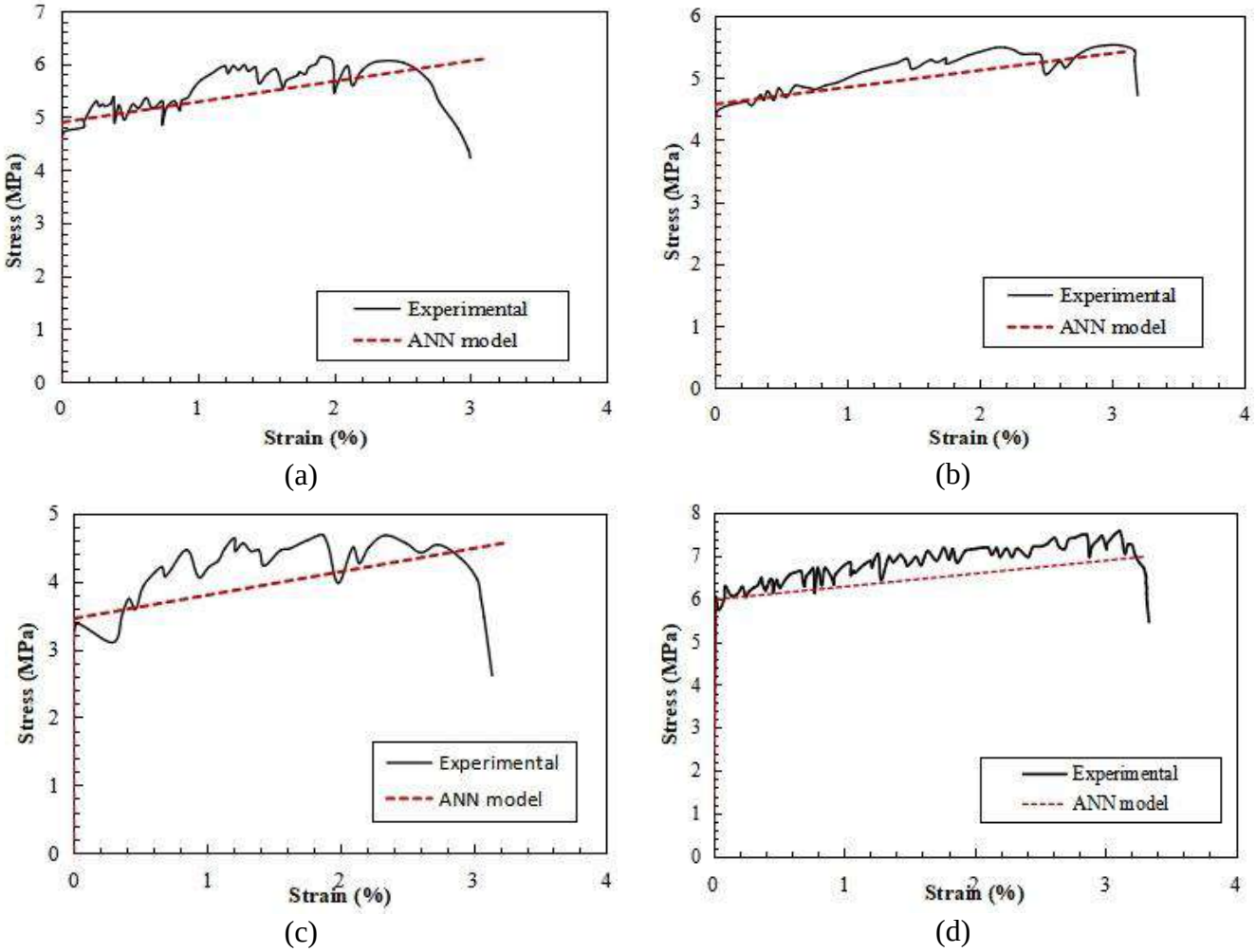

Figure 4.8. The experimental validation of the ANN model in terms of averaged tensile stress strain curve (a) for mix 1 (b) for mix 2 (c) for mix 3 (d) for mix 4.

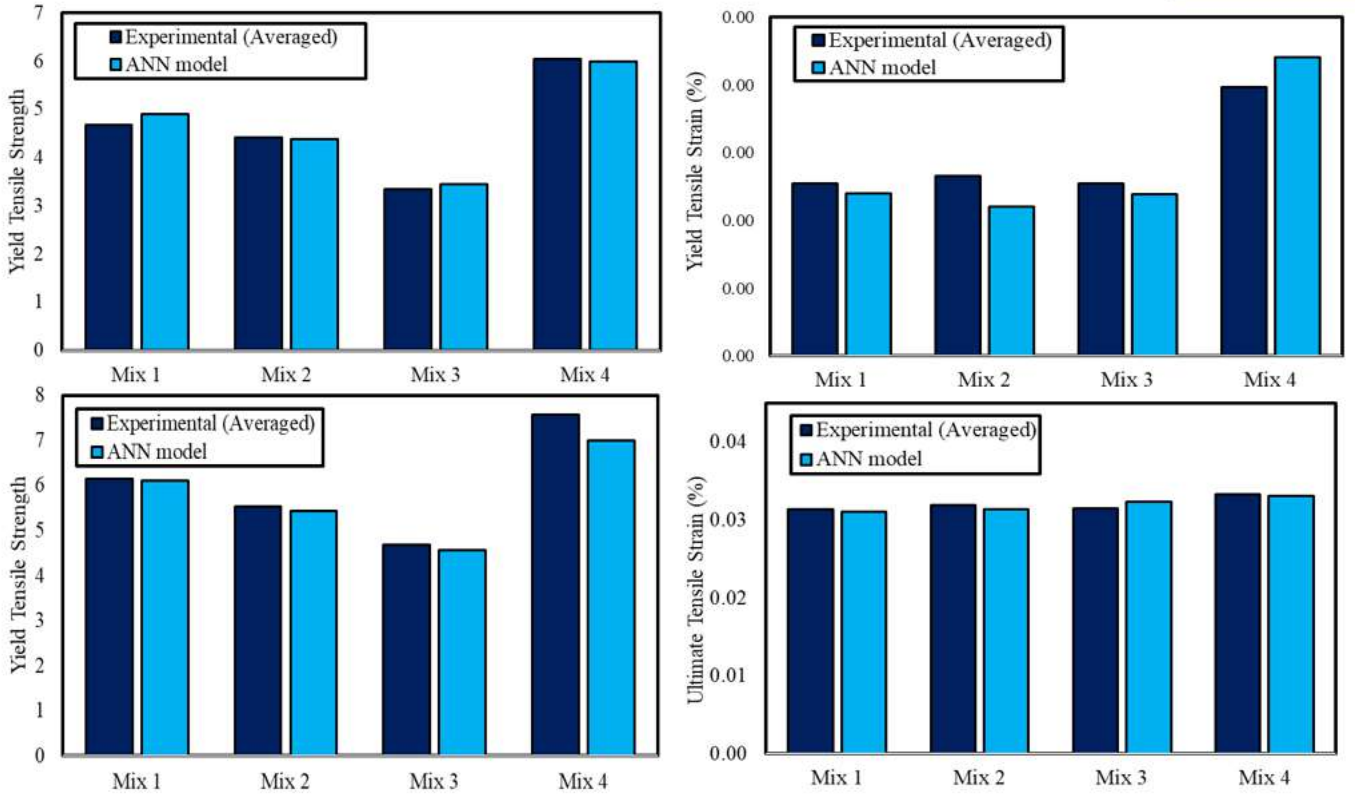

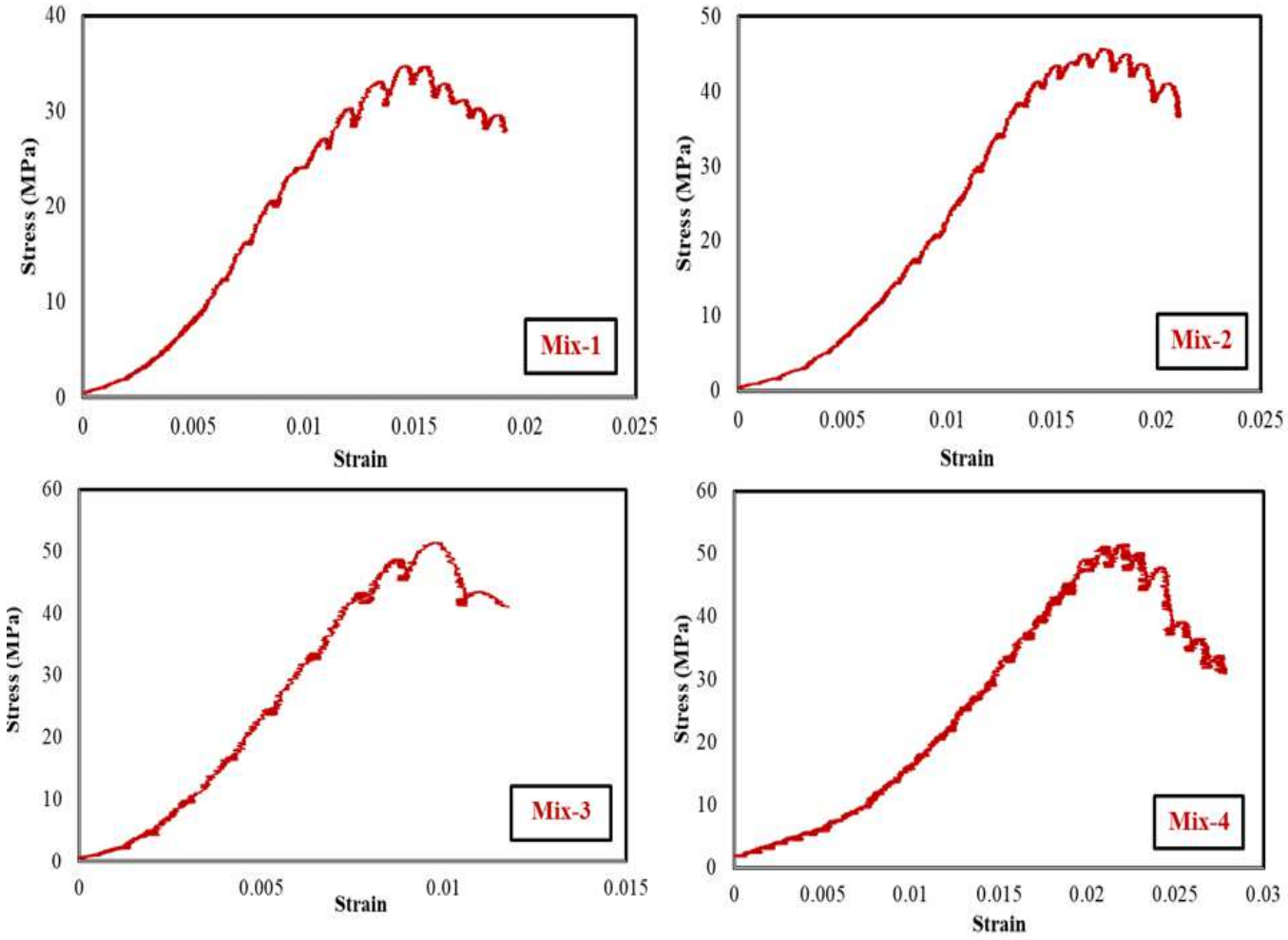

Figure 4.9. The experimental validation of the ANN model in terms of averaged compressive stress strain curve (a) for mix 1 (b) for mix 2 (c) for mix 3 (d) for mix 4.

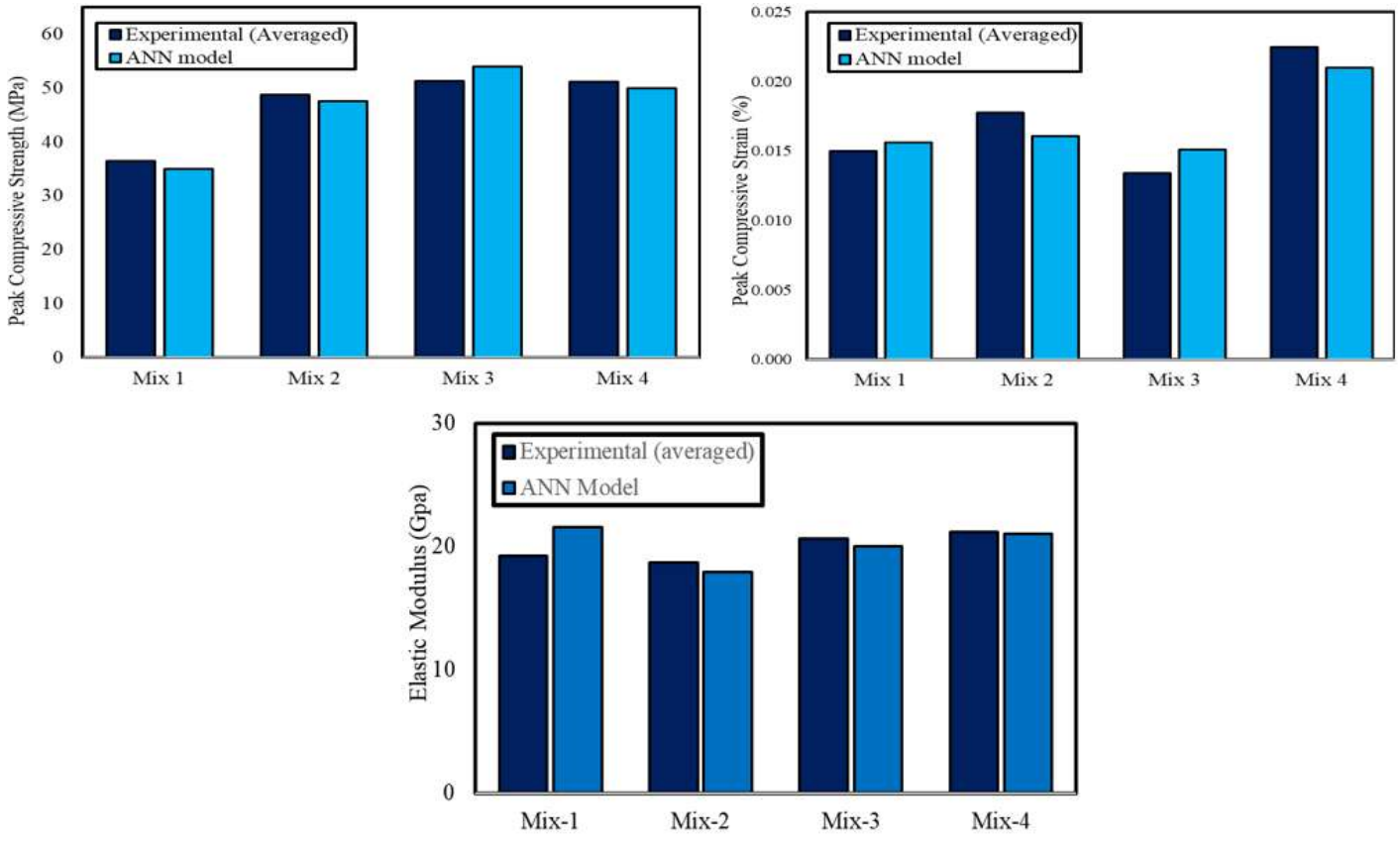

4.5. Conclusion and Recommendations

This study successfully introduced a novel approach for predicting fracture properties, including the tensile stress-strain curve, peak compressive stress-strain, and elastic modulus, of ECC through the utilization of machine learning techniques. Specifically, artificial neural network (ANN) models were developed to predict these properties based on 10 input parameters specific to engineered cementitious composite (ECC). The performance of each model was thoroughly evaluated, leading to the following conclusions:

- The developed predictive models exhibit a high level of accuracy, suggesting that they have the potential to replace the time-consuming and resource-intensive experimental trials typically required for optimizing engineering cementitious composite (ECC) according to specific needs and requirements.
- These models can be effectively used to predict fracture behavior as strain hardening or softening based on selected inputs as they are well trained for both types of behavior. ANN model shows 98.4% accuracy in segregating the fracture response of Engineering Cementitious Composite (ECC).
- These models can also be optimized in a way to make the mix economic with improved. mechanical properties along with minimizing the environmental impacts.

Future research is needed to find out other parameters and their dependence on different. important parameters of ECC and FRC, e.g., fresh properties, durability properties, use of other types of cement, or incorporating the packing density concept for high strength concrete. More research is also needed using these models for other types of special-purpose concretes.

References

[1] Romualdi, J.P.; Batson, G.B. Mechanics of Crack Arrest in Concrete. J. Eng. Mech. Div. 1963, 89, 147–168.

[2] Li, V.; Stang, H.; Krenchel, H. Micromechanics of crack bridging in fibre-reinforced concrete. Mater. Struct. 1993, 26, 486–494, doi:10.1007/BF02472808.

[3] Li, V.C.; Leung, C.K. Steady-state and Multiple Creaking of Short random fiber composites. J. Eng. Mech. 1992, 118, 2246–2264.

[4] Li, V.C. From micromechanics to structural engineering, The design of cementitious composites for civi for civil applications. Structrual Eng. Earthq. Eng. 1993, 10, 37s–48s.

[5] Li, V.C.; Mishra, D.K.; Wu, H.-C. Matrix Design for Pseudo Strain-Hardening Fiber Reinforced Cementitious Composites. Mater. Struct. 1995, 28, 586–595.

[6] Yang, C.C.; Mura, T.; Shah, S.P. Micromechanical Theory and Uniaxial Tensile Tests of Fiber Reinforced Cement Composites. 2015. Available online: http://journals.cambridge.org (accessed on 1 May 2021).

[7] McCartney, L. Mechanics of Matrix Cracking in Brittle-Matrix Fibre-Reinforced Composites. 1987. Available online: https://www.jstor.org/stable/2398127 (accessed on 1 May 2021).

[8] Leung, C.K. Design criteria for pseudoductile fiber-reinforced composites. J. Eng. Mech. 1996, 122, 10–18.

[9] Liu, H.; Zhang, Q.; Gu, C.; Su, H.; Li, V. Influence of microcrack self-healing behavior on the permeability of Engineered Cementitious Composites. Cem. Concr. Compos. 2017, 82, 14–22, doi:10.1016/j.cemconcomp.2017.04.004.

[10] Li, X.; Wang, J.; Bao, Y.; Chen, G. Cyclic behavior of damaged reinforced concrete columns repaired with highperformance fiber-reinforced cementitious composite. Eng. Struct. 2017, 136, 26–35, doi:10.1016/j.engstruct.2017.01.015.

[11] Fukuyama, H. Application of High Performance Fiber Reinforced Cementitious Composites for Damage Mitigation of Building Structures Case study on Damage Mitigation of RC Buildings with Soft First Story. J. Adv. Concr. Technol. 2006, 4, 35–44.

[12] Guo, P.; Meng, W.; Xu, M.; Li, V.; Bao, Y. Predicting Mechanical Properties of High-Performance FiberReinforced Cementitious Composites by Integrating Micromechanics and Machine Learning. Materials 2021, 14, 3143, doi:10.3390/ma14123143.

[13] Prasad, B.R.; Eskandari, H.; Reddy, B.V. Prediction of compressive strength of SCC and HPC with high volume fly ash using ANN. Constr. Build. Mater. 2009, 23, 117–128, doi:10.1016/j.conbuildmat.2008.01.014.

[14] Marani, A.; Jamali, A.; Nehdi, M.L. Predicting Ultra-High-Performance Concrete Compressive Strength Using Tabular Generative Adversarial Networks. Materials 2020, 13, 4757, doi:10.3390/ma13214757.

[15] Abu Yaman, M.; Elaty, M.A.; Taman, M. Predicting the ingredients of self compacting concrete using artificial neural network. Alex. Eng. J. 2017, 56, 523–532, doi:10.1016/j.aej.2017.04.007.

[16] Akande, K.O.; Owolabi, T.O.; Twaha, S.; Olatunji, S. Performance Comparison of SVM and ANN in Predicting Compressive Strength of Concrete. IOSR J. Comput. Eng. 2014, 16, 88–94.

[17] Dhanapal, J.; Jeyaprakash, S. Mechanical properties of mixed steel fiber reinforced concrete with the combination of micro and macro steel fibers. Struct. Concr. 2020, 21, 458–467, doi:10.1002/suco.201700219.

[18] Loh, Z.P.; Mo, K.H.; Tan, C.G.; Yeo, S.H. Mechanical characteristics and flexural behaviour of fibre-reinforced cementitious composite containing PVA and basalt fibres. Sadhana 2019, 44, 98, doi:10.1007/s12046-019-1072- 6S. 51

[19] Bagherzadeh, R.; Pakravan, H.; Sadeghi, A.-H.; Latifi, M.; Merati, A.A. An Investigation on Adding Polypropylene Fibers to Reinforce Lightweight Cement Composites (LWC). J. Eng. Fibers Fabr. 2012, 7, 1147.

[20] Abbass, A.; Abid, S.; Özakça, M. Experimental Investigation on the Effect of Steel Fibers on the Flexural Behavior and Ductility of High-Strength Concrete Hollow Beams. Adv. Civ. Eng. 2019, 2019, 245, doi:10.1155/2019/8390345.

[21] Wishwesh, K.; Anand, K.B. PVA Fiber-Fly Ash Cementitious Composite: Assessment of Mechanical Properties. 2017. Available online: http://iaeme.comhttp://iaeme.com (accessed on 5 june 2021).

[22] Lu, C. Mechanical Properties of Polypropylene Fiber Reinforced Concrete Pavement. Adv. Mater. Res. 2013, 739, 264–267, doi:10.4028/www.scientific.net/AMR.739.264.

[23] Liu, F.; Xu, K.; Ding, W.; Qiao, Y.; Wang, L. Microstructural characteristics and their impact on mechanical properties of steel-PVA fiber reinforced concrete. Cem. Concr. Compos. 2021, 123, 104196, doi:10.1016/j.cemconcomp.2021.104196.

[24] Zheng, Y.; Wu, X.; He, G.; Shang, Q.; Xu, J.; Sun, Y. Mechanical Properties of Steel Fiber-Reinforced Concrete by Vibratory Mixing Technology. Adv. Civ. Eng. 2018, 2018, 5715, doi:10.1155/2018/9025715.
[25] Babaie, R.; Abolfazli, M.; Fahimifar, A. Mechanical properties of steel and polymer fiber reinforced concrete. J. Mech. Behav. Mater. 2019, 28, 119–134, doi:10.1515/jmbm-2019-0014.
[26] Sustainable solutions in structural engineering and construction.
[27] Yao, Z.; Li, X.; Fu, C.; Xue, W. Mechanical Properties of Polypropylene Macrofiber-Reinforced Concrete. Adv. Mater. Sci. Eng. 2019, 2019, 214, doi:10.1155/2019/7590214.
[28] Singh, S.P. Investigation on the Strength and Flexural Toughness of Hybrid Fibre Reinforced Concrete. In Brittle Matrix Composites 9; Elsevier: Amsterdam, The Netherlands, 2009; pp. 91–100, doi:10.1533/9781845697754.91.
[29] Çavdar, A. A study on the effects of high temperature on mechanical properties of fiber reinforced cementitious composites. Compos. Part B Eng. 2012, 43, 2452–2463, doi:10.1016/j.compositesb.2011.10.005.
[30] Vafaei, D.; Hassanli, R.; Ma, X.; Duan, J.; Zhuge, Y. Sorptivity and mechanical properties of fiber-reinforced concrete made with seawater and dredged sea-sand. Constr. Build. Mater. 2021, 270, 121436, doi:10.1016/j.conbuildmat.2020.121436.
[31] Ede, A.N.; Ige, A.O. Optimal Polypropylene Fiber Content for Improved Compressive and Flexural Strength of Concrete. IOSR J. Mech. Civ. Eng. 2014, 11, 129–135.
[32] Zeyad, A.; Saba, A.M.; Shathly, A.B.; Alfaufy, T.H. Influence of steel fiber content on fresh and hardened properties of self-compacting concrete. AIP Conf. Proc. 2018, 2020, 20033, doi:10.1063/1.5062659.
[33] Thomas, J.; Ramaswamy, A. Mechanical Properties of Steel Fiber-Reinforced Concrete. J. Mater. Civ. Eng. 2007, 19, 385–392, doi:10.1061/ASCE0899-1561200719:5385.
[34] Leung, C.K.; Lai, R.; Lee, A.Y. Properties of wet-mixed fiber reinforced shotcrete and fiber reinforced concrete with similar composition. Cem. Concr. Res. 2005, 35, 788–795, doi:10.1016/j.cemconres.2004.05.033.
[35] Yao, W.; Li, J.; Wu, K. Mechanical properties of hybrid fiber-reinforced concrete at low fiber volume fraction. Cem. Concr. Res. 2003, 33, 27–30, doi:10.1016/S0008-8846(02)00913-4.
[36] Hajj, E.Y.; Sanders, D.H.; Weitzel, N.D. Development of Specifications for Engineered Cementitious Composites for Use in Bridge Deck Overlays. Cem. Concr. Res. 2016, 14, 456.
[37] Yu, J.; Wu, H.-L.; Leung, C.K. Feasibility of using ultrahigh-volume limestone-calcined clay blend to develop sustainable medium-strength Engineered Cementitious Composites (ECC). J. Clean. Prod. 2020, 262, 121343, doi:10.1016/j.jclepro.2020.121343.
[38] Li, M.; Li, V. High-Early-Strength ECC for Rapid Durable Repair-Material Properties. Available online:: https://www.researchgate.net/publication/280231620 (accessed on 5 june 2021).
[39] Ma, H.; Qian, S.; Zhang, Z.; Lin, Z.; Li, V.C. Tailoring Engineered Cementitious Composites with local ingredients. Constr. Build. Mater. 2015, 101, 584–595, doi:10.1016/j.conbuildmat.2015.10.146.
[40] Li, X.; Yang, X.; Ding, Z.; Du, X.; Wen, J. ECC Design Based on Uniform Design Test Method and Alternating Conditional Expectation. Math. Probl. Eng. 2019, 2019, 9575897, doi:10.1155/2019/9575897.
[41] Li, V.C. Engineered Cementitious Composites (ECC)-Material, Structural, and Durability Performance; Book Chapter in Concrete Construction Engineering Handbook, 2007. 52
[42] Huang, B.-T.; Weng, K.-F.; Zhu, J.-X.; Xiang, Y.; Dai, J.-G.; Li, V.C. Engineered/strain-hardening cementitious composites (ECC/SHCC) with an ultra-high compressive strength over 210 MPa. Compos. Commun. 2021, 26, 100775, doi:10.1016/j.coco.2021.100775.
[43] Yu, K.; Zhu, W.; Ding, Y.; Lu, Z.-D.; Yu, J.-T.; Xiao, J.-Z. Micro-str
[44] uctural and mechanical properties of ultra-high performance engineered cementitious composites (UHP-ECC) incorporation of recycled fine powder (RFP). Cem. Concr. Res. 2019, 124, 105813, doi:10.1016/j.cemconres.2019.105813.
[45] Ma, H.; Qian, S.; Li, V.C. Influence of fly ash type on mechanical properties and self-healing behavior of Engineered Cementitious Composite (ECC). Cem. Concr. Res. 2016, 11, 209, doi:10.21012/fc9.209. [46] Xu, M.; Clack, H.; Xia, T.; Bao, Y.; Wu, K.; Shi, H.; Li, V. Effect of TiO2 and fly ash on photocatalytic NOx abatement of engineered cementitious composites. Constr. Build. Mater. 2020, 236, 117559, doi:10.1016/j.conbuildmat.2019.117559.
[47] Xu, M.; Yu, J.; Zhou, J.; Bao, Y.; Li, V.C. Effect of curing relative humidity on mechanical properties of engineered

cementitious composites at multiple scales. Constr. Build. Mater. 2021, 284, 122834, doi:10.1016/j.conbuildmat.2021.122834.
[48] Yao, Q.; Li, Z.; Lu, C.; Peng, L.; Luo, Y.; Teng, X. Development of Engineered Cementitious Composites Using Sea Sand and Metakaolin. Front. Mater. 2021, 8, 1872, doi:10.3389/fmats.2021.711872.
[49] Yang, E.-H.; Li, V. Tailoring engineered cementitious composites for impact resistance. Cem. Concr. Res. 2012, 42, 1066–1071, doi:10.1016/j.cemconres.2012.04.006.
[50] Halvaei, M.; Jamshidi, M. The Effect of Nylon Fibers on Mechanical Properties of Engineered Cementitious Composites (ECCs) Preparation and Characterization of Chitosan/Sericin Nanoweb View Project Evaluating Piezoelectric Performance of PVDF Composite Nanofibers Pressure Sensor with Metal Nanoparticle View Project. 2013. Available online: https://www.researchgate.net/publication/262802066 (accessed on 5 June 2021).
[51] Bins, S.R.; Kumar, C.S.; Togi, S.; George, M. A Study of Engineered Cementitious Composites by Investigating its Compressive and Flexural Strength. Cem. Concr. Res. 2014, 11, 531950, doi:10.21203/rs.3.rs-531950/v1.
[52] Lin, J.-X.; Song, Y.; Xie, Z.-H.; Guo, Y.-C.; Yuan, B.; Zeng, J.-J.; Wei, X. Static and dynamic mechanical behavior of engineered cementitious composites with PP and PVA fibers. J. Build. Eng. 2020, 29, 101097, doi:10.1016/j.jobe.2019.101097.
[53] Rafiei, P.; Shokravi, H.; Mohammadyan-Yasouj, S.; Koloor, S.; Petrů, M. Temperature Impact on Engineered Cementitious Composite Containing Basalt Fibers. Appl. Sci. 2021, 11, 6848, doi:10.3390/app11156848.
[54] Sutrisno, W.; Komara, I.; Tambusay, A.; Suprobo, P. Beam-to-Column Connections for Medium-Rise Precast Reinforced Concrete SMRF with-L and-U Shaped Beam Reinforcement Anchored Outside The Panel View project Genetic Algorithm and SAP2000 View project Indra Komara Institut Teknologi Sepuluh Nopember Engineered Cementitious Compositeas An Innovative Durable Material: A Review. 2019. Available online: www.arpnjournals.com (accessed on 5 June 2021).
[55] Sherir, M.A.; Hossain, K.M.; Lachemi, M. Fresh state, mechanical & durability properties of strain hardening cementitious composite produced with locally available aggregates and high volume of fly ash. Constr. Build. Mater. 2018, 189, 253–264, doi:10.1016/j.conbuildmat.2018.08.204.
[56] Khan, S.W.; Shahzada, K.; Kamal, M.; Khan, S.W.; Alam, M. Experimental Investigation of the Mechanical Properties of Engineered Cementitious Composites (ECC) Intelligent Disaster Management in Pakistan View Project Improvement of Concrete Shielding to Nuclear Radiation using Barite View Project Experimental Investigation of the Mechanical Properties of Engineered Cementitious Composites (ECC). 2016. Available online: https://www.researchgate.net/publication/308694013 (accessed on 5 June 2021).
[57] Interface Tailoring for Strain-Hardening PVA-ECC. 2011. Available online: https://www.researchgate.net/publication/280224066 (accessed on 5 June 2021).
[58] Yu, K.; Wang, Y.; Yu, J.; Xu, S. A strain-hardening cementitious composites with the tensile capacity up to 8%. Constr. Build. Mater. 2017, 137, 410–419, doi:10.1016/j.conbuildmat.2017.01.060. 53
[59] Zhu, Y.; Zhang, Z.; Yang, Y.; Yao, Y. Measurement and correlation of ductility and compressive strength for engineered cementitious composites (ECC) produced by binary and ternary systems of binder materials: Fly ash, slag, silica fume and cement. Constr. Build. Mater. 2014, 68, 192–198, doi:10.1016/j.conbuildmat.2014.06.080.
[60] Wang, S., and Li, V. C. (2003). “Lightweight ECC.” Proc., HPFRCC, A. E. Naaman and H. W. Reinhardt, eds., RILEM, 379–390..
[61] Interface Tailoring for Strain-Hardening Polyvinyl Alcohol-Engineered Cementitious Composite (PVA-ECC). 2002. Available online: https://www.researchgate.net/publication/279938212 (accessed on 5 June 2021).
[62] Li, M.; Li, V. High-Early-Strength Engineered Cementitious Composites for Fast, Durable Concrete RepairMaterial Properties. Available online: https://www.researchgate.net/publication/298499593 (accessed on 5 June 2021).
[63] Li, V.C.; Wang, S.X.; Wu, C. Tensile strain-hardening behavior or polyvinyl alcohol engineered cementitious composite (PVA-ECC). Aci Mater. J. 2001, 14, 478.
[64] Li, V.; Lepech, M.D. General Design Assumptions for Engineered Cementitious Composites Measuring the Impact of Real-time Performance Feedback on Multi-Objective Conceptual Building Design Decisions View Project Protein Bound Concrete View Project. 2011. Available online: https://www.researchgate.net/publication/239553672 (accessed on 25 June 2021).

[65] Hossain, K.M.A.; Ranade, R.; Li, V. Influence of Aggregate Type and Size on Ductility and Mechanical Properties of Engineered Cementitious Composites. 2009. Available online: https://www.researchgate.net/publication/285773543 (accessed on 25 June 2021).
[66] Kanda, T.; Li, V. Effect of Fiber Strength and Fiber-Matrix Interface on Crack Bridging in Cement Composites. J. Eng. Mech. 1999, 125, 290–299, doi:10.1061/(asce)0733-9399(1999)125:3(290).
[67] Li, V.; Mishra, D.; Wu, H.-C. Matrix design for pseudo-strain-hardening fibre reinforced cementitious composites. Mater. Struct. 1995, 28, 586–595, doi:10.1007/BF02473191.
[68] Li, V.C.; Wu, C.; Wang, S.; Ogawa, A.; Saito, T. Interface Tailoring for Strain-Hardening Polyvinyl AlcoholEngineered Cementitious Composite (PVA-ECC). Aci Mater. J. 2019, 99, M47.
[69] Li, V.; Wu, H.C.; Maalej, M.; Mishra, D.K. Tensile Behavior of Engineered Cementitious Composites with Discontinuous Random Steel Fibers Biofuel Production by Pyrolysis of Biomass View Project Structural Characterization and Frictional Properties of Carbon Nanotube/Alumina Composites Prepared by Precursor Method View Project. Available online: https://www.researchgate.net/publication/233741819 (accessed on 25 June 2021).
[70] Qian, S.; Li, V. Elevating ECC Material Ductility to Structural Performance of Steel Anchoring to Concrete. 2011. Available online: https://www.researchgate.net/publication/267938800 (accessed on 25 June 2021).
[71] Flexural Behaviors of Glass Fiber-Reinforced Polymer (GFRP) Reinforced Engineered Cementitious Composite Beams. Available online: https://www.researchgate.net/publication/279577689 (accessed on 25 June 2021).
[72] General Design Assumptions for ECC. Available: https://www.researchgate.net/publication/268404234 (accessed on 25 June 2021). [73] Angadi, S.; Reddy, K.S.; Selvaprakash, S.; Prasad, J.S.R.; Venu, M. Experimental Studies on Structural Behaviour of Hybrid Fibre Reinforced Concrete. IOP Conf. Ser. Mater. Sci. Eng. 2018, 431, 42003, doi:10.1088/1757- 899X/431/4/042003.
[74] Qian, S.; Li, V.; Li, V.C.; Zhang, H.; Keoleian, G.A. Durable and Sustainable overlay with ECC. 2008. Available online: https://www.researchgate.net/publication/237135081 (accessed on 25 June 2021).
[75] Kanda, T.; Li, V.C. New Micromechanics Design Theory for Pseudostrain Hardening Cementitious Composite. J. Eng. Mech. 1999, 125, 373–381, doi:10.1061/(asce)0733-9399(1999)125:4(373).
[76] Li, V.; Mishra, D.; Naaman, A.E.; Wight, J.K.; LaFave, J.M.; Wu, H.-C.; Inada, Y. On the shear behavior of engineered cementitious composites. Adv. Cem. Based Mater. 1994, 1, 142–149, doi:10.1016/1065- 7355(94)90045-0.
[77] Ductile Engineered Cementitious Composite Elements for Seismic Structural Applications. 2000. Available online: https://www.researchgate.net/publication/228861959 (accessed on 18 july 2021). 54
[78] Li, M.; Li, V.C. Behavior of ECC/Concrete Layered Repair System Under Drying Shrinkage Conditions / Das Verhalten eines geschichteten Instandsetzungssystems aus ECC und Beton unter der Einwirkung von Trocknungsschwinden. Restor. Build. Monum. 2006, 12, 143–160.
[79] Yang, E.-H.; Yang, Y.; Li, V. Rheological Control in Production of Engineered Cementitious Composites. Available online: https://www.researchgate.net/publication/279541414 (accessed on 18 July 2021).
[80] Li, V. Development of Green ECC for Sustainable Infrastructure Systems Multi-Physics and Multi-Scale Modelling of Next Generation Sustainable Civil Infrastructure View Project Concrete Materials; Engineering Cementious Composites View Project Development of Green Ecc for Sustainable Infrastructure Systems. Available online: https://www.researchgate.net/publication/228998310 (accessed on 18 July 2021).
[81] A Study on Impact of Polypropylene (Recron 3S) Fibers on Compressive and Tensile Strength of Concrete. A Study on Impact of Polypropylene (Recron 3S) Fibers on Compressive and Tensile Strength of Concrete. IJIRSTInternational Journal for Innovative Research in Science & Technology. 2017. Available online: www.ijirst.org (accessed on 18 July 2021).
[82] Wu, F.; Xu, L.; Chi, Y.; Zeng, Y.; Deng, F.; Chen, Q. Compressive and flexural properties of ultra-high performance fiber-reinforced cementitious composite: The effect of coarse aggregate. Compos. Struct. 2020, 236, 111810, doi:10.1016/j.compstruct.2019.111810.
[83] Yang, E.-H.; Garcez, E.; Li, V.C. Development of pigmentable engineered cementitious composites for architectural elements through integrated structures and materials design. Mater. Struct. 2011, 45, 425–432, doi:10.1617/s11527-011-9774-1.
[84] Experimental Study on the M20 Grade Cement Concrete Containing Crimped Steel Fibres. 2016. Available online:

www.ijste.org (accessed on 18 July 2021).
[85] Zhou, J.; Qian, S.; Beltran, M.G.S.; Ye, G.; Van Breugel, K.; Li, V.C. Development of engineered cementitious composites with limestone powder and blast furnace slag. Mater. Struct. 2009, 43, 803–814, doi:10.1617/s11527- 009-9549-0.
[86] Eswari, S.; Raghunath, P.N.; Kothandaraman, S. Regression Modeling for Strength and Toughness Evaluation of Hybrid Fibre Reinforced Concrete. 2011. Available online: https://www.researchgate.net/publication/267785146 (accessed on 18 July 2021).
[87] Balanji, E.K.Z.; Sheikh, N.; Hadi, M.N.S.; Sheikh, M.N. Behaviour of High Strength Concrete Reinforced with Different Types of Steel Fibres Sea Sand and Seawater in Concrete View Project Rigid Pavements, Portland cement concrete, Geogrid View Project Behaviour of High Strength Concrete Reinforced with Different Types of Steel Fibres. Available online: https://www.researchgate.net/publication/311708009 (accessed on 18 July 2021).
[88] Ghugal, Y.M.; Sabale, V.; Ghugal, Y.M.; Sabale, V.D.; More, S.S. Experimental Investigation on High Strength Steel Fiber Reinforced Concrete with Metakaolin Stability of Plates and Shells View project Stability of Structures View Project Experimental Investigation on High Strength Steel Fiber Reinforced Concrete with Metakaolin. 2017. Available online: https://www.researchgate.net/publication/319184021 (accessed on 18 July 2021).
[89] Xu, M.; Bao, Y.; Wu, K.; Shi, H.; Guo, X.; Li, V.C. Multiscale investigation of tensile properties of a TiO2-doped Engineered Cementitious Composite. Constr. Build. Mater. 2019, 209, 485–491, doi:10.1016/j.conbuildmat.2019.03.112.
[90] Cheng, Z.; Yan, W.; Sui, Z.; Tang, J.; Yuan, C.; Chu, L.; Feng, H. Effect of Fiber Content on the Mechanical Properties of Engineered Cementitious Composites with Recycled Fine Aggregate from Clay Brick. Materials 2021, 14, 3272, doi:10.3390/ma14123272.
[91] Turk, K.; Nehdi, M.L. Coupled effects of limestone powder and high-volume fly ash on mechanical properties of ECC. Constr. Build. Mater. 2018, 164, 185–192, doi:10.1016/j.conbuildmat.2017.12.186.
[92] Ding, Y.; Yu, J.-T.; Yu, K.; Xu, S.-L. Basic mechanical properties of ultra-high ductility cementitious composites: From 40 MPa to 120 MPa. Compos. Struct. 2018, 185, 634–645, doi:10.1016/j.compstruct.2017.11.034.
[93] Yu, K.-Q.; Dai, J.-G.; Lu, Z.-D.; Poon, C.S. Rate-dependent tensile properties of ultra-high performance engineered cementitious composites (UHP-ECC). Cem. Concr. Compos. 2018, 93, 218–234, doi:10.1016/j.cemconcomp.2018.07.016. 55
[94] Chen, Z.; Li, J.; Yang, E.-H. Development of Ultra-Lightweight and High Strength Engineered Cementitious Composites. J. Compos. Sci. 2021, 5, 113, doi:10.3390/jcs5040113.
[95] Sun, M.; Chen, Y.; Zhu, J.; Sun, T.; Shui, Z.; Ling, G.; Zhong, H.; Zheng, Y. Effect of Modified Polyvinyl Alcohol Fibers on the Mechanical Behavior of Engineered Cementitious Composites. Materials 2018, 12, 37, doi:10.3390/ma12010037.
[96] Zhou, Y.; Xi, B.; Yu, K.; Sui, L.; Xing, F. Mechanical Properties of Hybrid Ultra-High Performance Engineered Cementitous Composites Incorporating Steel and Polyethylene Fibers. Mater. 2018, 11, 1448, doi:10.3390/ma11081448.
[97] Nanda, R.P.; Mohapatra, A.K.; Behera, B. Influence of metakaolin and Recron 3s fiber on mechanical properties of fly ash replaced concrete. Constr. Build. Mater. 2020, 263, 120949, doi:10.1016/j.conbuildmat.2020.120949.
[98] Said, S.; Razak, H.A. The effect of synthetic polyethylene fiber on the strain hardening behavior of engineered cementitious composite (ECC). Mater. Des. 2015, 86, 447–457, doi:10.1016/j.matdes.2015.07.125.
[99] Zhu, Y.; Yang, Y.; Yao, Y. Use of slag to improve mechanical properties of engineered cementitious composites (ECCs) with high volumes of fly ash. Constr. Build. Mater. 2012, 36, 1076–1081, doi:10.1016/j.conbuildmat.2012.04.031.
[100] Strength Characteristics of Glass Fiber Reinforced Concrete (GFRC) using Calcium Chloride Integral Curing Method. Int. J. Recent Technol. Eng. 2019, 8, 3040–3044, doi:10.35940/ijrte.B1392.0982S1119.

CHAPTER 5

MODULE 2

Experimental and Analytical evaluation of Section level Stiffness and proposed stiffness modifiers of Engineering Cementitious Composite (ECC).

Abstract

Engineering Cementitious Composites (ECC) have gained significant attention from researchers and practitioners in recent years due to their exceptional mechanical and fracture properties. This paper provides a comprehensive review of the stiffness characterization of ECC, aiming to present a thorough understanding of the material's behavior under different loading conditions. The study begins by introducing the fundamental properties and composition of ECC, emphasizing its unique microstructure comprising of short randomly distributed fibers within a cementitious matrix. In this section, the section scale stiffness is find out, where the flexural behavior of ECC members is analyzed. The study considers various cross-sectional shapes and sizes, as well as different fiber types and volume fractions. The results reveal that the effective stiffness of ECC members is significantly influenced by the fiber reinforcement and the cross-sectional geometry. This finding underscores the importance of considering these factors when developing stiffness modifiers for ECC. In conclusion, this study provides valuable insights into the flexural effective stiffness of ECC at various scales and proposes stiffness modifiers that are specifically tailored for this material. The findings contribute to a better understanding of the unique properties of ECC and their implications for structural design.

5.1 Introduction

Concrete is a hydraulic binder made of cement and different aggregates. It is a cement-based composite material that is composed of cement, water, and fine and coarse aggregate. Since the 20th century, constructions have evolved in a higher, larger, and deeper direction. Concrete is a versatile material that can be Widely used in building floors, walls, foundations, roads, bridges, and other structures. One of the main advantages of concrete is its durability and strength. It is ideal for building large structures as it can withstand weight and pressure. In addition, it is weather and corrosion-resistant, making it suitable for outdoor use. Another advantage of concrete is its low cost. It is generally cheaper than other building materials such as steel and wood, making it a popular choice for many construction projects.

Ordinary Cement concrete offers the advantages of high availability, low cost, and high strength, and it is widely used in construction, transportation, and water conservation. Despite the distinct benefits cement concrete has certain drawbacks, including poor tensile strength, brittleness, and low toughness. To overcome these properties a new material has been introduced into the concrete to attain maximum tensile and compressive strength which shaped it into a

ductile mode that leads to the development of high-performing concrete or fiber-reinforced concrete.

According to AC1 116R, Cement and Concrete Terminology, fiber-reinforced concrete (FRC) is simply concrete with a dispersion of randomly arranged fibers. The present era of fiber-reinforced concrete research and development commenced more than 30 years ago.

Engineered Cementitious Composite (ECC), a novel variety of fiber-reinforced cementitious composite, has just been discovered. Although having a strain capacity of 3–7%, ECC exhibits tensile strain-hardening behavior, and its usual fiber content is less than 2% by volume. By using micromechanical models to optimize the composite's microstructure and take into consideration the mechanical interactions between the fiber, matrix, and interface, extremely high ductility is made possible. For cementitious composites reinforced with randomly oriented short fibers, the micromechanics of tensile strain-hardening has been investigated in extreme detail. Guidelines for adjusting fiber, matrix, and interface to achieve strain-hardening with the least quantity of fibers are provided by the criteria for steady-state crack propagation required for composite strain-hardening behavior and the micromechanics of the relationship.

Following matrix initial breaking, the distinctive ECC strain hardening is accompanied by the sequential generation of several microcracks, and the tensile strain capacity is 300–500 times higher than that of conventional cement. It takes the development of numerous microcracks for a composite to have high tensile ductility. The crack width is still in the range of 50 to 80 micro-meters even at the maximum stress. This tiny crack width is self-controlled and independent of the rebar reinforcement ratio, regardless of whether the composite is employed in conjunction with traditional reinforcement or not.

The regulation of fracture width in conventional concrete and fiber-reinforced concrete (FRC) depends on steel reinforcement. ECC can improve structural durability as well as water tightness and other serviceability by suppressing fractures in the presence of significantly induced structural deformations. These characteristics make ECCs appropriate for a variety of civil engineering applications, in addition to their relative ease of manufacture, including self-consolidation casting and shotcreting. In conventional concrete, aggregates often make up a significant portion of the total volume and have a significant impact on a variety of material characteristics. The dimensional stability of cement-based materials may be thought of as consisting of a framework of cement paste with relatively substantial shrinkage movements restricted by aggregates. In addition to their function as an economical filler. However, the inclusion of coarse particles in a paste tends to make the fracture path more complex and create a hard matrix that delays crack initiation and stops steady-state flat-crack propagation in ECC, which reduces the tensile ductility of the material.

Paulay and Priestley examined a variety of variables that could affect the bending stiffness of RC elements and proposed average values. Mehanny et al. suggested straightforward methods for calculating the effective bending and shear stiffness coefficients of beams and columns while accounting for the level of axial load. Panagiotaki and Fardis proposed formulas to anticipate the effective elastic stiffness of broken RC elements for the yield and ultimate deformation capabilities of RC elements. For application in the design of buildings, for use in the

design of buildings, Kumar and Singh proposed two unique effective stiffness models for normal-strength and high-strength concrete members. Pan et al. explored the reduction factor and put forth various techniques to raise the stiffness prediction's precision. The effective stiffness of RC elements is determined using the cross-section properties and is expressed in seismic codes and guidelines as a percentage of their stiffness. To take effective stiffness into account, several approaches are offered.

The results of the analyses were compared to the effective section stiffness coefficients reported for RC members in various regulations. The moment-curvature connection can also be used to observe events such as how the section stiffness and strength change and the ductility state of the cross-section behavior. The section strength, flexural stiffness, and section ductility of structures can only be predicted via an inelastic analysis using the moment-curvature connection. Effective stiffness incorporates both the behavior of reinforced concrete components as predicted by moment-curvature analysis and the impact of cracking.

The element's cross-sectional behavior determines how reinforced concrete structural elements behave. The material employed in the section, the section's geometry, and the loads exerted on the section all affect how the section behaves. The nonlinear moment-curvature connection allows for the observation of reinforced concrete section behaviours such as stiffness, strength, and ductility. The ratio between the yield moment (My) and the yield curve ($\emptyset y$), accounting for the moment-curvature relationship, determines the effective section stiffness (EIe) of the cracked section in RC sections.

5.2 Experimental Methodology

5.2.1 Materials, mixture proportions and specimens' preparations

Polyvinyl alcohol (PVA) fibers are widely used in ECC mixes; however, steel and PE (polyethylene) fibers have also been utilized to obtain the desired characteristics for particular applications. PVA fibers are hydrophilic, creating a solid chemical connection between the matrix and the fibers.

Ordinary Portland cement (OPC), silica sand, fly ash (FA), water, polyvinyl alcohol (PVA), steel fibers, and a polycarboxylates-based superplasticizer were the components used to make the ECC mixture. The cement, silica sand, and fly ash employed in this investigation were readily available locally, and the table 5.1 below shows the chemical compositions of cement and fly ash. The fiber used in this study was polyvinyl alcohol (PVA) and its properties are shown in table 5.2.

Table 5.1. Chemical compositions of cement and fly ash

Material	SiO2 (%)	Al2O3 (%)	Fe2O3 (%)	CaO (%)	MgO (%)	SO3 (%)	Na2O (%)	K2O (%)
Cement	18.11	3.07	3.03	65.88	1.87	3.37	0.47	0.19
Fly ash	49.98	25.32	5.31	5.92	1.51	0.62	0.83	0.89

Table 5.2: Properties of PVA fibers

Length of fiber (mm)	**12**
Diameter of fiber (um)	39
Density (kg/m^3)	1300
Nominal Strength (Mpa)	1620
Young's Modulus (Gpa)	43
Elongation (%)	6

5.2.2 Specimens' preparations

The PVA-ECC was blended using a rotating blade mortar mixer. The first step was to properly mix the solid elements (cement, fly ash, and sand) for two minutes. The measured water was combined with the HRWR to create a liquid solution in the interim. The HRWR solution was then progressively added to the mixture. After the mixture had become equal and consistent, the fibers were gradually and manually added to produce an even dispersion of the mixture. All the ingredients were then carefully blended for 5 to 10 minutes. ECC was directly put into the beam moulds when the mixing process was complete, and it was then vibrated. Layered pouring method was used to create ECC beams, in which ECC was poured into the mould first and vibrated and then ECC was poured again and vibrated. After 24 hours, the beams were demoulded. At a steady temperature of 25 degrees Celsius, the beams were then cured for 28 days. Figure 5.1 shows the casting of beams.

Figure 5.1 shows the casting of beams.

5.2.3 Mix proportions

A total of 12 reinforced ECC-concrete composite beams were cast and tested. The main parameters studied were the length of beams, cross-section of beams, amount of reinforcement and different mix designs of ECC to investigate the effective section stiffness. Three groups of beams were created based on different mix designs. Each group contained a number of specimens with various beam lengths, beam cross sections, and reinforcement levels as shown in Table 5.3 (a) and Tables 5.3 (b) illustrate the columns details. A summary of the mix proportions used in this investigation is shown in Table 5.4. For compressive strength, three (100mm x 100mm x 100mm) cube specimens of each mix design were tested as per standard ASTM C39. Three dog bones of each mix design were prepared and then tested to find the tensile strength of ECC. The mechanical properties of steel reinforcements like yield strength, ultimate strength and elastic modulus were obtained from testing 3 samples of each grade as per standard ASTM A370.

Table 5.3 (a) Beams Details

Compressive Strength	Cross Section	Reinforcement Ratio	Area required	Steel Provided
35 MPA	6x6x48	1%	0.36	1#2 , 3#3
		1.25%	0.45	1#2 , 4#3
		1.5%	0.54	5#3
	6x5x48	1%	0.30	3#3
		1.25%	0.38	3#2 , 2#3
		1.5%	0.45	2#2 , 3#3
	7.5x8x108	1%	0.60	2#3 , 2#4
		1.25%	0.75	4#4
		1.5%	0.90	5#4
45 MPA	6x6x48	1%	0.36	1#2 , 3#3
		1.25%	0.45	1#2 , 4#3
		1.5%	0.54	5#3
	6x5x48	1%	0.30	3#3
		1.25%	0.38	3#2 , 2#3
		1.5%	0.45	2#2 , 3#3
	7.5x8x108	1%	0.60	2#3 , 2#4
		1.25%	0.75	4#4
		1.5%	0.90	5#4
55 MPA	6x6x48	1%	0.36	1#2 , 3#3
		1.25%	0.45	1#2 , 4#3
		1.5%	0.54	5#3
	6x5x48	1%	0.30	3#3
		1.25%	0.38	3#2 , 2#3
		1.5%	0.45	2#2 , 3#3
	7.5x8x108	1%	0.60	2#3 , 2#4
		1.25%	0.75	4#4
		1.5%	0.90	5#4
	7.5X8X96	1.25%	0.75	1#3 , 2#5

Table 5.3 (b) Column details

Mix design	Column ID	b x h (mm x mm)	Length H (mm)	Reinforcement Ratio	Steel Provided
Mix-1 35MPa	C-1	300 x 300	1092	1.5 %	12#4
	C-2	500 x 500	2070	1.5 %	20#5
	C-3	700 x 700	2798	1.5 %	24#6
Mix-2 45 MPa	C-1	300 x 300	1092	1.5 %	12#4
	C-2	500 x 500	2070	1.5 %	20#5
	C-3	700 x 700	2798	1.5 %	24#6
Mix-3 55 MPa	C-1	300 x 300	1092	1.5 %	12#4
	C-2	500 x 500	2070	1.5 %	20#5
	C-3	700 x 700	2798	1.5 %	24#6

Table 5.4 Mix proportion used for casting.

Mix ID	Cement (Kg/m^3)	Sand (Kg/m^3)	Fly ash (Kg/m^3)	Water (Kg/m^3)	Superplasticizer (Kg/m^3)	PVA Fiber (Kg/m^3)
Mix 1	572	456	686	332	7	26
Mix 2	447	456	763	332	7	26
Mix 3	412	456	824	326	6	26

Table-5.5 Mechanical Properties of Steel Bars.

Diameter	Specimen	Yield Strength		Ultimate Strength		Elastic Modulus	
		fy (Mpa)	μ (Mpa)	fu (Mpa)	μ (Mpa)	E (Mpa)	μ (Mpa)
φ2 (6.35mm)	1	51.415	52.189	4.575	4.158	4.575	4.158
	2	55.234		3.875		3.875	
	3	49.917		4.023		4.023	
φ3 (9.525mm)	1	50.897	48.632	4.484	4.340	4.575	4.158
	2	49.25		4.515		3.875	
	3	45.748		4.022		4.023	
φ5 (15.875mm)	1	35.422	32.816	4.178	4.012	4.575	4.158
	2	30.649		3.881		3.875	
	3	32.378		3.976		4.023	

5.2.4 Testing procedure

Strain gauges were installed on the surface of the beams and columns at predetermined locations to measure the strain distribution along the length of the specimens during testing. The strain gauges were connected to a data acquisition system to record the strain data in real time. The beams were subjected to three-point bending tests to obtain the moment-curvature relationship. The test setup consisted of a loading frame, hydraulic actuator, and load cell to apply and measure the applied load. The load was applied incrementally, and the corresponding strains were recorded at each load step. Figure 5.2 shows the experimental setup for flexural of beams.

Figure 5.2. Flexural Testing of beams.

The columns were subjected to axial compression tests to obtain the axial load-strain relationship. The test setup consisted of a loading frame, hydraulic actuator, and load cell to apply and measure the applied axial load. The load was applied incrementally, and the corresponding strains were recorded at each load step.

5.3 Analytical Methodology

Moment curvature analysis is a method used in structural engineering to determine the behavior of a structure under load. It involves plotting the moment and curvature of a beam or column as it is subjected to increasing levels of load. The resulting curve, known as the moment-curvature curve, provides valuable information about the strength and stiffness of the structure.

To perform moment-curvature analysis in Abaqus, we will need to create a 3D model of the beam or column. This can be done using the Abaqus/CAE graphical user interface, which allows us to create and modify models using a variety of tools and features.

Once we have created the model, we will need to define the material properties of the concrete. This includes the modulus of elasticity, Poisson's ratio, and the yield strength. These properties can be entered into Abaqus using the Material Editor, which allows us to define and modify material properties for use in our model. Next, we will need to define the cross-sectional properties of the beam or column. This includes the area, moment of inertia, and section modulus. These properties can be entered into Abaqus using the Section Editor, which allows us to define and modify cross-sectional properties for use in our model.

After defining the material and cross-sectional properties, we will need to apply the appropriate boundary conditions to the model. This includes fixed or pinned supports, which can be applied using the Constraints tool in Abaqus/CAE. Once the model is set up, we can define the load cases for the model. This includes the magnitude and direction of the applied loads, which can be entered into Abaqus using the Load Editor. We can also define the load steps for the analysis, which determine how the load is applied to the model over time. With the model set up and the load cases defined, we can run the analysis to obtain the moment curvature curves for the beam or column. This can be done using the Abaqus/Standard solver, which is a finite element analysis program that can simulate the behavior of complex structures under load.

After running the analysis, we can use the moment curvature curves to calculate the Flexural Effective Stiffness of the beam or column. This involves determining the slope of the moment curvature curve at various points along the curve, which provides information about the stiffness of the structure. It's important to note that the process of performing moment curvature analysis in Abaqus can be complex and requires a good understanding of the software and the principles of structural analysis. In conclusion, moment curvature analysis is a powerful tool used in structural engineering to determine the behavior of a structure under load. By plotting the moment and curvature of a beam or column as it is subjected to increasing levels of load, engineers can gain valuable insights into the strength and stiffness of the structure. Abaqus provides a powerful platform for performing moment curvature analysis, allowing engineers to create and modify models, define material and cross-sectional properties, apply boundary conditions and loads, and run the analysis to obtain moment curvature curves and calculate Flexural Effective Stiffness.

5.1 Result and Discussion

5.4.1 Moment curvature curves of beams

The moment-curvature relationship for the beams was obtained by plotting the applied moment

(calculated from the applied load and the span length) against the curvature (calculated as the difference in strain between the top and bottom fibers divided by the depth of the section). The moment-curvature curve was used to determine the flexural stiffness of the ECC beams. Figure 5.3 shows the moment-curvature curves of different beams.

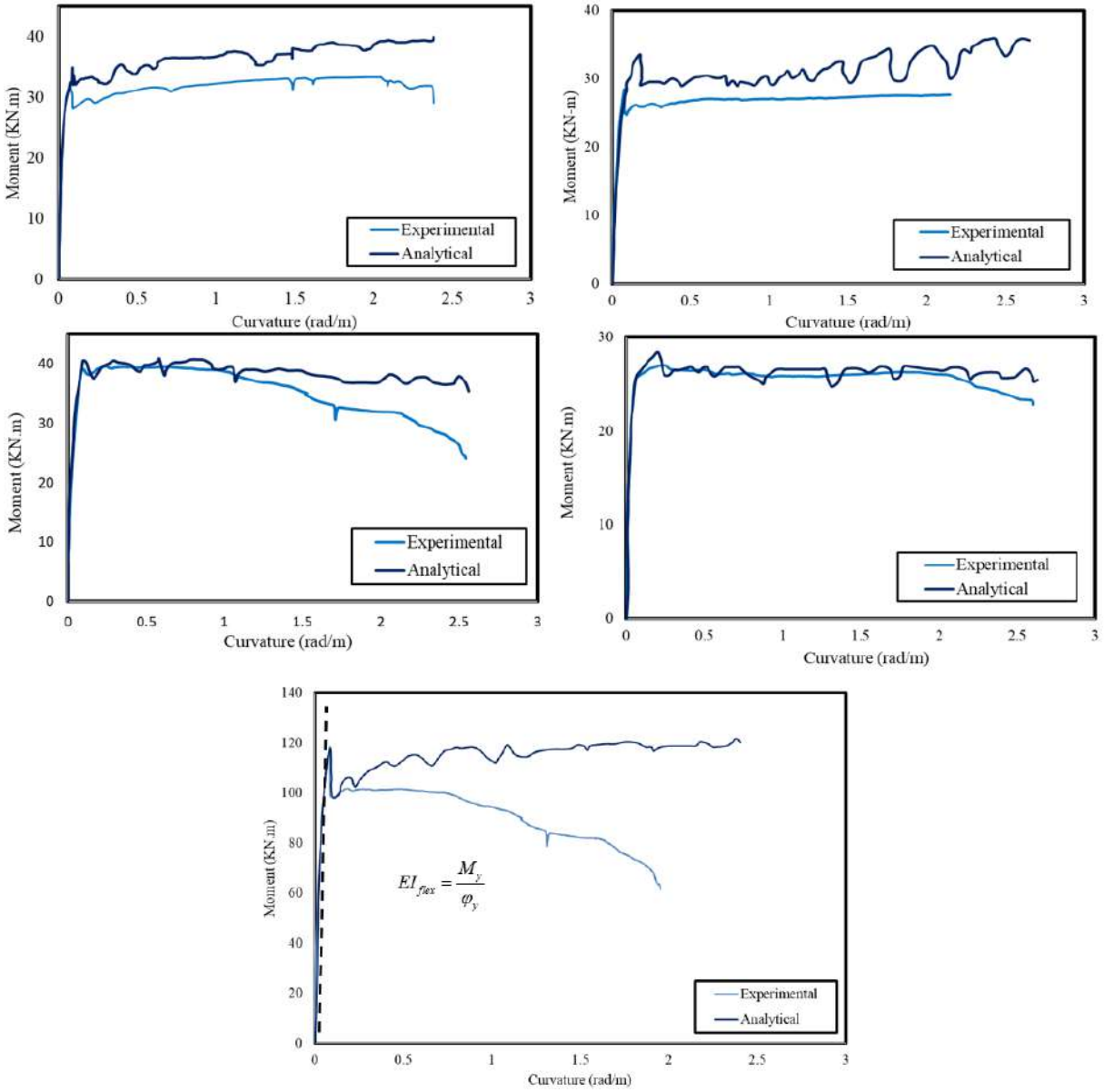

Figure 5.3 Beams Moment Curvature Curve.

5.4.2 Moment curvature curves of columns

The axial load-strain relationship for the columns was obtained by plotting the applied axial load against the average axial strain (calculated from the strain gauges installed on the column surface). The axial load-strain curve was used to determine the axial stiffness of the ECC columns. Figure 5.4 shows moment-curvature curves of different columns.

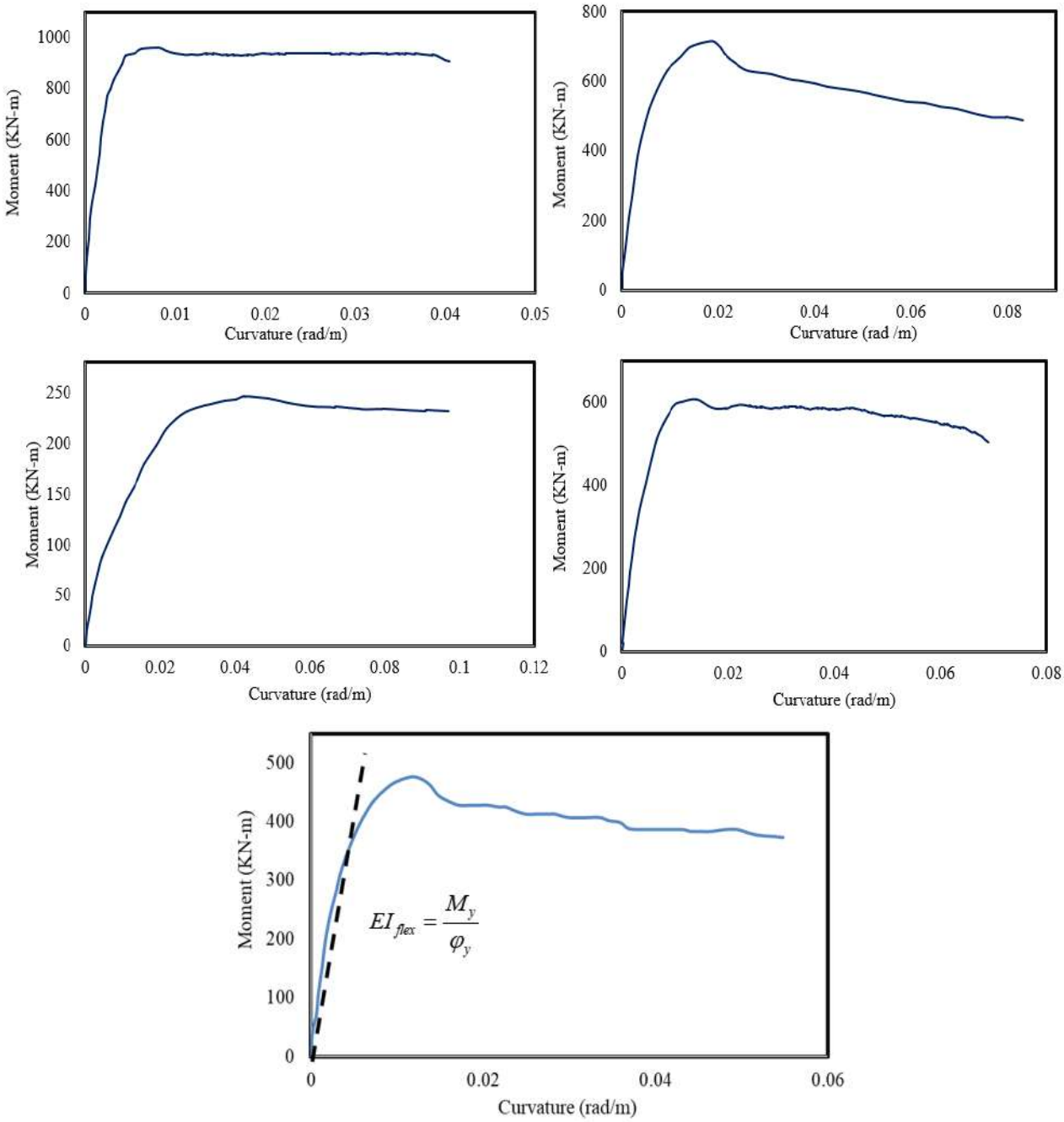

Figure 5.4 shows moment-curvature curves of different columns.

5.4.3 Stiffness modifiers of Beams

Stiffness modifiers were calculated based on the moment-curvature and axial load-strain relationships. These modifiers were used to adjust the theoretical stiffness values obtained from the material properties and section geometry to account for the actual behavior of the ECC specimens under load. The theoretical flexural stiffness (EI) of the ECC beams was calculated using the following formula:

$$EI = E * I$$

where E is the elastic modulus of the ECC material, and I is the moment of inertia of the beam section.

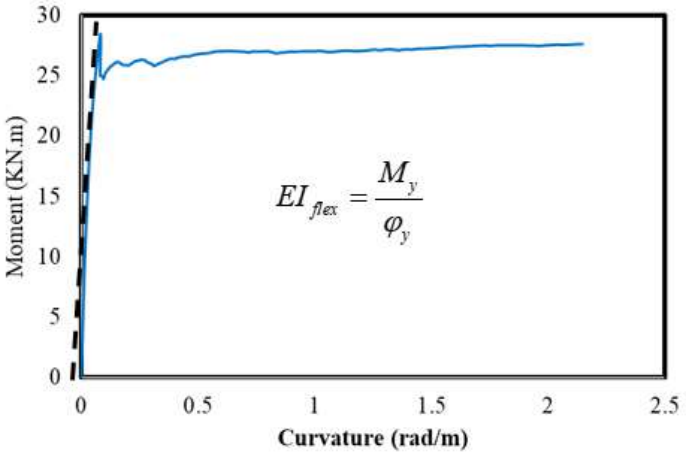

Elastic Modulus(E)=19.27 GPa

Moment of Inertia:

$$I_g = \frac{1}{12} \times (0.127) \times (0.1524)^3 = 3.746 \times 10^{-5} m^4$$

Slope of the Curve:

$$\frac{M}{\varphi} = \frac{28.395 \times 1000}{0.081} = 350555.556$$

Stiffness Modifier is given as:

$$SM = \frac{350555.556}{19.27 \times 10^9 \times 3.746 \times 10^{-5}} = \mathbf{0.467}$$

Table 5.6 Stiffness modifiers of beams.

Beam ID	Analytical	Experimental
B-1	0.4731	0.531
B-2	0.4187	-
B-3	0.52322	0.443
B-4	0.49112	0.4718
B-5	0.4601	0.407
B-6	0.467	0.467
B-7	0.421	0.529
B-8	0.394	0.471
B-9	0.482	0.402
B-10	0.419	-
B-11	0.527	0.5
B-12	0.492	0.47

Mean	0.4754
Standard Deviation	0.046911

5.4.4 Stiffness modifiers of columns

Stiffness modifiers were calculated based on the moment-curvature and axial load-strain relationships. These modifiers were used to adjust the theoretical stiffness values obtained from the material properties and section geometry to account for the actual behavior of the ECC specimens under load. The theoretical axial stiffness (EA) of the ECC columns was calculated using the

following formula:

$$EA = E * A$$

where E is the elastic modulus of the ECC material, and A is the cross-sectional area of the column.

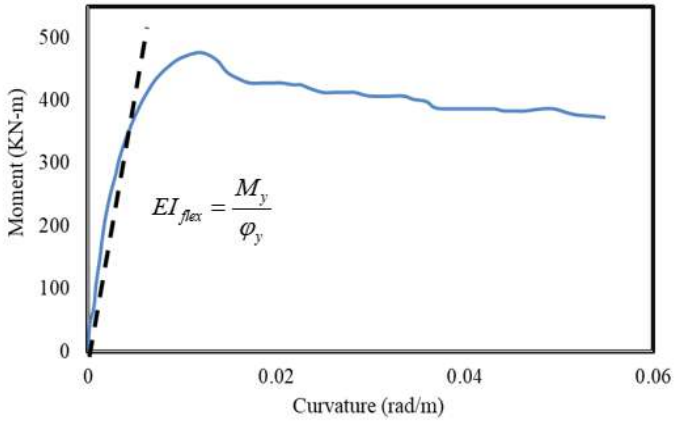

Elastic Modulus(E) =19.27 GPa

Moment of Inertia:

$$I_g = \frac{1}{12}(0.5)(0.5)^3 = 5.2083 \times 10^{-3}$$

Slope of the Curve:

$$\frac{M}{\varphi} = \frac{339.67603 \times 1000}{0.004022064} = 84453164.89$$

Stiffness Modifier is given as:

$$SM = \frac{84453164.89}{5.2083 \times 10^{-3} \times 19.27 \times 10^{9}} = \mathbf{0.841}$$

Table 5.5 Stiffness modifiers of beams.

Mix design	Column ID	Stiffness Modifiers
	C-1	0.863
Mix-1	C-2	0.881
	C-3	0.789
	C-4	0.793
Mix-2	C-5	0.761
	C-6	0.732
	C-7	0.841
Mix-3	C-8	0.843
	C-9	0.799

Mean	0.8093
Standard Deviation	0.0480

5.5. Conclusions and Recommendations

In this module we presents a detailed methodology for calculating the flexure effective stiffness of Engineered Cementitious Composites (ECC) based on experimental and analytical data obtained from beam and column tests. The methodology includes specimen preparation, instrumentation,

testing procedures, data analysis, and calculation of flexure effective stiffness values. By incorporating stiffness modifiers derived from moment-curvature and axial load-strain relationships, this method accounts for the actual behavior of ECC specimens under load, resulting in more accurate stiffness values for use in structural design and analysis.

- Beams stiffness modifiers are calculated from moment curvature curves which are 0.47 I_g and ECC beams stiffness modifiers are much higher than RCC.

- Columns stiffness modifiers are calculated from moment curvature curves which are 0.80 I_g and ECC columns stiffness modifiers are much higher than RCC.

Future research can investigate the effect of different fiber types and volume fractions on the flexure-effective stiffness of ECC materials. This will help identify the optimal fiber type and volume fraction for achieving the desired stiffness and performance characteristics in ECC structures. Further studies can be conducted to evaluate the long-term behavior and durability of ECC materials under various environmental conditions and loading scenarios. This will provide valuable information on the performance and service life of ECC structures, which can be used to inform maintenance and repair strategies.

References

[1] Bentur, A., Mindess, S.: Fibre Reinforced Cementitious Composites, 2nd edn. E & FN Spon,London (2007)
[2] Li, V.C., Wang, S., Wu, C.: Tensile strain-hardening behavior or polyvinyl alcohol engineered cementitious composite (PVA ECC). ACI Mater. J. 98(6), 483–492 (2001)
[3] Li, V.C.: On engineered cementitious composites (ECC). A review of the material and its applications. J. Adv. Concr. Technol. 1(3), 215–230 (2003)
[4] Li, V.C.: From micromechanics to structural engineering – the design of cementitious composites for civil engineering applications. JSCE J. Struct. Mech. Earthq. Eng. 10(I-24), 37s–48s(1993)
[5] V.C. Li, H.-C. Wu, Conditions for pseudo strain-hardening in fiber reinforced brittle matrix composites, Appl. Mech. Rev. 45 (1992) 390–398.
[6] V.C. Li, On engineered cementitious composites (ECC), J. Adv. Concr. Technol. 1 (2003) 215–230.
[7] T.A. Boden, R.J. Andres, G. Marland, Global, Regional, and National Fossil-Fuel CO2 Emissions, Carbon Dioxide Information Analysis Center, Oak Ridge National Laboratory, U.S. Department of Energy, Oak Ridge, Tenn., USA, 2017. Available at: https://cdiac.ess-dive.lbl.gov/trends/emis/meth_reg.html.
[8] S. H. Teh, T. Wiedmann, A. Castel, and J. de Burgh, "Hybrid life cycle assessment of greenhouse gas emissions from cement, concrete and geopolymer concrete in Australia," *J. Clean. Prod.*, vol. 152, pp. 312–320, 2017, doi: 10.1016/j.jclepro.2017.03.122.
[9] A. Akbarnezhad, M. Huan, S. Mesgari, and A. Castel, "Recycling of geopolymer concrete," *Constr. Build. Mater.*, vol. 101, pp. 152–158, 2015, doi: 10.1016/j.conbuildmat.2015.10.037.
[10] Hendriks, C. A., Worrell, E., Jager, D. De, Blok, K., & Riemer, P. (2004) (n.d.). Emission Reduction of Greenhouse Gases from the Cement Industry, 1–11.
[11] Ali, M. B., Saidur, R., & Hossain, M. S. (2011). A review on emission analysis in cement industries. Renewable and Sustainable Energy Reviews, 15(5), 2252–2261. https://doi.org/10.1016/j.rser.2011.02.014
[12] A.M. Rashad, Metakaolin as cementitious material: history, scours, production and composition–A comprehensive overview, Construct. Build. Mater. 41 (2013) 303–318.
[13] A. Tafraoui, G. Escadeillas, T. Vidal, Durability of the ultra high performances concrete containing metakaolin, Construct. Build. Mater. 112 (2016) 980–987.
[14] K. Scrivener, F. Martirena, S. Bishnoi, S. Maity, Calcined clay limestone cements (LC3), Cement Concr. Res. 114 (2018) 49–56.
[15] R. Fernandez, F. Martirena, K.L. Scrivener, The origin of the pozzolanic activity of calcined clay minerals: a comparison between kaolinite, illite and montmorillonite, Cement Concr. Res. 41 (1) (2011) 113–122.
[16] D.Zhang, B.Jaworska, H.Zhu, K.Dahlquist,V.C.Li, "Engineered Cementitious Composites (ECC) with limestone calcined clay cement (LC3)" Cem. Conc. Comp., doi: https://doi.org/10.1016/j.cemconcomp.2020.103766
[17] M. J.M. Canut, S. Miller, Calcined clay: process impact on the reactivity and color, in: S. Bishnoi (Ed.), Calcined Clays for Sustainable Concrete. RILEM Bookseries, Springer, 2020.
[18] E.C. Arvaniti, et al., Physical characterization methods for supplementary cementitious materials, Mater. Struct. 48 (11) (2015)

3675–3686, https://doi. org/10.1617/s11527-014-0430-4.
[19] Benjamin A.G.: Material Property Characterization of Ultra-High Performance Concrete, no. FHWA-HRT-06-103, p. 186 (2006)
[20] Andersen PJ, Johansen V (1991) Particle packing and concrete properties. Material Science of Concrete: II, Skalny J and Mindess S (Edited), The American Ceramic Society, Inc., Westerville, Ohio, 111–14
[21] Stovall T, De Larrard F, Buil M (1986) Linear packing density model of grain mixtures. Powder Technol 48:1–12
[22] Andersen, P.J. and Johansen, V. Particle packing and concrete properties, Material Science of Concrete: II, 1991, Skalny J and Mindess S (Edited), The American Ceramic Society, Inc., Westerville, Ohio. Pp.111-147.
[23] Senthilkumar V, Manu Santhanam, "Particle packing theories and their applicationinconcrete mixture proportioning: a review" The Indian Concrete Journal 2003:1324–31.
[24] Golterman, P., Johansen, V., Palbfl, L., "Packing of Aggregates: An Alternative Tool to Determine the Optimal Aggregate Mix," ACI Materials Journal, Vol. 94, No. 5, 1997, p 435.
[25] Fuller, W.B. and Thompson, S.E., The Laws of Proportioning Concrete, American Society of Civil Engineers, Vol.33, 1907, pp.223-298. [13] T. Stovall, F. De Larrard and M. Buil, "Linear Packing Density Model of Grain Mixtures", Powder Technology, 48 (1986), pp 1 – 12.
[26] Franqois De Larrard, "Ultrafine Particles for the Making of Very High Strength Concretes", cement and concrete research. Vol. 19, 1989, pp. 161-172.
[27] F. De Larrard and T. Sedran, "Optimization of Ultra-HighPerformance Concrete by the use of a Packing Model" Cement and Concrete Research, Vol. 24, No. 6, 1994, pp.997-1009. [16] M. Glavind, E. J. Pedersen, "Packing Calculations Applied for Concrete Mix Design" Proceedings Creating with Concrete, May 1999, University of Dunde, pp.1-10.
[28] Francois De Larrard, Thierry Sedran, "Mixture-proportioning of high-performance concrete", Cement and Concrete Research 32 (2002) pp.1699–1704.
[29] L.M. Vizcaíno Andr´es, M.G. Antoni, A. Alujas Diaz, J.F. Martirena Hern´andez, K. L. Scrivener, Effect of fineness in clinker calcined clays-limestone cements, Adv. Cement Res. 27 (9) (2015) 546–556.
[30] Z. Ge, K. Wang, R. Sun, D. Huang, Y. Hu, Properties of self-consolidating concrete containing nano-CaCO3. J. Sustain. Cem Based Mater. 3(3–4), 191–200 (2014)
[31] X. Liu, L. Chen, A. Liu, X. Wang, Effect of nano-CaCO3 on properties of cement paste. Energy Proc. 16, 991–996 (2012) 388.
[32] J. Camiletti, A.M. Soliman, M.L. Nehdi, Effects of nano- and micro-limestone addition on early-age properties of ultra-high performance concrete. Mater. Struct. 46(6), 881–898 (2013)
[33] S. Kawashima, P. Hou, D.J. Corr, S.P. Shah, Modification of cement-based materials with nanoparticles. Cem. Concr. Compos. 36, 8–15 (2013)
33[34] S. Kawashima, J.T. Seo, D. Corr, M.C. Hersam, S.P. Shah, Dispersion of CaCO3 nanoparticles by sonication and surfactant treatment for application in fly ash-cement systems. Mater. Struct. 47(6), 1011–1023 (2014)
[35] S.W.M. Supit, F.U.A. Shaikh, Effect of nano-CaCO3 on compressive strength development of high volume fly ash mortars and concretes. J. Adv. Concr. Technol. 12, 178–186 (2014)
[36] W.M.S. Steve, U.A.S. Faiz, Effect of nano-CaCO3 on compressive strength development of high volume fly ash mortars and concretes. J. Adv. Concr. Technol. 12(6), 178–186 (2014)
[37] P. Jinchang, L. Ronggui, Improvement of performance of ultra-high performance concrete based composite material added with nano materials. Frattura ed Integr. Strutt. 10(36), 130– 138 (2016)
[38] F.U.A. Shaikh, S.W.M. Supit, Mechanical and durability properties of high volume fly ash (HVFA) concrete containing calcium carbonate (CaCO3) nanoparticles. Constr. Build. Mater. 70, 309–321 (2014)
[39] Volpe R, Taglieri G, Daniele V, et al. A process for the synthesis of Ca(OH)2 nanoparticles by means of ionic exchange resin. European patent EP2880101. 2016.
[40] Taglieri G, Felice B, Daniele V, et al. Analysis of the carbonatation process of nanosized Ca(OH)2 particles synthesized by exchange ion process. Proceedings of the Institution of Mechanical Engineers, Part N: Journal of Nanoengineering and Nanosystems. 2016;230(1):25-31.
[41] Andreasen, AHM (1930). On the relation between grain gradation and spacing in loose grain products (with some experiments). *Colloid Journal*, 50(3), 217-228. doi:10.1007/bf01422986
[42] Li, V.; Stang, H.; Krenchel, H. Micromechanics of crack bridging in fibre-reinforced concrete. *Mater. Struct.* **1993**, *26*, 486–494.
[43] Li, V.C.; Leung, C.K. Steady-state and Multiple Creaking of Short random fiber composites. *J. Eng. Mech.* **1992**, *118*, 2246–2264.
[44] Li, V.C. From micromechanics to structural engineering—The design of cementitious composites for civi for civil applications. *Structrual Eng. Earthq. Eng.* **1993**, *10*, 37s–48s.
[45] Li, V.C.; Mishra, D.K.; Wu, H.-C. Matrix Design for Pseudo Strain-Hardening Fiber Reinforced Cementitious Composites. *Mater. Struct.* **1995**, *28*, 586–595.
[46] Yang, C.C.; Mura, T.; Shah, S.P. Micromechanical Theory and Uniaxial Tensile Tests of Fiber Reinforced Cement Composites. 2015. Available online: http://journals.cambridge.org
[47] McCartney, L. Mechanics of Matrix Cracking in Brittle-Matrix Fibre-Reinforced Composites. 1987. Available online: https://www.jstor.org/stable/2398127

CHAPTER 6

MODULE 3

Effective stiffness of engineered cementitious composite (ECC) structures and its Performance Assessment.

Abstract

Engineered Cementitious Composite (ECC) is an exclusive type of cement mixture with unique composition of low volume fibers and different composites so as to impart high ductility, high tensile strength besides ability to repair. Conventional concrete and fiber reinforced concrete has a brittle nature and hence crack easily. This paper presents a comprehensive performance assessment of Engineered Cementitious Composite (ECC) using three different analytical methods: Monotonic Pushover Analysis (MPA), Cyclic Pushover Analysis (CPA), and Nonlinear Time History Analysis (NTHA). Additionally, the Cyclic Pushover Analysis provided valuable information about the hysteric behavior, stiffness, and strength degradation of ECC structures. The Nonlinear Response History Analysis (NLRHA) procedure was employed to evaluate the seismic performance of the structures, and the results of the study indicate that ECC has superior seismic performance compared to conventional concrete. MPA and CPA are found to be effective in predicting the behavior of ECC under seismic loads, but NTHA provides a more detailed and accurate representation of the actual response of the structure. The study also highlights the importance of incorporating the material properties and behavior of ECC into the analytical models to accurately predict its performance.

Graphical Abstract

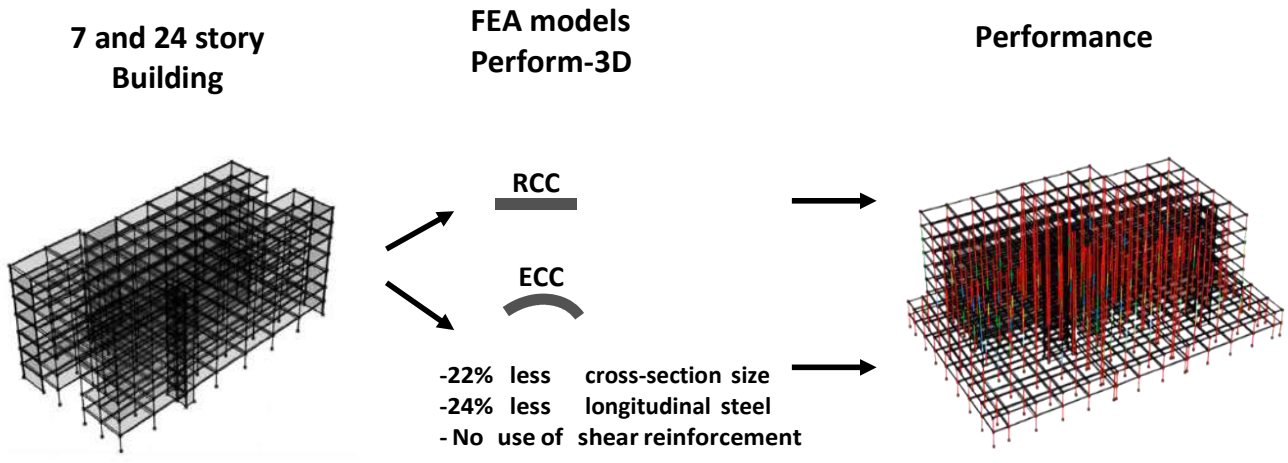

6.1. Introduction:

Building structures have always been instrumental in shaping civilizations across the world. As the population continues to grow, efficient land utilization becomes crucial. Nowadays, people are migrating to urban areas at a rapid pace due to better amenities. To accommodate this trend and address population growth, vertical development has emerged as an effective solution for maximizing land use. However, designing structures in the vertical direction presents challenges, particularly in dealing with high moments that lead to undesired tensile stresses. Additionally, most construction materials, except for steel, have limited strength when subjected to tension [1]. In ancient times, the challenge of dealing with high moments and tensile stresses was addressed by utilizing arches and domes in structural design. These architectural elements effectively reduced moments and generated axial compressive stresses [2]. Reinforced Concrete (RCC) was introduced during the 1940s as a construction material suitable for medium to long-span structures and tall buildings that demanded significant steel reinforcement [3]. Subsequently, for long-span structures, pre-stressed and post-tensioned members were employed, which eliminated the need for excessive reinforcement and bulky cross-sections. However, these methods were associated with certain drawbacks, particularly concerning ductility. [4,5]. In areas prone to earthquakes, the aforementioned limitation becomes a critical concern, as seismic design codes emphasize the necessity for structures and their elements to possess ductility in order to withstand seismic forces effectively. [6]. Hence, in seismic regions, the use of Reinforced Concrete (RCC) with ample reinforcement, cross-sections, and proper confinement becomes imperative to ensure structural ductility. Although RCC exhibits improved ductility compared to pre-stressed concrete, it often results in uneconomical designs due to heavy material usage. Therefore, there arises a need for innovative materials that can provide ductility without compromising cost-effectiveness.

Several innovative solutions have been proposed to improve the seismic performance of structures [7,8]. To improve the ductility of the cementitious matrix, one approach is to introduce fibers, leading to the development of Fiber Reinforced Concrete (FRC) composites [9]. A special class of high performance FRC that exhibits strain-hardening behavior in uniaxial tension is classified as Engineered Cementitious Composite (ECC) [10-12]. Due to its improved tensile capacity, Engineered Cementitious Composite (ECC) has the potential to reduce cross-sections and reinforcement requirements. Furthermore, ECC's lightweight nature and high ductility can contribute to enhanced seismic performance in structures [13]. The material processing and design of Engineered Cementitious Composite (ECC) are more complex compared to conventional concrete, as it necessitates the utilization of a micro-mechanical model to achieve the desired strain hardening behavior [14]. In order to analyze the structural mechanics of ECC, Integrated Structures and Materials Design (ISMD) methodologies are employed, which incorporate the material properties of ECC [15] approach proposed by Li. which specifies that material design should be carried out first to obtain the necessary constitutive model for structural analysis and design.

Several studies have focused on different aspects of ECC to study its behavior at the member

level using the ISMD [15] approach. The studies demonstrate that Engineered Cementitious Composite (ECC), owing to its inherent ductility, exhibits superior performance under cyclic loading conditions compared to conventional concrete [16]. Extensive research has substantiated that Engineered Cementitious Composite (ECC) possesses a remarkable load carrying capacity, demonstrating its ability to sustain high loads without compromising structural integrity [17]. Maalej and Li [18] and Szerszen et al. [19] studied the behavior of reinforced Engineered Cementitious Composite (ECC) members under moments was investigated, leading to the development of a moment-curvature relationship for steel-reinforced ECC beams. Furthermore, comprehensive studies were conducted on columns, shear walls, and beam-column connections, analyzing their response to various types of static and dynamic loadings [20-24]. Although numerous studies have focused on Engineered Cementitious Composite (ECC) at the member and material levels, there is a notable lack of comprehensive performance-based assessments conducted at the structural scale. Therefore, in order to effectively compare the seismic response of ECC and conventional Reinforced Concrete (RCC), it is crucial to conduct a thorough structural-level investigation on a long-span structure. This study should involve subjecting the structure to realistic loadings while utilizing detailed performance-based design and assessment procedures.

This study focuses on the structural design and performance based seismic evaluation through monotonic and cyclic pushover analysis of ECC structures and NLTHA (Non-Linear Time History Analysis) were employed to calculate the seismic demands of buildings. First, material design was performed following the ISMD approach [15]to obtain material properties for analyses using a simplified machine learning based approach which were also verified by experimentation [25]. For the purpose of comparative analysis, two case study buildings a 7-story mid-rise structure and a 24-story high-rise structure were chosen. A comprehensive finite element model of Engineered Cementitious Composite (ECC) at the complete structural level was developed using ETABs software. Additionally, finite element models of Reinforced Concrete (RCC) were developed for the same case study structures. The linear static analysis method was employed to calculate the design actions in response to dead, live, and seismic loads. For Elastic design, JSCE [26] guidelines were used for ECC, while ACI 318-19 [27] were used for RCC. The design results revealed that the reinforcement requirements for ECC were significantly lower and impractical. The practical approach would be to use a reduced cross-section model for ECC. As ECC is a new material, nonlinear modelling and analyses should be conducted to capture its actual behavior on structural scale. For performance-based evaluation, non-linearity was induced only in frame elements, while other elements were modelled as linear elastic. For beams, plastic hinges were assigned using moment rotation curves as per ASCE 41-17 [28], while the fiber modelling technique was employed for columns. Nonlinear time history analysis (NLTHA) was performed to find the actual behavior of the structure against lateral loadings, monotonic and cyclic pushover analysis used to calculate structural stiffness, strength and stiffness degradation on large scale. Finally, the economic potential of ECC is investigated through material cost estimation and cost comparison with RCC.

6.2. Development of ECC Mix

Usually, the material and structural design are performed by two distinct parties and the only connection between the two is the compressive strength of concrete irrespective of which design is done first. For ECC, this approach stands invalid as its constitutive model can only be constructed once material design is finalized. It will be very difficult for a material designer to proportionate a mix from a particular stress-strain curve. Therefore, the structural design of ECC should be performed after finalizing the material design first. Integrated Structures and Materials Design (ISMD) [15] method proposed by Li enables the structural performance to be linked with ECC constituent selection and tailoring. For the usefulness of the ISMD [15] approach, A constitutive model is required to simulate material properties at the structural level when used in conjunction with the finite element method. Figure 6.1 illustrates the ISMD approach, which establishes a connection between structural performance and material properties.

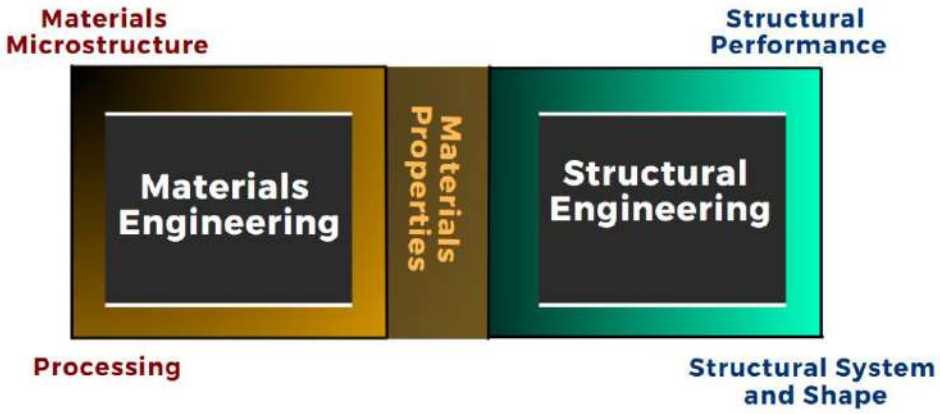

Figure 6.1. ISMD approach linking Structural performance with composite's material properties

Material designing of ECC is quite complex as it shows strain-hardening behavior in uniaxial tension [10-12]. Initially it was believed that strain hardening could be achieved solely by increasing the amount of fibers in a material. However, this approach is not considered feasible due to the high cost involved and concerns regarding the workability of the mixture. Subsequent research has suggested that fiber content is not the sole determining factor for achieving strain hardening behavior. [29]. Other important factors that can affect how Fiber-Reinforced Concrete (FRC) behaves when subjected to tension include the toughness and strength of the matrix material, the properties of the fibers (such as their stiffness, strength, and shape), and how well the matrix material and fibers are bonded together [30-31]. Several researchers have proposed their approaches to determine the critical volume fraction, which represents the minimum amount of fibers required to achieve strain hardening. These investigations involve establishing correlations between the aforementioned properties to uncover the relationship between fiber content and the desired behavior of strain hardening. [29-35].

Developing a mix design technique to achieve strain hardening in concrete relies on

extensive experimentation, which can be a lengthy, time-consuming, and costly process. [36]. Therefore, a relatively new technique is adopted, based on a machine learning (ML) model, for getting a desiredmix design along with its ductility and mechanical properties [25]. To determine the appropriate mix for Engineered Cementitious Composite (ECC) with a target compressive strength of 35 MPa, a machine learning model was utilized. The model provided the ECC mix proportions, as well as the associated tensile strength and strain values. Table 6.1 presents the ECC mix design, fiber properties, and the predicted output parameters generated by the machine learning model. Given that PVA fibers are commonly employed in ECC, a mix incorporating PVA fibers was utilized in this study.

Table 6.1. Selected mix of ECC sample, Properties of fibers, and Output parameters of ML model

Selected mix of ECC				
Cement	**Fly ash**	**Sand**	**W/B**	**HRWR***
1	0.6	0.6	0.55	0.6%
Properties of Fiber				
Volume fraction	**Elastic modulus**	**Length**		**Diameter**
2%	40 GPa	12 mm		40 µm
Output parameters of ML model				
Compressive Strength	**Tensile Strength**	**Tensile Strain**		**Post Cracking Response**
35.2 MPa	4.7	3.7%		Strain-hardening

∗High range water reducer (Polycarboxylate ether based)

6.3. Selection of a Case Study Building

For finding the effective stiffness at structure level two case study buildings were taken one is 7 story which represents low rise structure and 24 story which represents high rise structure. The selection of a 7-story and 24-story building provides a significant variation in height, allowing for the investigation of stiffness properties across different scales. This range helps to capture the behavior of structures under various vertical loads and gravitational forces. The chosen buildings exhibit diverse architectural and structural characteristics. This selection enables the examination of different construction methods, materials, and structural systems, offering valuable insights into the effect of these variables on the overall stiffness of the buildings. The selection process aims to ensure that the chosen buildings represent typical multi-story structures encountered in real-world scenarios. This enhances the applicability of the research findings and facilitates the extrapolation of results to other similar structures. The selected buildings encompass a range of complexities in terms of architectural design and construction techniques. By including both a relatively simpler 7-story building and a more intricate 24-story building, the study can assess the impact of complexity on the overall stiffness and structural behavior. This variation allows for an exploration of how different structural systems influence the stiffness characteristics and response of multi-story buildings. Figure 6.2 illustrates the architectural details of case study structures (a) floor plan of 7 story building (b) 3D model of 7 story building (c) floor plan of 24 story

building (d) 3D model of 24 story building.

Assumptions made during the modeling of the building linearly in Etabs software are as follows:

1. Beam Column joints are modelled as rigid joints.
2. Frame is modeled as intermediate moment resisting frame.
3. Soil structure interaction is not considered while carrying out analysis of structures. Fixed support is taken at the base.
4. Only structural elements with significant stiffness; beams and columns are modelled.

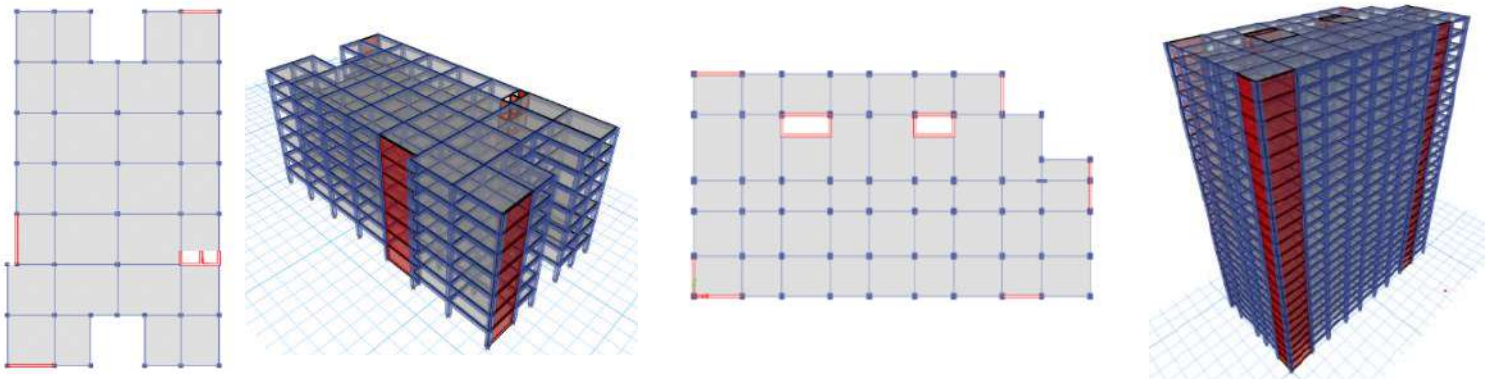

(a) (b) (c) (d)

Figure 6.2. The architectural details of case study structures (a) floor plan of 7 story building (b) 3D model of 7 story building (c) floor plan of 24 story building (d) 3D model of 24 story building.

To gain a comprehensive understanding of the performance of Engineered Cementitious Composite (ECC), a comparative study was conducted. In addition to the ECC model, an RCC model was constructed for analysis and design purposes. Two finite element models were developed to compare the structural performance of these materials. Table 6.2 presents the input material properties considered for the analysis and design of the structures. The seismic and live load specifications were kept consistent for both models, while the dead load varied due to differences in the unit weight of the materials. The study assumed a location in Karachi, Sindh, Pakistan, and the seismic coefficients were selected according to the building code of Pakistan 2021 (BCP-2021) [37]. Detailed numerical values of the loading patterns and specifications for seismic loading are summarized in Table 6.3. This comparative analysis aimed to provide valuable insights into the behavior and performance of ECC in comparison to RCC under specific loading conditions and geographical considerations.

Table 6.2. Input materials parameters for concrete, ECC, and steel reinforcement

	Concrete	**ECC**	**Steel Rebars**
Compressive Strength	25.58 MPa	46.16 MPa	420 MPa
Tensile Strength	-	4.96 MPa	420 MPa
Elastic Modulus	24.85 GPa	18 GPa	200GPa
Poisson Ratio	0.2	0.226	0.28
Tensile Strain Capacity	-	3.74%	10.8 %
Unit Weight	2400 kg/ m^3	1800 kg /m^3	7850 kg /m^3

Table 6.3. Dead, Live, and Seismic load use for design of buildings

Load Pattern	Factors	Values
Dead Load	-	As per unit Weight
Live Load	-	4.78 KN/m^2
Seismic Load	S_s	1.302
	S_1	0.381
	Site Class	D
	Long-Period Transition Period	8 sec
	Response Modification Factor	5
	Over strength factor	3
	Deflection amplification	4.5
	Occupancy Importance Factor	1

Both the ECC and RCC models underwent static linear analysis, in which loads such as dead load, live load, and seismic load, as well as their combinations, were selected based on ASCE 7-16 [38]. The objective of the analysis was to determine the design actions for each structural member by employing the Response Spectrum Analysis (RSA) procedure to simulate earthquakes. Through the static analysis, it was observed that the design actions for ECC members were significantly reduced compared to RCC members. This reduction can be attributed to the lower unit weight of the ECC composite, resulting in lower dead loads and seismic loads acting on the structure. The findings from the analysis highlight the potential advantages of ECC, as its lighter weight contributes to reduced structural demands under various loading conditions.

6.4. Design of a Case Study Building

After analysis the next step was to design the structural members. The design of conventional concrete is performed directly by aid of ACI 318-19 code [27]. As ECC possesses significant tensile strength which needs to be consider for structural design, and ACI 318-19 [27] ignores tensile capacity of concrete hence it cannot be use for ECC design. Therefore, for the elastic design of ECC, calculations were performed using JSCE Guidelines [26]. JSCE provides a simplified stress and strain distribution for both compression and tension along the depth for flexural members as shown in Figure 6.3. Longitudinal reinforcement for beams and slabs is computed against design bending moments. Furthermore, in reinforced ECC a major proportion of shear is resisted by fibers which can be incorporated in shear design by using JSCE guidelines [26], as shown in equation (1) and (2). For column design, three-dimensional capacity interaction surfaces were used. Reinforcements are assumed and trial cross-sections are employed in ascending order. The design actions and the three-dimensional capacity surface are compared to calculate adequate cross-section and optimum amount of steel for ECC columns.

$$V_u = V_c + V_s + V_f \qquad (1)$$

Where Vs represents the shear capacity provided by the concrete, Vs represents the shear capacity provided by the transverse steel, and Vf represents the shear capacity provided by the fibers. On the other hand, Vu refers to the ultimate shear capacity of the member.

$$V_f = \left(\frac{f_{vd}}{\tan(\beta_u)}\right) . b_w . \frac{z}{\gamma_b} \quad (2)$$

f_{vd}: design tensile yield strength of ECC, $f_{vd} = 0$ when f_{vd} is smaller than 1.5 N/mm^2.
β_u: angle of the diagonal crack surface to the member axis. $\beta_u = 45^0$.
γ_b: 1.3 for shear (Factor of safety)
Z: distance between location of compressive stress resultant to centroid of tensile steel, may generally use d/1.15.

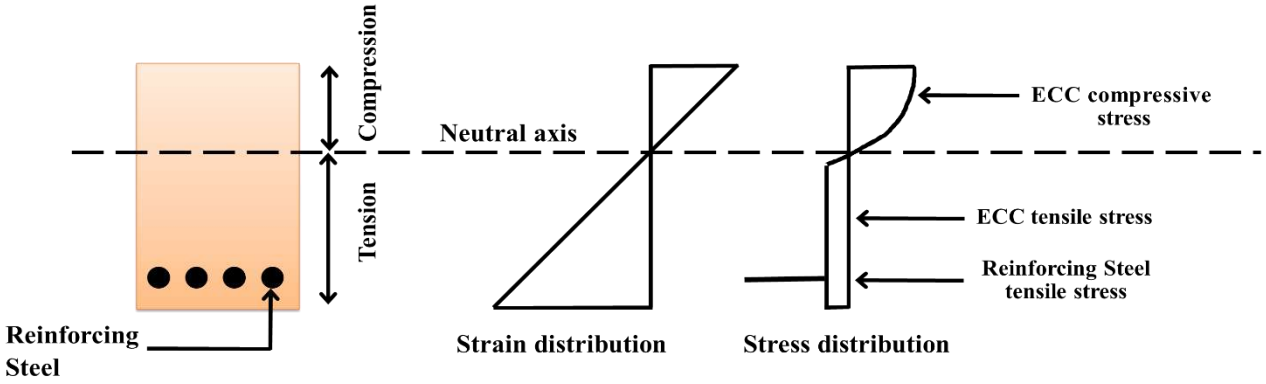

Figure 6.3. Flexural stress & strain profile as per JSCE guideline

Table 6.4 provides a comparison of the reinforcement requirements for both ECC and RCC materials. The data clearly indicates that ECC members require significantly less reinforcement compared to the minimum reinforcement requirements. This implies that the cross-section of the ECC model can be further reduced to achieve a more economical and practical design. During the static analysis, it was observed that the design actions were further reduced by an average of 20% in the reduced cross-section ECC model. This reduction can be attributed to the lower self-weight of the ECC elements.

The reinforcement requirement for ECC models was significantly lower compared to RCC, primarily due to the lower unit weight of ECC. This lower weight helped to mitigate the dead and seismic loads acting on the structure. By further reducing the cross section, the demands on ECC members were decreased, resulting in a more cost-effective design. The design, following the guidelines of JSCE [26], showcased an average reduction of 30% in the area of longitudinal steel and a 25% reduction in cross-section for beams. Similar findings were reported by Szerszen et al. [19], who observed an increase in strength of up to 230% for smaller values of reinforcement while maintaining comparable cross sections in ECC members. Remarkably, due to ECC's excellent shear performance, no shear reinforcement was required throughout the entire structure. Li et al. [39] found that the shear capacity of an ECC beam without stirrups was comparable to an RCC beam with sufficient shear reinforcement. This result was also supported by Shimizu et al. [40], who studied reinforced PVA-ECC beams. The design results for

columns also demonstrated improvements compared to RCC. Experimental investigations on reinforced ECC columns subjected to cyclic loading [20] revealed increased capacity compared to RCC columns. Figure 6.4 and 6.5 illustrates the reduced cross section of buildings beams and columns respectively.

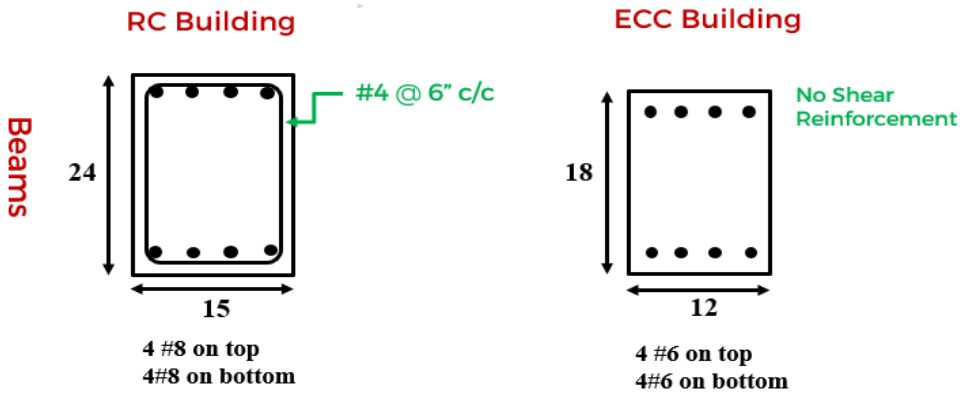

Figure 6.4. Beams Cross section

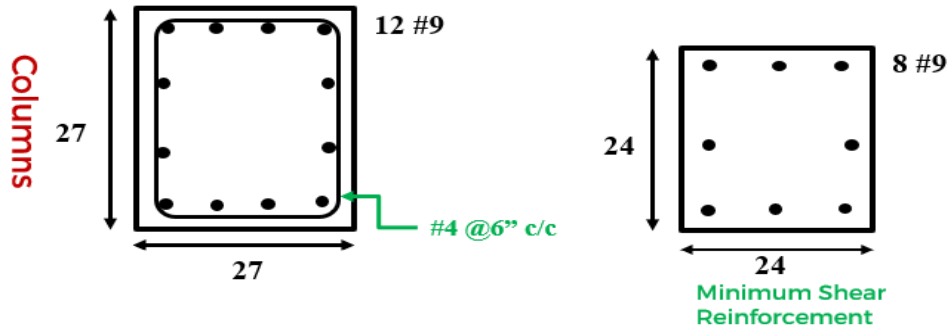

Figure 6.5.Columns Cross section

Table 6.4. Design results for beams and columns

Table 6.4. Design results for beams and columns

	RC Structure			ECC Structure		
	Structural Element (B x H) mm	**Longitudinal Reinforcement**	**Shear Reinforcement**	**Structural Element (B x H) mm**	**Longitudinal Reinforcement**	**Shear Reinforcement**
7th Story	Column-1 (600 X 600)	12#9	#4 @6" c/c	Column-1 (500 X 500)	8#9 bars	No Shear Reinforcement
	Column-2 (675 X 675)	12#9	#4 @6" c/c	Column-2 (600 X 600)	8#9 bars	No Shear Reinforcement
	Beam-1 (375 X 600)	4 #6 bars on top and bottom	#3 @6"c/c	Beam-1 (300 X 450)	4 #6 bars on top and bottom	No Shear Reinforcement
24 Story	Column-1 (900 X 1050)	40#9	5-#3 @10" c/c	Column-1A (750 X 900)	40#9	No Shear Reinforcement
	Column-2 (900 X 900)	32#8	4-#3 @10" c/c	Column-2A (750 X 750)	32#8	No Shear Reinforcement
	Column-3 (900 X 900)	32#8	4-#3 @10" c/c	Column-2W (750 X 750)	32#8	No Shear Reinforcement
	Column-4 (450 X 1800)	32#8	4-#3 @10" c/c	Column-6 (450X 1500)	32#8	No Shear Reinforcement
	Beam-1 (375 X 675)	10#6 on top and 8#6 bottom	#3 @6" c/c	Beam-1a (375 X 600)	8#6 on top and 8#6 bottom	No Shear Reinforcement
	Beam-2 (375 X 825)	12#6 in2 on top and 8#6 bottom	#3 @6" c/c	Beam-2a (375 X 750)	10#6 in2 on top and 8#6 bottom	No Shear Reinforcement
	Beam-3 (375 X 675)	8#6 on top and 8#6 on bottom	#3 @6" c/c	Beam-3a (375 X 600)	8#6 on top and 8#6 on bottom	No Shear Reinforcement

Modal analysis was conducted to assess the stiffness of the structures in terms of time-period. The results of the modal analysis are summarized in Table 6.5. It is observed that the ECC structure exhibits a relatively higher time-period compared to RCC due to its lower modulus of elasticity, as mentioned in Table 6.2, and reduced cross-sections. To account for cracked moment of inertia of concrete, stiffness modifiers are typically utilized in structural design based on various codes. However, in the case of ECC, the presence of fibers bridges the cracks, leading to improved damage tolerance and enhanced tension stiffening response in reinforced ECC members. Tension stiffening refers to the increase in stiffness beyond the bare steel reinforcement caused by the tensile load carried by the concrete material after cracking occurs [41-42]. It is estimated that the stiffness modifiers should be double as those for RCC [26]. But due to unavailability of numeric values of the stiffness modifiers for ECC, being on conservative side, same stiffness modifiers areused for both materials in this study.

Table 6.8. Modal analysis result summary OF 7 story building

Time Period	RC sec	ECC sec
1st Mode	1.03	1.38
2nd Mode	0.89	1.17
3rd Mode	0.6	0.77

6.5. Performance Based Evaluation

The occurrence of structural failures during seismic events has highlighted the limitations of code-based design procedures and emphasized the necessity for methodologies that can evaluate and design structural performance more effectively. The main challenge lies in addressing the significant uncertainties associated with loadings and the complex nonlinear behavior of structures. Proper consideration and treatment of these uncertainties are essential for ensuring reliable and robust structural designs. [43]. Performance based analysis allows us to capture complete material behavior, even after the linear range. Since ECC shows excellent post-cracking behavior, it is necessary to perform non-linear analyses to completely capture its response on the structural level. In addition to that, there may be uncertainties involved with a new and novel material like ECC, these are catered for by performance-based evaluation.

In this study, a comparative performance-based seismic evaluation of the two materials was conducted using pushover analysis and non-linear time history analysis. The evaluation was carried out considering both the design basis earthquake (DBE) and the maximum considered earthquake (MCE). The DBE-level earthquake represents a 10% probability of exceedance in 50 years, while the MCE-level earthquake represents a 2% exceedance in 50 years. To gain a deeper understanding of the seismic performance of ECC, the results obtained from the non-linear analysis of the conventional concrete model were compared with two different ECC models. To summarize there are a total of 4 structural models, and all 4 models are analyses earthquakes yielding a total of 8 seismic responses.

6.5.1. Non-linear modelling

Perform 3D is a powerful software solution specifically designed for the analysis and design of building structures. It follows a systematic analysis procedure, starting with a linear elastic analysis when the materials exhibit linear response to loads. This initial analysis provides an approximate understanding of the structural elements' capabilities and helps assess the structure's behavior under typical loads. What sets Perform 3D apart is its advanced analysis tools, which go beyond linear behavior. These tools are capable of capturing intricate behaviors by considering both geometric and material nonlinearities. Geometric nonlinearities account for significant deformations and member instability, while material nonlinearities address phenomena like concrete cracking and steel yielding. To

accurately capture these nonlinear behaviors, Perform 3D allows for the inclusion of material properties and relevant parameters in the model. These adjustments introduce nonlinear effects, enabling a more realistic representation of the structure's response. The software then performs a comprehensive nonlinear analysis, accounting for the behavior of the structure after yielding, including the redistribution of forces while considering nonlinear factors. This approach provides a more accurate assessment of the structure's performance and ensures reliable design outcomes.

6.5.1.1. Non-Linearity at the Material Level

In the linear elastic model, it is assumed that all input curves in the software are linear, represented by fixed numerical values. However, when utilizing a non-linear model, actual action-deformation curves are incorporated to accurately depict the material behavior. For concrete, the Mander's unconfined stress-strain curve is commonly employed due to its reliability. Steel, on the other hand, is typically modeled using a bilinear curve with strength degradation and no strain hardening. Defining the nonlinearity of materials at the material level is essential for correctly assigning hinges to columns and shear walls. This process involves considering performance levels and acceptance criteria for both steel and concrete, ensuring precise results. Engineers establish specific standards to assess steel performance under compression and tension. For compression, acceptance criteria include the point at which compression yielding begins for Immediate Occupancy (IO), twice the value of compression yielding for Life Safety (LS), and three times the value of compression yielding for Collapse Prevention (CP). Regarding tension, acceptance criteria consist of the point at which tensile yielding initiates for IO, three times the value of tensile yielding for LS, and five times the value of tensile yielding for CP.

Similarly, for concrete under compression, acceptance criteria involve the initiation of compression cracking for IO, the highest stress reached for LS, and the onset of significant strength degradation for CP. For tension, acceptance criteria consider the initiation of tensile cracking for IO. By defining these performance levels and corresponding acceptance criteria, it becomes possible to accurately incorporate the nonlinear properties of steel and concrete at the material level. This process entails assigning specific parameters and models to effectively capture the nonlinear behavior of these materials during the analysis process. Stress-strain models for steel, conventional concrete and ECC are added to the models as shown in Figure 6.6. ECC possesses significant stress taking capability in both tension and compression, therefore, both behaviors must be considered to simulate the actual behavior of the composite. For this purpose, Ding et al. [46] model for compression and Quan et al. [47] model for tension are used as material stress-strain curves incorporating the mix properties as shown in Figure 6.7. Elastic modulus is calculated directly from stress-strain curve [27]. Whereas Poisson’s ratio and unit weight are calculated using JSCE guidelines [26] as mentioned in Table 6.2.

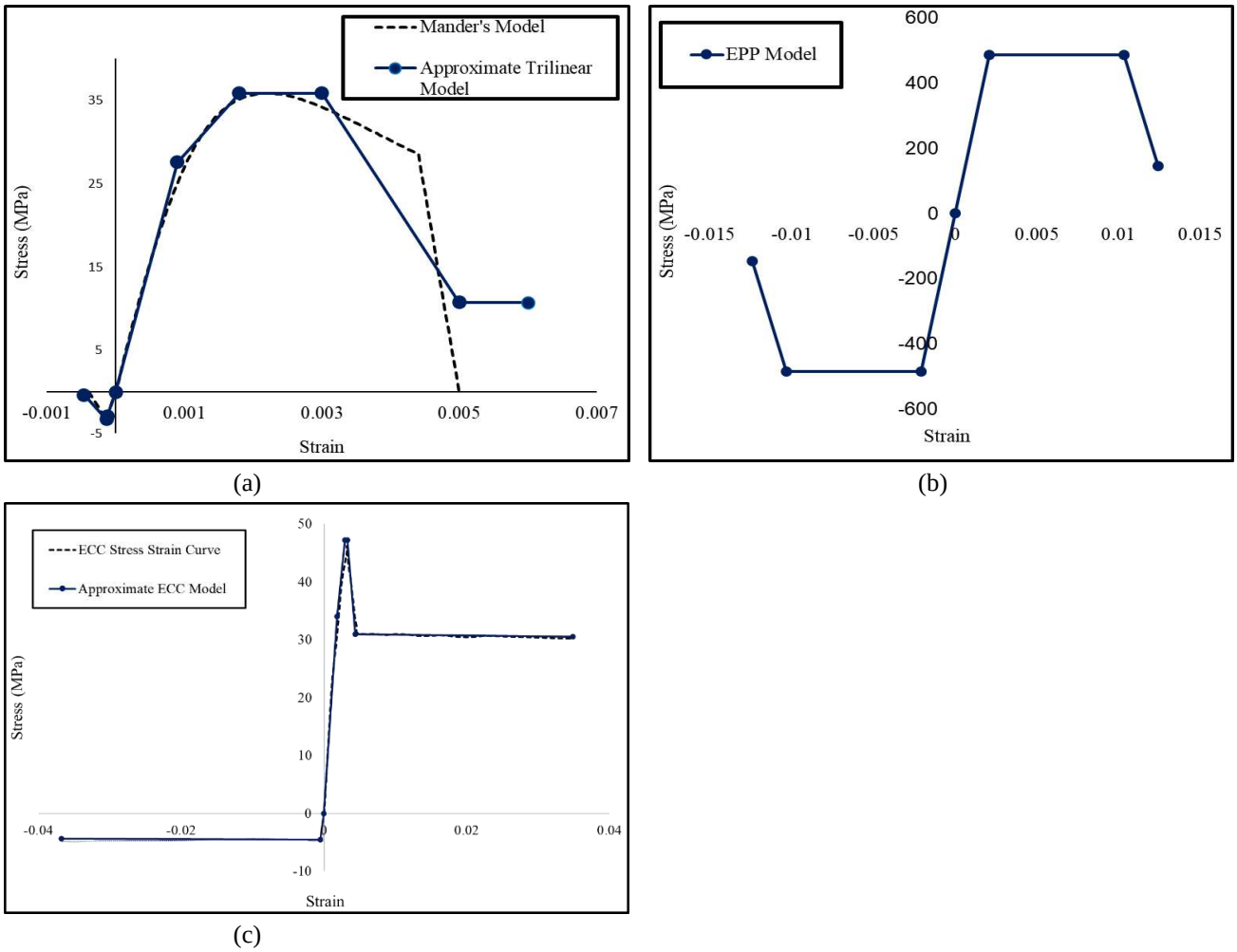

Figure 6.6. Stress-strain curves (a) for Normal Concrete, (b) Elastic-perfectly plastic model for Grade -60 steel reinforcement (c) ECC.

6.5.1.2. Non-Linearity at the Section Level

Non-linear modeling techniques provide an accurate representation of the structural behavior of beams, columns, and shear walls. These techniques utilize force-deformation curves to capture the plastic hinge behavior of beams, following the recommendations outlined in ASCE 41-17 for automatic hinge assignment. This thorough approach uses force-deformation curves to explain the plastic hinge behavior of beams in accordance with the recommendations made in ASCE 41-17 for automatic hinge assignment.

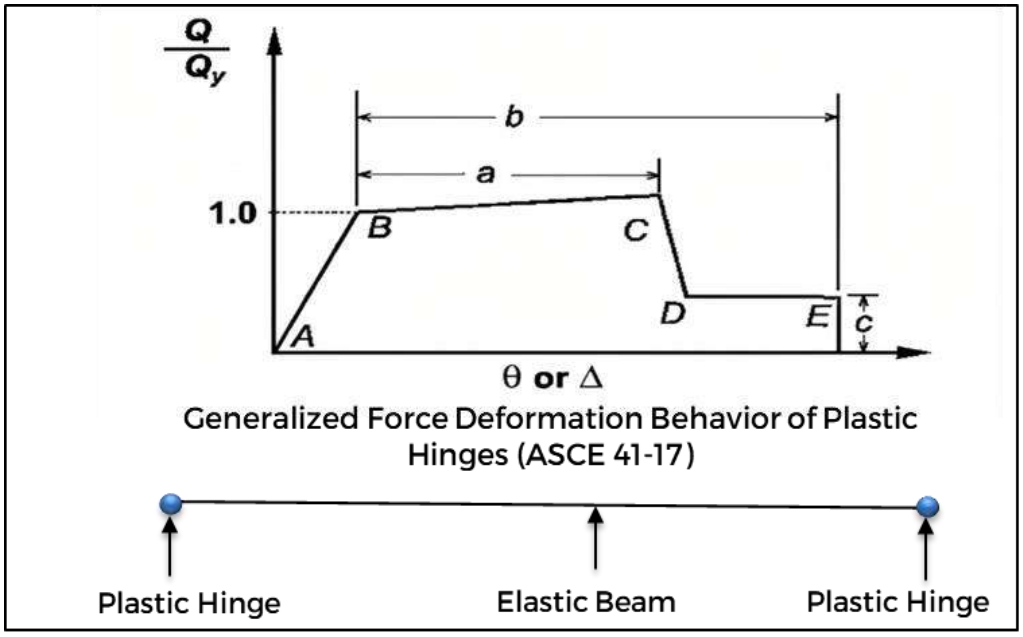

Figure 6.7. Plastic Hinge modeling Approach

In the case of columns subjected to biaxial loading, the interaction of P-M2-M3 fiber hinges is employed to represent the inelastic behavior. These fiber hinges, positioned at the ends of the column, depict the localized plastic hinge length, enabling an accurate reflection of the column's inelastic response. For shear walls, out-of-plane actions are often assumed to remain elastic, while inelastic behavior is considered only in the in-place direction for simplification purposes. In this context, a useful model incorporating interacting P-M3 fiber hinges is utilized to study the interaction of moment with axial loads in a single direction. As inelastic movement can occur anywhere along the height of the building, this model incorporates fiber hinges throughout the entire height of the shear walls. This model is particularly suitable for taller shear walls exhibiting column-like behavior.

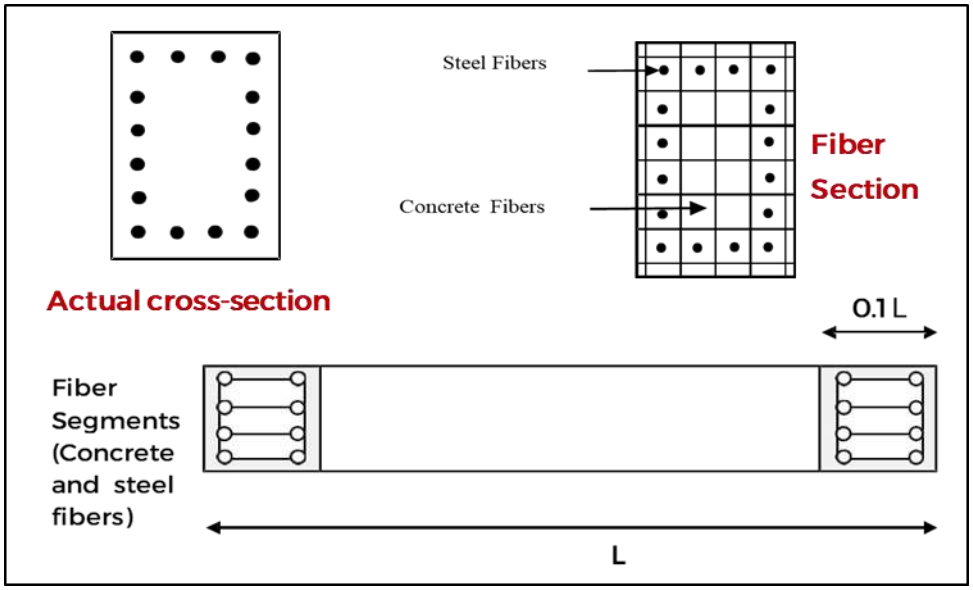

Figure 6.8. Fiber Modeling Approach

The table shows fibers assigned to a column and a shear wall of original design:

Fiber	Area	Coordinate 3	Coordinate 2	Material
1	0.38	4.9312	-12.4312	Steel
2	0.38	4.9312	-6.2156	Steel
3	0.38	4.9312	0	Steel
4	0.38	4.9312	6.2156	Steel
5	0.38	4.9312	12.4312	Steel
6	0.38	-4.9312	-12.4312	Steel
7	0.38	-4.9312	-6.2156	Steel
8	0.38	-4.9312	0	Steel
9	0.38	-4.9312	6.2156	Steel
10	0.38	-4.9312	12.4312	Steel
11	0.38	0	-12.4312	Steel
12	0.38	0	12.4312	Steel
13	16.6	-6.5321	13.0988	Concrete
14	13.1	0	13.0988	Concrete
15	16.6	6.5321	13.0988	Concrete
16	26.3	-6.5321	0	Concrete
17	26.3	6.5321	0	Concrete
18	16.6	-6.5321	-13.0988	Concrete
19	13.1	0	-13.0988	Concrete
20	16.6	6.5321	-13.0988	Concrete
21	30	-4.257	9.8341	Concrete
22	30	0	9.8341	Concrete
23	30	4.257	9.8341	Concrete
24	30	-4.257	0	Concrete
25	60	0	0	Concrete
26	30	4.257	0	Concrete
27	30	-4.257	-9.8341	Concrete
28	30	0	-9.8341	Concrete
29	30	4.257	-9.8341	Concrete

Table 6.9.: Concrete Column Fiber Sections

Fiber	Area	Coordinate 2	Material
1	113.1	-80.2778	Concrete
2	226.1	-66.1111	Concrete
3	226.1	-47.2222	Concrete
4	226.1	-28.3333	Concrete
5	226.1	-9.4444	Concrete
6	226.1	9.4444	Concrete
7	226.1	28.3333	Concrete
8	226.1	47.2222	Concrete
9	226.1	66.1111	Concrete
10	113.1	80.2778	Concrete
11	0.57	-75.5556	Steel
12	0.57	-56.6667	Steel
13	0.57	-37.7778	Steel
14	0.57	-18.8889	Steel
15	0.57	0	Steel
16	0.57	18.8889	Steel
17	0.57	37.7778	Steel
18	0.57	56.6667	Steel
19	0.57	75.5556	Steel

Table 6.10. Shear wall Fiber Section

6.5.2. Selection of ground motions:

The site is assumed located in Islamabad, Pakistan. Site class is assumed to be D and using ASCE 7-16 [38] the seismic design coefficients are found to be $S_s = 1.308$; $S_1 = 0.381$ [37] Other parameters required for the selection of ground motion are taken from published literature as mentioned in Table 6.11.

Table 6.11. Site hazard parameters

Sr. No.	**Selection Criteria**	**Values**
1	Fault Type	Reverse/Oblique
2	Magnitude	6.3-7.8
3	R_{JB} (Km)	10 to 50 Km
4	R_{RUP} (Km)	10 to 50 Km
5	V_{S30} (m/s)	490 to 620 m/s
6	D5-95 (sec)	30 to 50 sec
7	Pulse	No Pulse-like Records

The ground motions are obtained from the PEER website using the above parametric criteria.

ground motions were selected. Spectral matching is done to scale the selected ground motion according to our design spectrum of the site [38], so that lateral loadings are within the limit for which structureis to be designed. The key seismic parameters for the ground motions are shown in Table 6.11. The time histories are shown in Table 6.12 for each earthquake. Figure 6.10 and 6.11. illustrates the selected earthquake matched with the response spectrum of Islamabad and match ground motion respectively.

Table 6.12. Time histories selected for NLTHA

Earthquake Name	Magnitude	Recording Station	Mechanism	Rjb (km)	Rrup (km)
Parkfield (1966)	6.19	Cholame - Shandon Array #12	strike slip	17.64	17.64
San Fernando (1971)	6.61	Castaic - Old Ridge Route	Reverse	19.33	22.63
San Fernando (1971)	6.61	Palmdale Fire Station	Reverse	24.16	28.99
Imperial Valley-06 (1979)	6.53	Cerro Prieto	strike slip	15.19	15.19
Chuetsu-Oki_ Japan (2007)	6.8	Joetsu Kita	Reverse	28.97	29.45
Chichi Taiwan (1999)	7.62	CHY088	Reverse Oblique	37.48	37.48
Kern County (1952)	7.36	Taft Lincoln School	Reverse	38.42	38.89

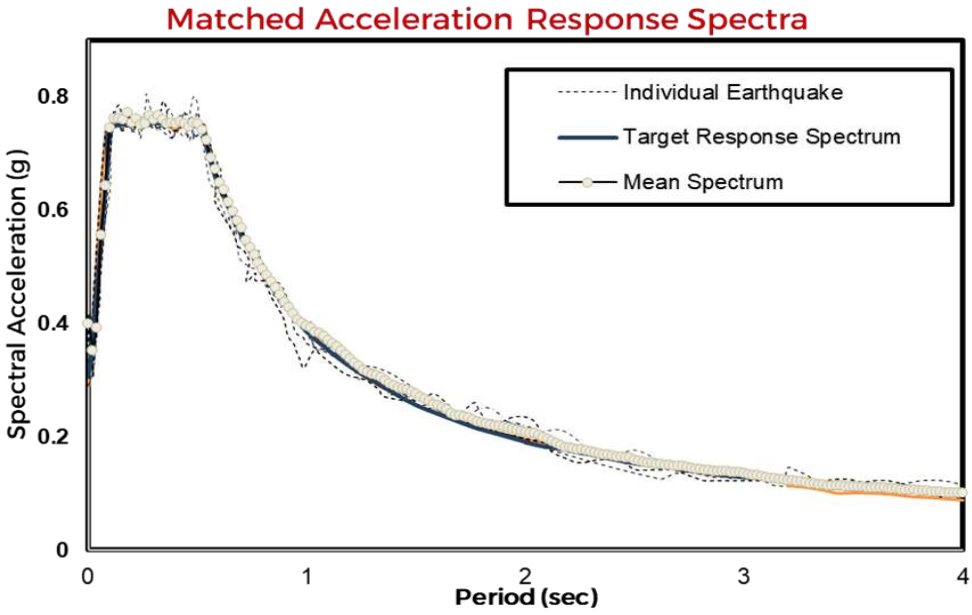

Figure 6.9. Mean Match Response spectrum.

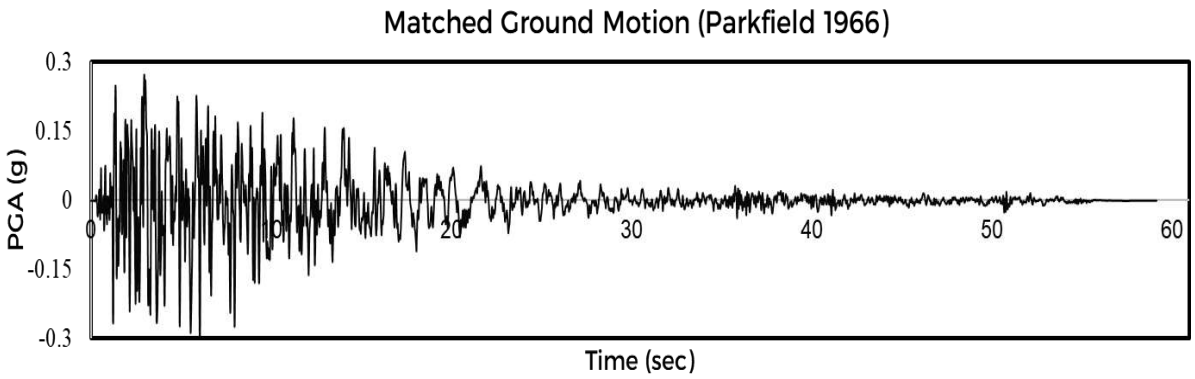

Figure 6.10. Matched Ground Motion

6.5.2. *Pushover Analysis*

Pushover analysis is a nonlinear static analysis method used to evaluate the seismic performance of structures. It assesses the response of a structure under increasing lateral loads until it reaches a state of collapse or a predefined performance limit. This analysis technique is commonly employed in structural engineering to assess the capacity and behavior of buildings under seismic forces. During pushover analysis, a series of load patterns are applied incrementally to the structure, typically starting with a gravity load followed by lateral loads. The loads are increasing gradually, allowing the structure to deform and redistribute internal forces. The analysis considers both the geometric nonlinearity (such as large deformations and member instabilities) and material nonlinearity (such as concrete cracking and steel yielding). The primary output of pushover analysis is the capacity curve, which depicts the relationship between the applied base shear and the corresponding top displacement or inter-story drift. This curve provides valuable information about structural behavior, including the yield point, ultimate capacity, and potential failure modes.

Modal pushover analysis is a specialized technique used in structural engineering to evaluate the seismic performance of buildings and other structures. It combines the benefits of modal analysis and pushover analysis to provide more accurate and detailed information about the structure's behavior under seismic loads. In modal pushover analysis, the structure's response is assessed by considering the mode shapes and corresponding modal participation factors. The mode shapes represent the different vibration patterns of the structure, and the modal participation factors indicate the contribution of each mode to the overall response. By considering multiple modes, the analysis captures the dynamic characteristics and interactions of the structure more effectively.

For cyclic analysis, a loading protocol is followed to simulate the repeated loading and unloading cycles that structures experience during earthquakes. The loading protocol typically involves applying cyclic loads with a specific amplitude and cycle increment. In the case mentioned, the loading protocol is specified as 0.125% per cycle, which means that the applied load increases by

0.125% of its maximum value in each cycle. Cyclic analysis allows for the assessment of the structure's behavior under repetitive loading, which is essential for evaluating its durability and performance under seismic events. By considering the cyclic loading effects, engineers can gain insights into the structure's ability to withstand multiple seismic events and assess the potential for cumulative damage.

6.6. Results and Discussion

6.6.1. Monotonic Pushover analysis result:

To assess the lateral performance of the structure, it is subjected to increasing displacement, specifically the roof displacement, in order to determine its base shear capacity. The roof drift plays a crucial role in determining when the structure begins to yield. Static pushover analysis is employed to generate pushover curves, which provide a measure of the structure's base shear capacity. In this study, the behavior of reinforced ECC and RCC materials is compared at the structural level. Static pushover curves are obtained for all four models, considering the first mode pattern along the x and y axes. Figures 6.12 and 6.13 illustrate these curves. Additionally, the damage to the models is monitored at the point of maximum displacement, ensuring that the maximum number of hinges has formed.

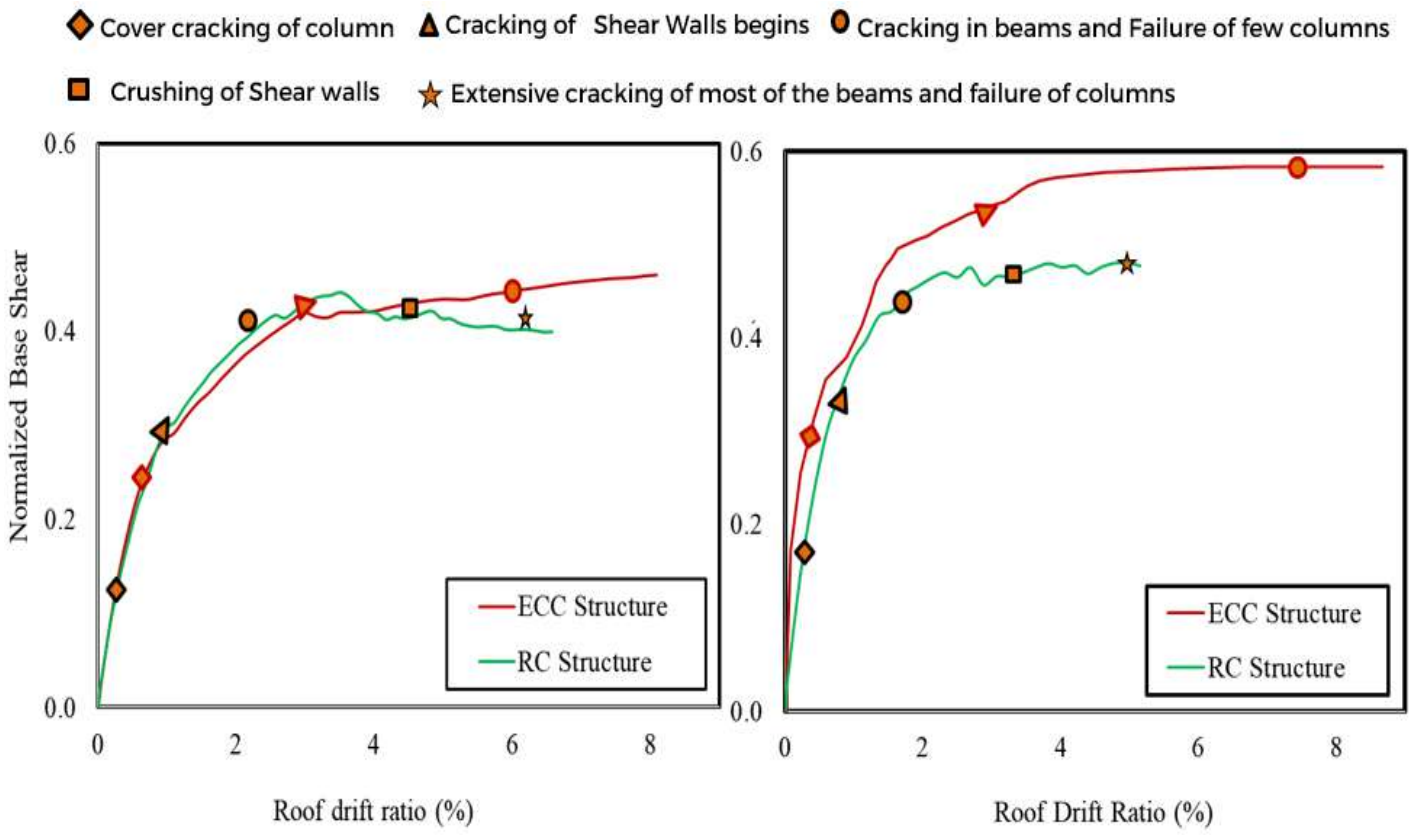

Figure 6.11. The normalized static pushover curves (a) along Y-axis (b) X-axis of 7 story building.

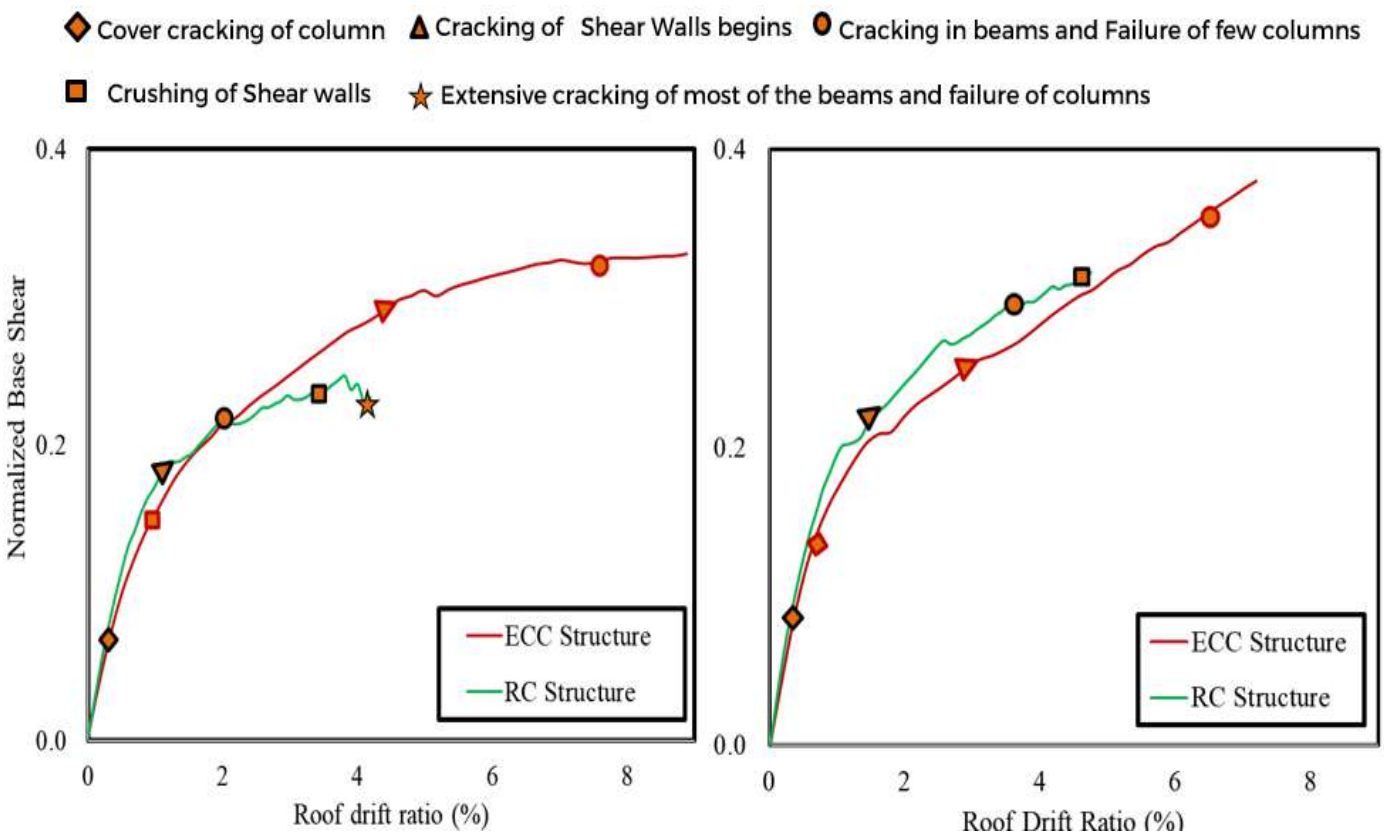

Figure 6.12. The normalized static pushover curves (a) along Y-axis (b) X-axis of 24 story building.

The comparison between Figure 6.12 and Figure 6.13 reveals the superior performance of ECC compared to RCC when subjected to lateral loading. The curves indicate that the stiffness of both materials is similar, but ECC exhibits a higher base shear capacity despite having reduced cross-sections. This finding supports the economic advantages of ECC without compromising the structural capacity. Moreover, the analysis of plastic hinges confirms that ECC structures exhibit fewer plastic hinges compared to RCC structures due to the inherent ductility of ECC.

6.6.2. Cyclic Pushover Analysis result:

The cyclic pushover analysis results for both the 7-story and 24-story normal concrete RC (reinforced concrete) and ECC (engineered cementitious composite) buildings are presented. These results provide insights into the behavior of the structures under cyclic loading. In the case of the 7-story normal concrete RC building, the cyclic pushover analysis revealed a gradual accumulation of damage and a decrease in stiffness as the loading increased. The structure exhibited significant lateral drift and experienced considerable plastic deformation at certain locations. The plastic hinges formed in critical columns and beams indicated the areas of maximum damage and energy dissipation. For the 7-story ECC building, the cyclic pushover analysis demonstrated enhanced performance compared to the normal concrete RC building. The ECC structure exhibited higher stiffness and better energy dissipation capacity, resulting in reduced damage and smaller plastic hinge formation. The inherent ductility of ECC contributed

to its improved resilience and ability to withstand cyclic loading. Figure 6.14. and 6.15 illustrates the cyclic pushover curves of 7 story and 24 story buildings respectively.

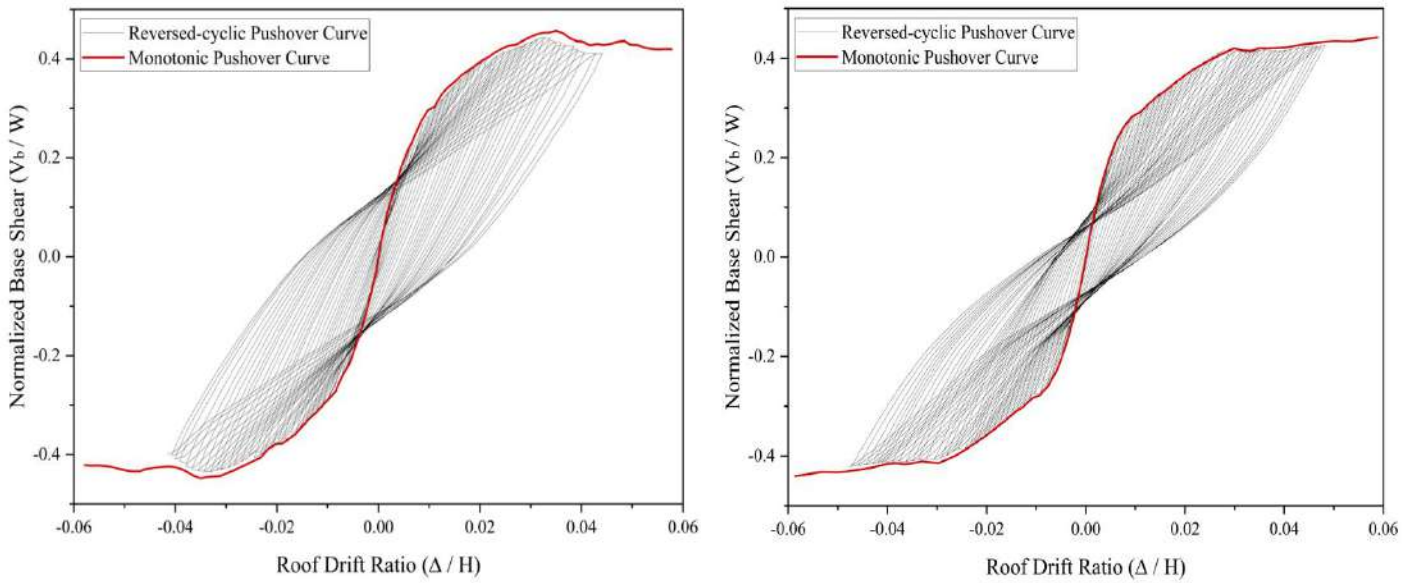

(a) (b)

Figure 6.13. Cyclic Pushover of 7 story (a) RC buildings (b) ECC buildings.

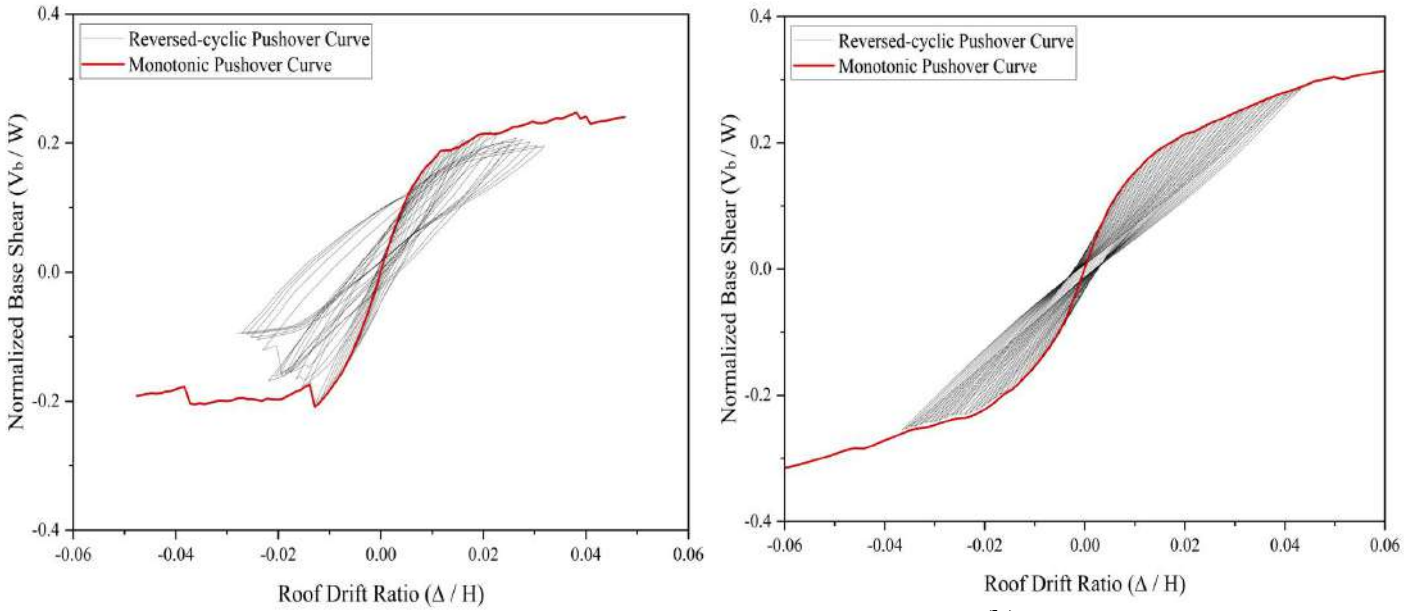

(a) (b)

Figure 6.14. Cyclic Pushover of 24 story (a) RC buildings (b) ECC buildings.

Moving on to the 24-story buildings, similar trends were observed. The normal concrete RC building experienced significant damage and reduced stiffness as the loading increased during the cyclic pushover analysis. Plastic hinges formed in multiple columns and beams, indicating significant structural degradation. In contrast, the 24-story ECC building demonstrated superior performance. It exhibited higher stiffness and energy dissipation capacity, leading to reduced damage and plastic hinge formation. The ECC structure displayed enhanced ductility and resilience, indicating its potential for mitigating the effects of cyclic loading. Overall, the cyclic pushover analysis results highlight the superior behavior of ECC buildings compared to normal concrete RC buildings. ECC structures demonstrate improved stiffness, energy dissipation, and damage tolerance, making them a promising alternative for seismic-resistant construction.

6.6.3. Results of non-linear time history analysis (NLTHA):

The NLTHA (Non-Linear Time History Analysis) requires a representative ground motion input that can be applied to the structure. In this study, the ground motion used was carefully selected following the guidelines outlined in above section. Prior to application, the ground motion was spectrally matched to the design response spectrum to ensure its compatibility with the structural characteristics. The NLTHA analysis was conducted on all four non-linear models, namely reinforced concrete (RC), engineered cementitious composite (ECC). The responses of these models to the applied ground motion were compared and summarized in Figure 6.16 and Figure 6.17. The results of the NLTHA analysis provide valuable insights into the dynamic behavior of the structures under the influence of the ground motion. By comparing the responses of the RC, ECC, and reference models, it is possible to assess the performance and effectiveness of each material in terms of their ability to withstand seismic loading.

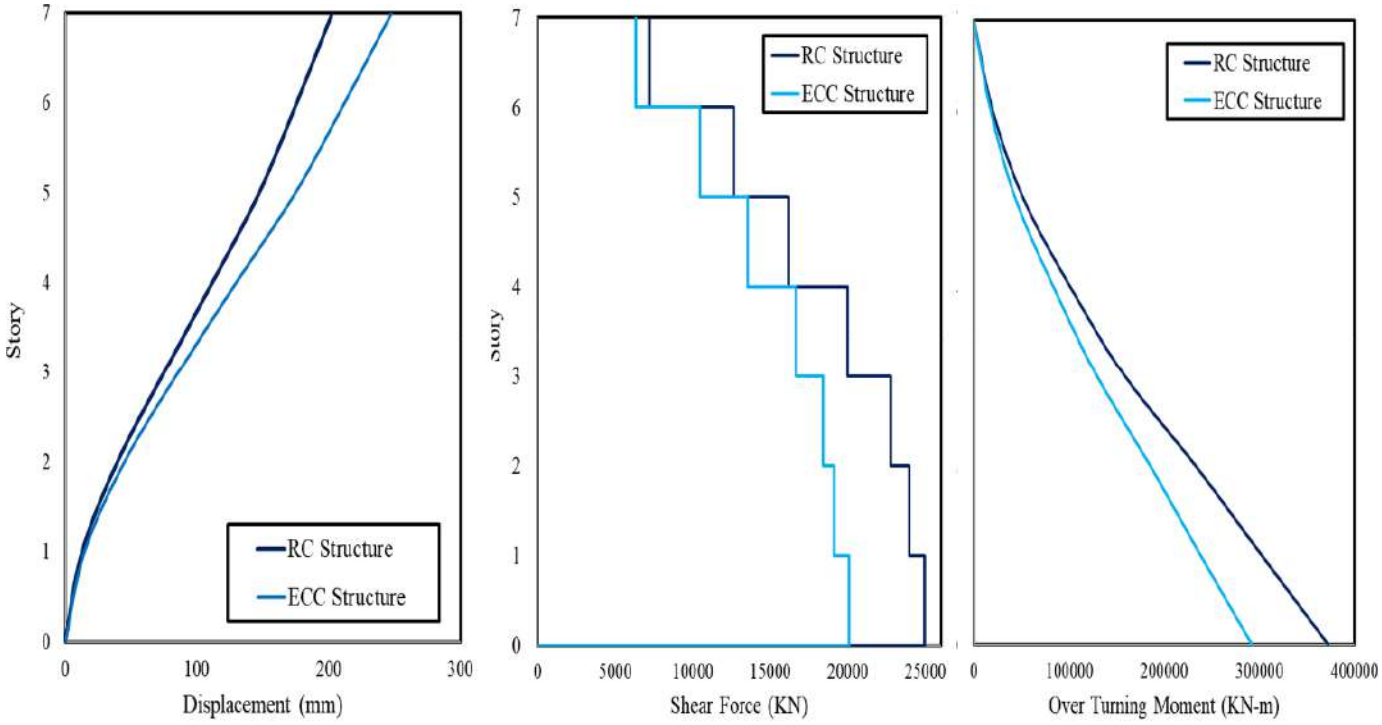

Figure 6.15. (a) Displacement vs Story, (b) Shear Force vs story and (c) Overturning moment vs story.

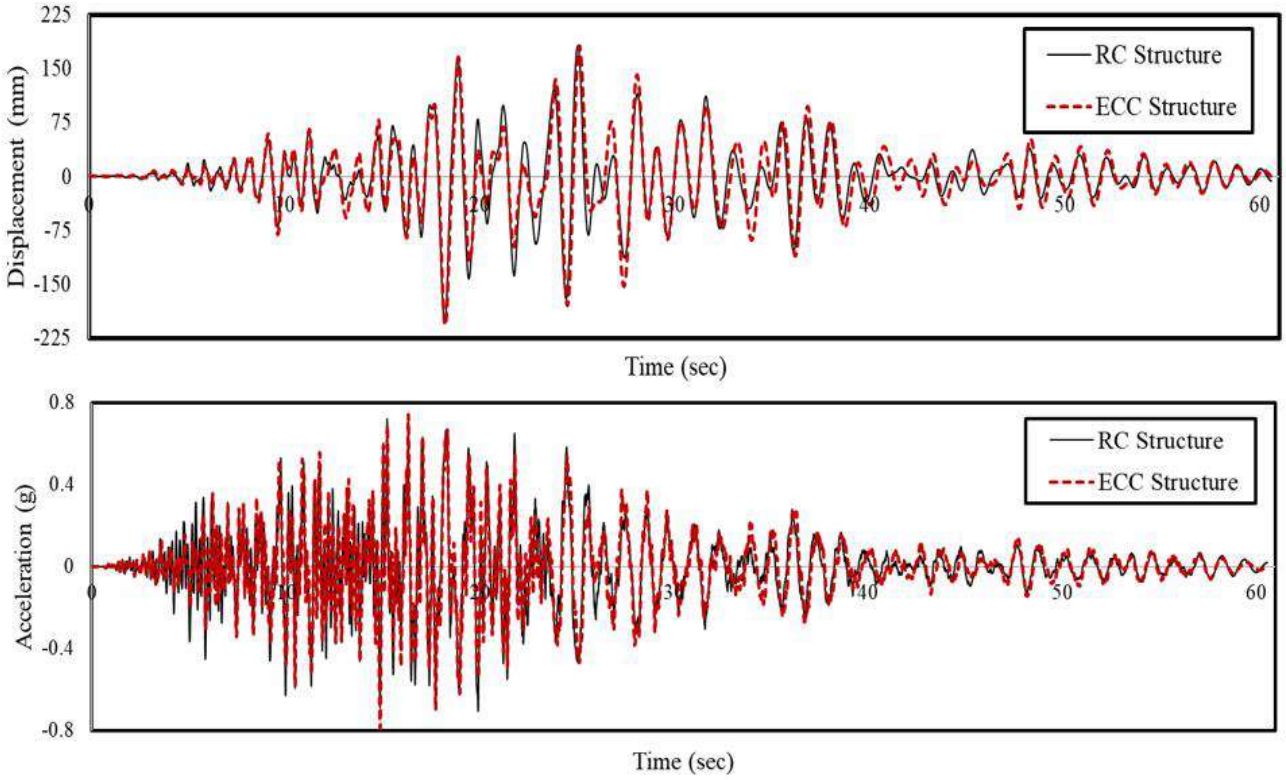

Figure 6.16. (a) Displacement vs time, (b) Acceleration vs story.

The analysis results indicate that the utilization of engineered cementitious composite (ECC) results in increased story drift and displacement compared to traditional reinforced concrete (RCC) structures, primarily due to the lower stiffness of ECC. It is important to note that the prescribed drift and displacement limits specified by building codes are specifically intended for RCC structures. However, since ECC has the ability to withstand significant deformation while remaining structurally safe, the higher drift and roof displacement observed in ECC structures can still be considered within acceptable limits. On the other hand, the overturning moments experienced in ECC structures are reduced, particularly in the case of reduced cross-section ECC. This reduction can be attributed to the lower unit weight of ECC. The results of the analysis clearly demonstrate that ECC structures exhibit a minimal formation of plastic hinges, thanks to their enhanced ductility.

6.7. Conclusions and Recommendations

This study effectively confirmed the outstanding material characteristics of engineered cementitious composite (ECC) through a comprehensive analysis at the structural level, utilizing a 7-story and 24-story building as case studies. The research involved the development of linear and non-linear finite element analysis (FEA) models for ECC, considering its constitutive behavior at the material level. Structural design and non-linear analyses were conducted for ECC structures, and a comparative analysis with reinforced concrete (RCC) structures was performed. The following conclusions were drawn from the study:

- Due to the lower unit weight of ECC, the design actions for structural members were approximately reduced by 22% because of reduction in dead and seismic loads.
- Due to the better tensile capacity of ECC, the cross-sectional sizes were reduced by 25%, making ECC a good alternative to RCC in the case of long-span structures.
- The design performed using JSCE guidelines showed over 24% reduction of longitudinal steel in flexural members and about 15% reduction in longitudinal steel of compression members. Alongside, theoretically shear reinforcement requirement throughout the structure was eliminated.
- The non-linear analyses clearly showed better seismic performance of ECC due to its increased capacity and lower inertial forces developed within the structure.
- Non-Linear static (pushover) analysis of both buildings shows that ECC buildings have greater capacity and lower base shear. However, due to the lower material stiffness of ECC, the displacements and drifts were higher as compared to RCC.
- Cyclic Pushover analysis shows that ECC have greater stiffness, No strength and stiffness degradation till 32 cycles while there is strength and stiffness degradation occur in RC buildings.

It is recommended that future research should be carried out to find actual parameters to avoid assumptions in design process. The design procedure and certain assumptions, being on safer side,adopted in this paper give conservative designs. These conservative approaches are due tounavailability of authentic numeric data for ECC. For example, Damping ratio for ECC should be investigated for further accuracy in design and analysis procedures. Alongside, the structural response of ECC in other special structures should be investigated.

References

[1] Jiansinlapadamrong, C.; Park, K.; Hooper, J.; M.ASCE.; Chao, S. Seismic Design and Performance Evaluation of Long-Span Special Truss Moment Frames. J. Struct. Eng., 2019, 145(7): 04019053

[2] Fuentes, Paula, and Santiago Huerta.: Islamic Domes of Crossed-Arches: Origin, Geometry and Structural Behavior. Arch' 10. 6th International Conference on Arch Bridges, oct 2010, Fuzhou, China. ISBN 978-953-7621-10-0 (2010)

[3] Rodriguez, S.: Design of Long Span Concrete Box Girder Bridges: Challenges and Solutions. ASCE structures. (2004)

[4] Wang, C., Shen, Y., Yang, R., Wen, Z.: Ductility and Ultimate Capacity of Prestressed Steel Reinforced Concrete Beams. Hindawi Mathematical Problems in Engineering Volume 2017, Article ID 1467940. https://doi.org/10.1155/2017/1467940

[5] Kaur, H., Singh, J.: A Review on External Prestressing In Concrete. International Research Journal of Engineering and Technology (IRJET). Volume: 04 Issue: 05 (2017)

[6] International Code Council. International Building Code. Falls Church, Va. :International Code Council, (2021)

[7] M. Chey, J. Chase, J. Mander, A. Carr.: Innovative seismic retrofitting strategy of added stories isolation system. Frontiers Struct Civil Eng, 7 (2013), pp. 13-23

[8] H.L. Hsu, H. Halim **Improving seismic performance of framed structures with steel curved dampers.** Eng Struct, 130 (2017), pp. 99-111, 10.1016/j.engstruct. (2016)

[9] Bentur, A., Mindess, S.: Fiber Reinforced Cementitious Composites, 2nd edn. E & FN Spon, London (2007)

[10] Li, V.C.: From micromechanics to structural engineering – the design of cementitious composites for civil engineering applications. JSCE J. Struct. Mech. Earthq. Eng. 10(I-24), 37s–48s (1993)

[11] Li, V.C., Wang, S., Wu, C.: Tensile strain-hardening behavior or polyvinyl alcohol engineered cementitious composite (PVA-ECC). ACI Mater. J. 98(6), 483–492 (2001)

[12] Li, V.C.: On engineered cementitious composites (ECC). A review of the material and its applications. J. Adv. Concr. Technol. 1(3), 215–230 (2003)

[13] Li, V.C., Hashida, T.: Engineering ductile fracture in brittle-matrix composites. J. Mater. Sci. Lett. 12(12), 898–901 (1993)

[14] Kanda, T., Li, V.C.: Practical design criteria for saturated pseudo strain hardening behavior in ECC. J. Adv. Concr. Technol. 4(1), 59–72 (2006)

[15] Li, V.C.: Integrated structures and materials design. Mater.Struct. 40(4), 387–396 (2007)

[16] Li, X.; Wang, J.; Bao, Y.; Chen, G. Cyclic behavior of damaged reinforced concrete columns repaired with high-performance fiber-reinforced cementitious composite. Eng. Struct. 2017, 136, 26–35. [CrossRef]

[17] Fukuyama, H.: Application of high performance fiber reinforced cementitious composites for damage mitigation of building structures case study on damage mitigation of RC buildings with soft first story. J. Adv. Concr. Technol. 4(1), 35–44 (2006)

[18] Maalej, M., Li, V.C.: Flexural/tensile strength ratio in engineered cementitious composites. J. Mater. Civ. Eng. 6(4), 513–528 (1994)

[19] Szerszen, M.M., Szwed, A., Li, V.C.: Flexural response of reinforced beam with high ductility concrete material. In: BMC-8, Woodland Publishing, Warsaw, Poland, pp. 263–274 (2006)

[20] Fukuyama, H., Matsuzaki, Y., Sato, Y., Iso, M., Suwada, H.: Structural Performance of Engineered Cementitious Composite Elements, Composite and Hybrid Structures, 6th ASCCS International Conference on Steel-Concrete Composite Structures, pp. 969–976 (2000) 222 6 Resilience of Engineered Cementitious Composites (ECC) Structural Members

[21] Parra-Montesinos, G., Wight, J.K.: Seismic response of exterior RC column-to-steel beam connections. J. Struct. Eng. 126, 1113–1121 (2000)

[22] Qudah, S., Maalej, M.: Application of engineered cementitious composites (ECC) in interior beam-column connections for enhanced seismic resistance. Eng. Struct. 69, 235–245 (2014)

[23] Said, S.H., Abdul Razak, H.: Structural behavior of RC engineered cementitious composite (ECC) exterior beam-column joints under reversed cyclic loading. Constr. Build. Mater. 107, 226–234 (2016)
[24] Hosseini, F., Gencturk, B., Aryan, H., Cadaval, G.: Seismic behavior of 3-D ECC beam-column joints subjected to bidirectional bending and torsion. Eng. Struct. 172, 751 (2017)
[25] Khokhar, S.A.; Ahmed, T.; Khushnood, R.A.; Ali, S.M.; Shahnawaz. A Predictive Mimicker of Fracture Behavior in Fiber Reinforced Concrete Using Machine Learning. Materials 2021, 14, 7669.
[26] Japan Society of Civil Engineers: Recommendations for design and construction of high performance Fiber reinforced cement composites with multiple fine cracks (HPFRCC). Concrete Engineering Series, vol. Concrete L. (2008)
[27] ACI Committee 318. Building Code Requirements for Structural Concrete : (ACI 318-19) ; and Commentary (ACI 318R-19). Farmington Hills, MI :American Concrete Institute, 2019.
[28] ASCE/SEI 41-17.(2017). Seismic evaluation and retrofit of existing buildings. https://doi.org/10.1061/9780784414859. American Society of Civil Engineers (ASCE).
[29] Li, V.C., Leung, C.: Steady-state and multiple cracking of short random fiber composites. J. Eng. Mech. 118(11), 2246–2264 (1992)
[30] Lin, Z., Li, V.C.: Crack bridging in fiber reinforced cementitious composites with sliphardening interfaces. J. Mech. Phys. Solids. 45(5), 763–787 (1997)
[31] Li, V.; Stang, H.; Krenchel, H. Micromechanics of crack bridging in fiber-reinforced concrete.Mater.Struct. (1993)
[32] Li, V.C.; Mishra, D.K.; Wu, H.-C. Matrix Design for Pseudo Strain-Hardening Fiber Reinforced Cementitious Composites. Mater.Struct. (1995)
[33] Yang, C.C.; Mura, T.; Shah, S.P. Micromechanical Theory and Uniaxial Tensile Tests of Fiber Reinforced Cement Composites. 2015. Available online: http://journals.cambridge.org (accessed on 1 May 2021).
[34] McCartney, L. Mechanics of Matrix Cracking in Brittle-Matrix Fiber-Reinforced Composites. 1987. Available online: https://www.jstor.org/stable/2398127 (accessed on 1 May 2021).
[35] Leung, C.K. Design criteria for pseudoductile fiber-reinforced composites. J. Eng. Mech. (1996)
[36] Guo, P.; Meng, W.; Xu, M.; Li, V.; Bao, Y. Predicting Mechanical Properties of High-Performance Fiber-Reinforced Cementitious Composites by Integrating Micromechanics and Machine Learning. Materials (2021)
[37] Pakistan Engineering Council. Building Code of Pakistan. Islamabad, Pakistan. : Pakistan Engineering Council, (2021)
[38] ASCE. 2016. Minimum design loads for buildings and other structures. ASCE/SEI 7.Reston, VA: ASCE.
[39] Li, V.C., Mishra, D.K., Naaman, A.E., Wight, J.K., Lafave, J.M., Wu, H.-C., Inada, Y.: On the shear behavior of engineered cementitious composites. Adv. Cem. Based Mater. 1, 142–149 (1994)
[40] Shimizu, K., Kanakubo, T., Kanda, T., and Nagai, S.: Shear Behavior of PVA-ECC Beams, in Proc., Int'l RILEM Workshop HPFRCC in Structural Applications. In: Fischer, G., and Li, V.C. (eds.) published by RILEM SARL, pp. 443–451 (2006)
[41] Li, V.C.: Damage tolerance of engineered cementitious composites. In: Advances in Fracture Research, Proceedings of 9th ICF Conference on Fracture, pp. 619–630 (1997)
[42] Fischer, G., Li, V.C.: Influence of matrix ductility on tension-stiffening behavior of steel reinforced engineered cementitious composites (ECC). ACI Struct. J. 99(1), 104–111 (2015)
[43] Wen, Y.K. Reliability and performance-based design. Structural Safety 23 (2001)
[44] Computers and Structures, Inc, ETABS Nonlinear v9.7.4, Extended Three Dimensional Analysis of Building System, Version 9.7.4, Computers and Structures, Inc, Berkeley, CA 2011.
[45] ASCE/SEI 41-17.(2017). Seismic evaluation and retrofit of existing buildings. https://doi.org/10.1061/9780784414859. American Society of Civil Engineers (ASCE).
[46] Ding, Y.; Yu,K.; Mao, W. Compressive performance of all-grade engineered cementitious composites: Experiment and theoretical model. Construction and Building Materials (2020)
[47] Quan, K; Lu, Z; Dai, J; Shah, S.P. Direct Tensile Properties and Stress–Strain Model of UHP-ECC. J. Mater. Civ. Eng., 2020, 32(1): 04019334

[48] Zaman, S., Ornthammarath, T., Warnitchai, P., 2012. Probabilistic Seismic Hazard Maps for Pakistan. In Proceedings of the 15th World Conference on Earthquake Engineering WCEE, 1–10.
[49] Li, M., Ranade, R., Kan, L., Li, V.C.: On improving the infrastructure service life using ECC to mitigate rebar corrosion. In: van Breugel, K.,Ye, G., Yuan, Y. (eds.) Proceedings of the Second International Symposium on Service Life Design for Infrastructure, Delft, The Netherlands, RILEM PRO 70, pp. 773–782 (2010)
[50] Yang, Y., Lepech, M.D., Yang, E.-H., Li, V.C.: Autogenous healing of engineered cementitious composites under wet-dry cycles. Cem. Concr. Res. 39(5), 382–390 (2009)
[51] Kan, L.L., Shi, H.S., Sakulich, A.R., Li, V.C.: Self-healing characterization of engineered cementitious composite materials. ACI Mater. J. 107(6), 617–619 (2010).

CHAPTER 7
CONCLUSIONS & RECOMMENDATIONS

7.1. Conclusions:

In this thesis, three level of stiffness of engineered cementitious composite has been found out and proposed stiffness modifiers for ECC. The study is able to resolve the concerns related to the sustainable high-strength matrix, material, and structural designing in the form of modules respectively. Following conclusions are made as a result of this study

1) The stiffness at the material level was calculated by the Machine learning tool and experiment. A simplified model was developed that could predict the complete behavior of the stress-strain curve of ECC in compression and in tension. Also, experimental work is done to validate our predicted model. The developed code can predict compressive strength, tensile strength, tensile strain, and fracture behavior with an accuracy of 99%.

2) The stiffness at the section level was calculated by the Experiment and Analytical. Moment curvatures are found out both beams and columns. Flexural stiffness are found out from moment-curvature curves and proposed stiffness modifiers which are 0.47 for ECC beams and 0.80 for ECC columns.

3) A complete structural level study revealed better performance of ECC in terms of lower damages in nonlinear analyses. A complete structural level study was performed on ECC 7 and 24 story buildings as a case study. For design JSCE guidelines were used, after which performance-based analyses were carried out to simulate its actual behavior on structural scale. On large scale structural stiffness is find out using pushover curve and cyclic analysis is used to calculate cyclic, strength and stiffness degradation of structure.

- **Recommendations:**

  - Future research is needed to find out other parameters and their dependence on different important parameters of FRC, e.g., fresh properties, durability properties, use of other types of cement, or incorporating the packing density concept
  - A further structural level should be conducted by using the damping ratio for ECC members.